

University of Southern Queensland
Faculty of Health, Engineering & Sciences

Extraction of ECGs for Twin Pregnancies

A dissertation submitted by

Jarkko Jarvinen

in fulfilment of the requirements of

ENG4112 Research Project

towards the degree of

Bachelor of Electrical & Electronic Engineering

Submitted: October, 2016

Abstract

The wellbeing of a fetus or fetuses can be monitored by the fetal heart rate (fHR). There are several proposed methods for fHR monitoring; these include fetal phonocardiography (fPCG), fetal cardiography (fCTG) and fetal magnetocardiogram (fMCG). Although, according to the research reviewed, none of these methods are ideal for monitoring or estimating fHR. The fPCG method is highly sensitive to noise and can only be used late in the pregnancy. With fCTG, the ultrasound transducer used for measuring the fHR needs to be properly aligned, otherwise the maternal heart rate (mHR) can be recorded instead of the fHR. In addition, the ultrasound high frequency exposure is not completely proven to be safe for the fetus. fMCG can detect fHR very accurately in comparison to the other methods but the method is unwieldy and expensive; thus not widely used in a clinical environment.

Therefore, there is a need for technology which would be able to provide more information about the cardiac health of a fetus, delivered in a cost-effective, streamlined manner. Based on the research reviewed and captured within this dissertation, non-invasive fetal electrocardiography (fECG) has been identified as a promising fetal cardiac monitoring method and if researched further, has the potential to become the next mainstream approach for monitoring fetal health. Within this dissertation, the fECG extraction methods have been explored and the findings captured. The research revealed that the fECG method can be used from early stages of pregnancy (20 weeks gestational age onwards). It is relatively low cost and does not necessarily require a highly skilled user. Continuous monitoring is also possible. The main challenge identified when using the non-invasive fECG extraction method is poor Signal-to-Noise Ratio (SNR) of the fECG signal on the abdominal signal which consists of fECG, maternal ECG (mECG) and noise.

Eleven different fECG extraction methods were tested as part of this dissertation. The

extraction methods were based on Adaptive Methods (AM), Template Subtraction (TS) or Blind Source Separation (BSS). Synthetic test signals were used for the testing the methods. The test signals included five different noise levels across seven different single pregnancy physiological cases and one twin pregnancy case. Each recording included 34 channels (32 abdominal and two maternal reference channels).

For single pregnancy cases all of the extraction methods were able to extract the fECG from the test signals with varying degrees of success. Overall, the BSS-JADE method was the top performing method for single pregnancy cases getting a median F_1 score of 99.85 %. Furthermore, the twin pregnancy case was tested using BSS methods. The BSS FastICA algorithm using symmetric approach was the top performing method for the twin pregnancy case receiving a median F_1 score of 99.93 %.

ENG4111/2 *Research Project*

Limitations of Use

The Council of the University of Southern Queensland, its Faculty of Health, Engineering & Sciences, and the staff of the University of Southern Queensland, do not accept any responsibility for the truth, accuracy or completeness of material contained within or associated with this dissertation.

Persons using all or any part of this material do so at their own risk, and not at the risk of the Council of the University of Southern Queensland, its Faculty of Health, Engineering & Sciences or the staff of the University of Southern Queensland.

This dissertation reports an educational exercise and has no purpose or validity beyond this exercise. The sole purpose of the course pair entitled “Research Project” is to contribute to the overall education within the student’s chosen degree program. This document, the associated hardware, software, drawings, and other material set out in the associated appendices should not be used for any other purpose: if they are so used, it is entirely at the risk of the user.

Dean

Faculty of Health, Engineering & Sciences

Certification of Dissertation

I certify that the ideas, designs and experimental work, results, analyses and conclusions set out in this dissertation are entirely my own effort, except where otherwise indicated and acknowledged.

I further certify that the work is original and has not been previously submitted for assessment in any other course or institution, except where specifically stated.

JARKKO JARVINEN

0061012762

Acknowledgments

I would like to sincerely thank my supervisor, John Leis, for all his support and assistance during the project. Furthermore, a big thanks to goes to my employer Olympus Australia and especially to my managers Graham Maxwell and Andrew Taylor.

Most importantly, I would like to thank my beautiful wife Megan for all her support, not only during this dissertation, but also during my studies in general.

JARKKO JARVINEN

Contents

Abstract	i
Acknowledgments	v
List of Figures	xi
List of Tables	xiv
Chapter 1 Research Background	1
Chapter 2 Fetal ECG Background	4
2.1 Physiology of the Fetal Heart	5
2.1.1 Development of the fetal heart	5
2.1.2 Fetal presentation	6
2.1.3 Anatomy and electrical activity of the fetal heart	6
2.1.4 Fetal heart rate	10
2.2 fECG Signal Extraction During Singleton Pregnancies	11
2.2.1 Brief history	11
2.2.2 Recent work	12

CONTENTS	viii
2.2.3 Adaptive Methods	12
2.2.4 Template Subtraction	13
2.2.5 Wavelet Transform	14
2.2.6 Singular Value Decomposition	15
2.2.7 Independent Component Analysis	16
2.3 fECG Signal Extraction During Multiple Pregnancies	19
2.4 fECG Signal Databases	23
2.5 Synthetic fECG Signal Generation Models	24
2.6 Chapter Summary	25
Chapter 3 ECG Data Transfer and Storage Formats	26
3.1 Major Formats	26
3.2 Detailed Review	28
3.2.1 HL7 aECG	29
3.2.2 DICOM supplement 30	30
3.2.3 SCP-ECG	33
3.2.4 EDF and EDF+	34
3.2.5 GDF	36
3.2.6 MFER	37
3.2.7 ISHNE Holter Standard Output File Format	40
3.2.8 WFDB	40
3.3 MATLAB Implementation	42

CONTENTS	ix
3.4 Test File ECG Waveforms	45
3.5 Chapter Summary	47
Chapter 4 Fetal ECG Signal Extraction Methods	48
4.1 Test Signal	48
4.2 Test Signal Preprocessing	50
4.3 fECG Extraction Methods	52
4.3.1 Blind Source Separation	53
4.3.2 Template Subtraction	55
4.3.3 Adaptive Methods	56
4.4 fQRS Detection	57
4.5 Performance Metrics	58
4.6 MATLAB Implementation	60
4.7 Chapter Summary	64
Chapter 5 fECG Signal Extraction Results and Performance Comparison	65
5.1 Single Pregnancy Case	65
5.2 Twin Pregnancy Case	80
5.3 Comparison of Results	83
5.4 Chapter Summary	84
Chapter 6 Conclusion and Future Work	86
6.1 Dissertation Summary	86

CONTENTS	x
6.2 Future Work	88
References	90
Appendix A Project Specification	101
Appendix B fECG Extraction Raw Results	103
B.1 Case 0 - Baseline + Noise	104
B.2 Case 1 - Fetal Movement + Noise	109
B.3 Case 2 - C2 - mHR / fHR Acceleration and Deceleration + Noise	114
B.4 Case 3 - Uterine Contraction + Noise	119
B.5 Case 4 - Ectopic Beats + Noise	124
B.6 Case 5 - Twin Pregnancy + Noise	129

List of Figures

1.1	Typical Abdominal fECG and Scalp fECG Signals	3
2.1	Fetal Heart Development Timeline	5
2.2	Fetomaternal Compartments	6
2.3	Fetal Presentations	7
2.4	Fetal Heart Anatomy	7
2.5	Heart Depolarisation Path	8
2.6	PQRST Waveform	9
2.7	Fetal Heart Rate	10
2.8	Diurnal fHR Variation	11
2.9	Example of the Signal Outputs	14
2.10	Extracted fECG Signals (Ayat)	16
2.11	Extracted fECG Signals (Wan)	18
2.12	Extracted fECG Signals (Kam)	20
2.13	Simulated Electrode and Signal Source Positions	21
2.14	Binary Series for the Detected fQRS Complexes	22

2.15	PI Metric for the Different Contrast Functions	22
3.1	HL7 aECG Syntax	30
3.2	HL7 aECG sequenceSet Element Syntax	30
3.3	E-R Diagram for DICOM	31
3.4	SCP-ECG File Structure	34
3.5	EDF Header and Data Sections	35
3.6	MFER Frame Attributes	38
3.7	MFER Frame Header	38
3.8	MFER Data Alignment	39
3.9	MFER Tag	39
3.10	ISHNE Fixed Header	41
3.11	WFDB Header	41
3.12	SPC-ECG MATLAB Header	43
3.13	Test ECG Waveforms	46
4.1	Electrode Configuration	50
4.2	ECG Signal Components Frequency Domain	51
4.3	Effect of High-Pass Filter Cut-Off Frequencies	52
4.4	ESN Adaptive Algorithm	56
4.5	fECG Extraction MATLAB Program Flowchart (p. 1)	62
4.6	fECG Extraction MATLAB Program Flowchart (p. 2)	63

5.1	Extracted Single Pregnancy fECG Waveform Examples	66
5.2	C0 F_1 Results	68
5.3	C0 MAE Results	69
5.4	C1 F_1 Results	70
5.5	C1 MAE Results	71
5.6	C2 F_1 Results	72
5.7	C2 MAE Results	73
5.8	C3 F_1 Results	74
5.9	C3 MAE Results	75
5.10	C4 F_1 Results	76
5.11	C4 MAE Results	77
5.12	Overall Single Pregnancy F_1 Results	78
5.13	Overall Single Pregnancy MAE Results	79
5.14	Extracted Twin Pregnancy fECG Waveform Examples	81
5.15	Overall Twin Pregnancy F_1 and MAE Results	82

List of Tables

2.1	Results Comparison for the Different ICA Algorithms	18
3.1	The Most Common ECG Data Transfer and Storage Formats	27
3.2	DICOM ECG Waveform IO Attributes	32
3.3	SCP-ECG Section Header	34
3.4	ECG Test Signals	44
4.1	Simulated Physiological Events	49
4.2	Selected Abdominal Channels	50
5.1	Best Performing fECG Extraction Methods	80
5.2	Median F_1 Score for Anroetti	84
5.3	Median F_1 Score for Eight Abdominal Channels	84
B.1	Raw Results - C0 (0 dB)	104
B.2	Raw Results - C0 (3 dB)	105
B.3	Raw Results - C0 (6 dB)	106
B.4	Raw Results - C0 (9 dB)	107

B.5 Raw Results - C0 (12 dB)	108
B.6 Raw Results - C1 (0 dB)	109
B.7 Raw Results - C1 (3 dB)	110
B.8 Raw Results - C1 (6 dB)	111
B.9 Raw Results - C1 (9 dB)	112
B.10 Raw Results - C1 (12 dB)	113
B.11 Raw Results - C2 (0 dB)	114
B.12 Raw Results - C2 (3 dB)	115
B.13 Raw Results - C2 (6 dB)	116
B.14 Raw Results - C2 (9 dB)	117
B.15 Raw Results - C2 (12 dB)	118
B.16 Raw Results - C3 (0 dB)	119
B.17 Raw Results - C3 (3 dB)	120
B.18 Raw Results - C3 (6 dB)	121
B.19 Raw Results - C3 (9 dB)	122
B.20 Raw Results - C3 (12 dB)	123
B.21 Raw Results - C4 (0 dB)	124
B.22 Raw Results - C4 (3 dB)	125
B.23 Raw Results - C4 (6 dB)	126
B.24 Raw Results - C4 (9 dB)	127
B.25 Raw Results - C4 (12 dB)	128

LIST OF TABLES

B.26 Raw Results - C5 (0 dB) 129

B.27 Raw Results - C5 (3 dB) 130

B.28 Raw Results - C5 (6 dB) 131

B.29 Raw Results - C5 (9 dB) 132

B.30 Raw Results - C5 (12 dB) 133

Chapter 1

Research Background

Electrocardiogram (ECG, ECC or EKG) can be used to monitor the human heart's cardiac activity and is known as a reliable technique for the diagnosis of heart related diseases in humans. A fetal heart's cardiac activity (the fECG signal) can be measured by two different methods: invasive and non-invasive. With the invasive method, an electrode is placed directly on the scalp of the fetus. With the non-invasive method, an ECG electrode or electrodes are placed on the mothers abdomen. The fECG signal from the invasive method offers better Signal-to-Noise (SNR) ratio compared to the fECG signal from the non-invasive method. However, the invasive method can only be used during labor so it is not useful for monitoring the electrical signals of a fetus's heart during the early stages of pregnancy.

So why is it important to monitor the cardiac activity of a fetus? Firstly, cardiovascular abnormality is one of the most common birth defects and heart related defects are one of the most common causes of neonatal and infant deaths in Australia (Hill 2016, VIC DHHS 2012). Furthermore, in the USA 1 out of 125 babies are born with some form of heart defect (AHA 2008). The human heart is one of the very first organs to develop in a fetus and a heart defect could originate from the early stages of the development process (Rajesh & Ganesan 2014, AHA 2008). However, it could take days, weeks or even years before a heart defect is detected after the birth. With timely detection, treatment can be started early and a potentially fatal outcome could be prevented.

Multiple pregnancies occurs when the pregnant woman carries two or more fetuses simultaneously. Multiple pregnancies carry inherently higher health risks for the fetuses. There

are several reasons why this is the case. Firstly, during multiple pregnancies the fetuses may compete for nutrients. It is also possible that the placenta cannot support the growth of both fetuses. This condition is called Intrauterine Growth Restriction (IUGR). Furthermore, multiple pregnancies carry higher risk for other complications during pregnancy for example: premature labour, gestational diabetes, hypertension, pre-eclampsia, twin-to-twin transfusion syndrome, fetal hypoxia and placental abruption (*Pregnant with twins: potential complications* 2012, *Complications In A Multiples Pregnancy* 2015, UPMC 2016).

Non-invasive fECG recorded on the maternal abdomen offers one method to monitor fetal wellbeing. However, the abdominal composite signal is corrupted by noise which makes it difficult to extract the fECG signal. Some of the interfering elements are:

- Maternal ECG signal (mECG)
- Maternal Electromyogram (mEMG)
- Fetal movement inside the uterus
- 50Hz Noise
- Baseline wander
- Electrical noise from the measuring equipment

Mathematically, the problem can be defined as: $lead_A = mECG + fECG + noise$, where $lead_A$ is an abdominal lead.

Figure 1.1 shows typical fECG signals measured using both invasive and non-invasive methods. The circled parts in the waveform are showing the respective fetal QRS complex in each signal. On the non-invasive recordings, the fetal QRS complex is hardly visible. In addition, during multiple pregnancies, the non-invasive abdominal ECG signal recordings have two or more fECG signals present. This adds further complexity to the situation.

This dissertation focuses on researching novel signal processing methods and techniques for non-invasive fECG signal extraction for singleton and multiple pregnancies. The most promising methods were then implemented to MATLABTM software for comparative analysis. Furthermore, ECG data transfer and storage formats have also been researched and some of the formats have been implemented to MATLAB. The dissertation is organised as follows; Fetal ECG Background, ECG Data Transfer and Storage Formats, Fetal

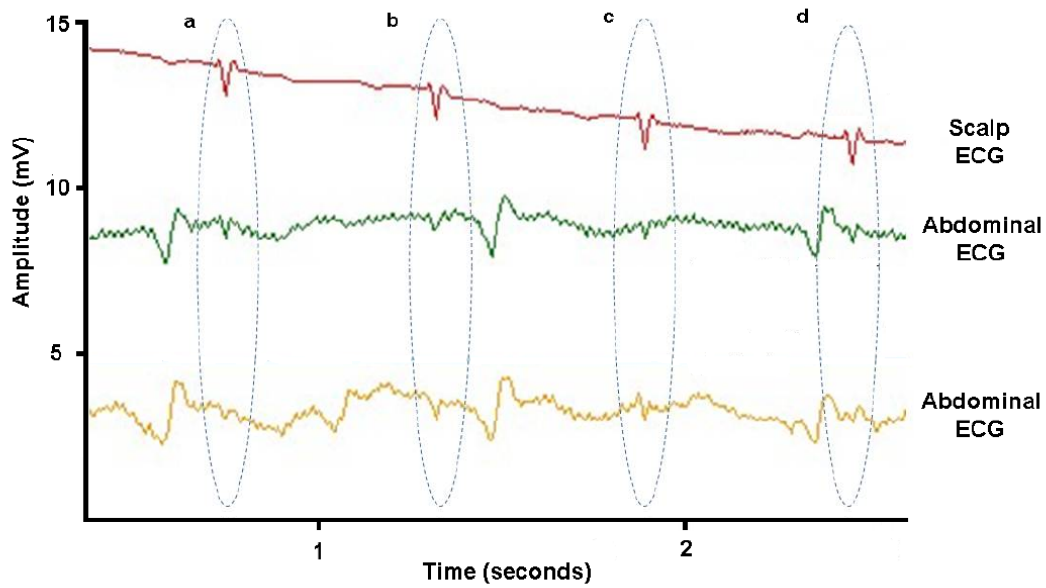


Figure 1.1: Fetal ECG signal recorded through invasive (Scalp ECG) and non-invasive (Abdominal ECG) methods. Reproduced from Sameni et al. (2010).

ECG Extraction Methods, Fetal ECG Extraction Results and Performance Comparison, Conclusion and Future Work.

In conclusion, this chapter provided an overview of the research background, including the definition of the research problems. In the next chapter, the background of fetal ECG, including physiology of the fetal heart and current fetal ECG extraction methods for singleton and multiple pregnancies, will be discussed in more detail.

Chapter 2

Fetal ECG Background

This chapter introduces the main physiological concepts of the fECG and includes a review of the fECG extraction methods. More specially following topics are covered:

- Physiology of the fetal heart
- fECG signal extraction during singleton pregnancies
- fECG signal extraction during multiple pregnancies
- ECG data storage formats
- fECG online signal databases
- Synthetic fECG signal generation models

Even though, the main focus of this project is the fECG signal extraction methods during multiple pregnancies, in the early stages of the literature researches, it became apparent that the fECG extraction methods for multiple pregnancies are based on the same methods which are used for singleton pregnancies. Therefore, for this dissertation it appears crucial to understand the fECG signal extraction methods, not only for the multiple pregnancy case, but also for the singleton pregnancy case.

Furthermore, testing of the fECG extraction methods requires appropriate test signals. Thus, the fECG online signal databases and synthetic fECG signal generation models are discussed.

2.1 Physiology of the Fetal Heart

2.1.1 Development of the fetal heart

The fetus's heart is one of the first organs to develop during pregnancy, with the most critical part being between three and seven weeks from fertilisation. This is when the heart develops from a simple tube shape to a four chambered heart. Figure 2.1 describes the development processes. By the third week, the heart starts beating and roughly a week later, the blood starts flowing through the separate closed circulatory system (Sameni & Clifford 2010).

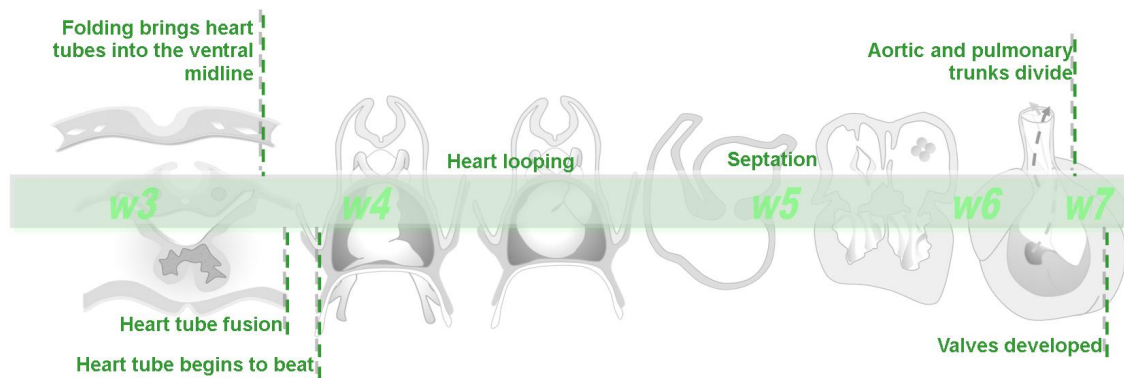


Figure 2.1: Basic fetal heart development timeline from week 3 to week 7. Reproduced from Hill, M.A. (2016).

Ultrasound imaging will be able to pick up the fetal heartbeat around seven to nine weeks into the pregnancy. However, the cardiac waveforms cannot be measured nor can the fetal heart rate (fHR) be accurately extracted using this technique. At around 20 weeks, the fetus's heartbeat can be heard without amplification and the fHR can be measured using acoustic techniques (Sameni & Clifford 2010).

The fECG can be measured from the mother's abdomen from 18 weeks after conception (Peters, Crowe, Piéri, Quartero, Hayes-Gill, James, Stinstra & Shakespeare 2001). The fetus is surrounded by several different layers with different electrical conductivities (Oostendorp, Van Oosterom & Jongasma 1989) as shown in Figure 2.2. These different layers form a so called volume conductor in which the fECG signal propagates from the fetus's heart through to the surface electrodes on the mother's abdomen. The volume conductor's electrical conductivity and the geometric shape changes constantly throughout the pregnancy. Specifically, after 28 to 32 weeks of gestation, a very low conductivity

vernix caseosa layer is formed (Oostendorp et al. 1989). The vernix caseosa layer makes fECG measurement through abdominal surface electrodes very difficult. This layer slowly dissolves around the 38th week of the pregnancy.

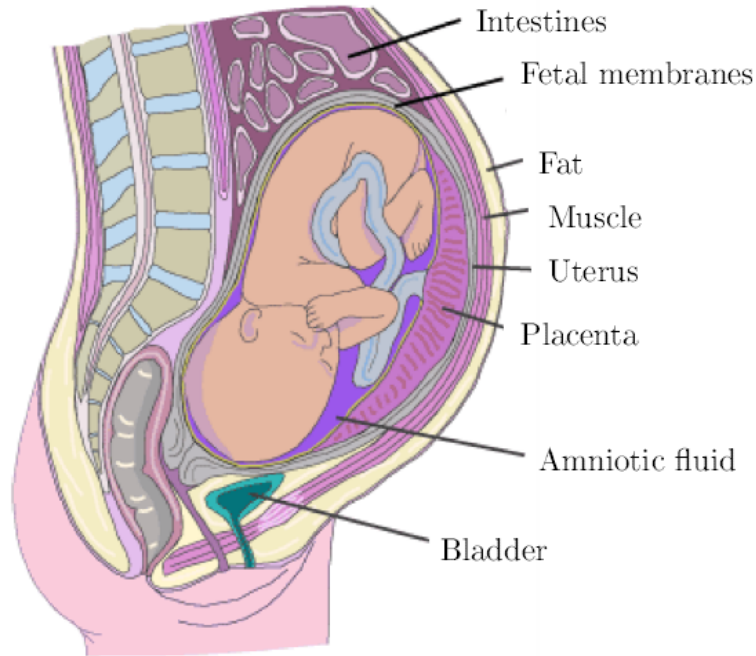


Figure 2.2: The major fetomaternal compartments are shown which affect the fECG signal propagation through the volume conductor. The vernix caseosa layer forms over the fetus's skin after 28 to 32 weeks of gestation. Reproduced from Stinstra, J.G. (2001).

2.1.2 Fetal presentation

During the first two trimesters of pregnancy, the fetus moves around inside the mother's womb. During the third trimester, the fetus assumes a so called *vertex* presentation in 96.8% of pregnancies. The vertex presentation is ideal for birth, but other fetal presentations are also possible as shown in Figure 2.3. The fetal presentation affects the fECG electric potentials recorded on the electrodes placed on the mother's abdomen (Van Oosterom 1989).

2.1.3 Anatomy and electrical activity of the fetal heart

Figure 2.4 shows a fully developed fetal heart. The anatomy of the fetal and adult hearts are similar. However, there are some functional differences. The right side of the adult

heart pumps oxygen poor blood from the veins in to the lungs. The lungs get rid of the carbon dioxide in the blood and replaces it with oxygen. The left side of the heart receives the oxygen rich blood from the lungs and deliveries it to the rest of the body through the arteries (NEALS 2008).

The fetus receives oxygen and nutrients from the placenta via the umbilical cord. Carbon dioxide, and other waste products, are returned from the fetus back to the mother via the umbilical cord and the mother's lungs and the liver removes the waste. The fetus does not use lungs for breathing and actually both sides of the fetus's heart pump blood through the fetus's body. After birth, when the baby takes it's first breath, the *foramen ovale* closes and the fetus's heart starts operating like an adult heart (Pope & Latson 2011).

Even though the operation of the fetal heart is somewhat different to the adult heart,

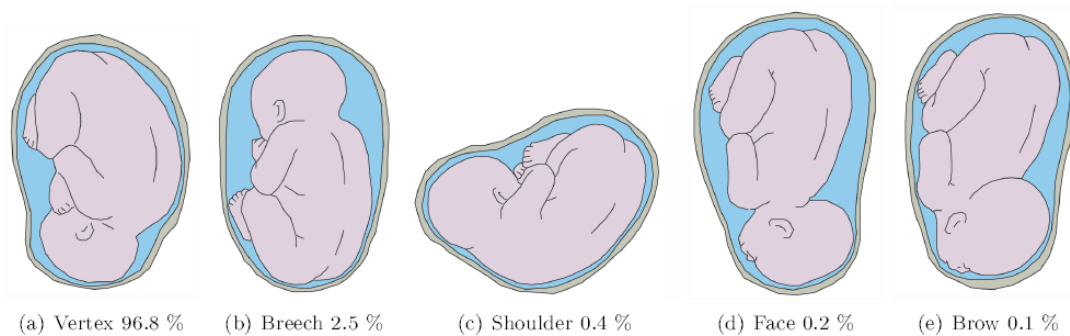


Figure 2.3: Fetal presentations inside the maternal womb towards the end of pregnancy. Reproduced from Stinstra, J.G. (2001).

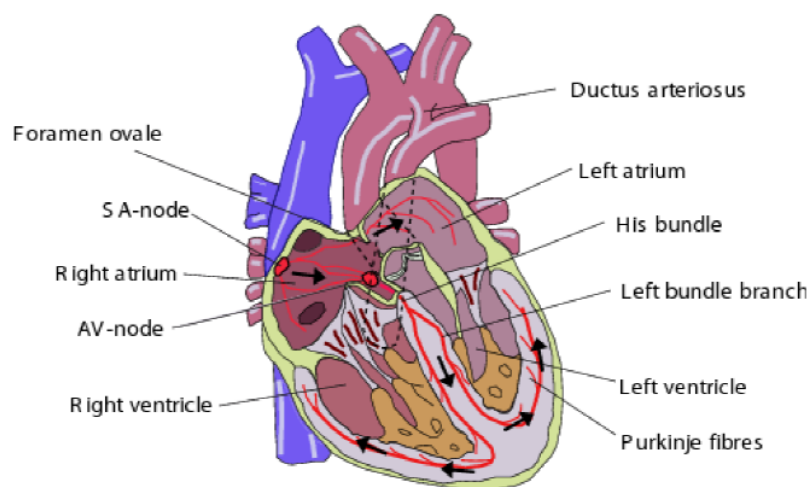


Figure 2.4: Anatomy of the fetal heart. Reproduced from Stinstra J.G. (2001).

the beat-to-beat electrical activity is similar. The heart's wavelike pumping action is controlled by a network of nerve fibres which contracts and relaxes the cardiac muscle tissue (myocardium). The *sinoatrial node* (SAN) is the heart's pacemaker. The SAN sends a depolarisation wave (DW) which spreads through the atria to the *atrioventricular node* (AVN) where the impulse is delayed briefly. Next the DW continues to the bundle of HIS where the DW splits to left and right bundle branches. The DW continues Purkinje system which distributes the DW into the ventricular walls. This will cause the left and right ventricles to contract. Figure 2.5 shows the depolarisation path (Ashley & Niebauer 2004).

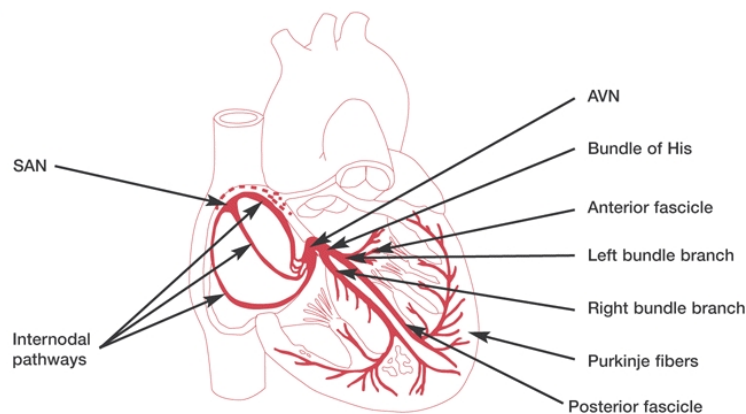


Figure 2.5: The depolarisation wave route of the heart. Reproduced from Ashley et al. (2004).

The electrical signals produced by the contraction and the relaxation action of the myocardium (the ECG) can be measured through electrodes placed on the patient's skin. A typical ECG waveform produced by the heart can be seen in Figure 2.6. This waveform is called the PQRST-complex and was named by a Dutch doctor Willem Einthoven (Hurst 1998). Dr Einthoven was the first researcher to be able to build a device capable of measuring ECG signals (Bass & Shouldice 2002).

The different parts of the PQRST-complex represent different stages of depolarisation taking place in the myocardium as follows:

P wave - represents atrial depolarisation.

PR interval - represents the time between the first deflection of the P wave and the first deflection of the QRS complex.

QRS wave complex - represents ventricular depolarisation.

Q wave - represents depolarisation of the interventricular septum.

R wave - represents depolarisation of the main mass of the ventricles.

S wave - represents the final depolarisation of the ventricles, at the base of the heart.

ST interval - represents the time between the end of the QRS complex and the start of the T wave; the period of zero potential between ventricular depolarisation and repolarisation.

T wave - represents ventricular repolarisation; atrial repolarisation is obscured by the QRS complex.

QT interval - represents the time between the beginning of the QRS complex and end of the T wave.

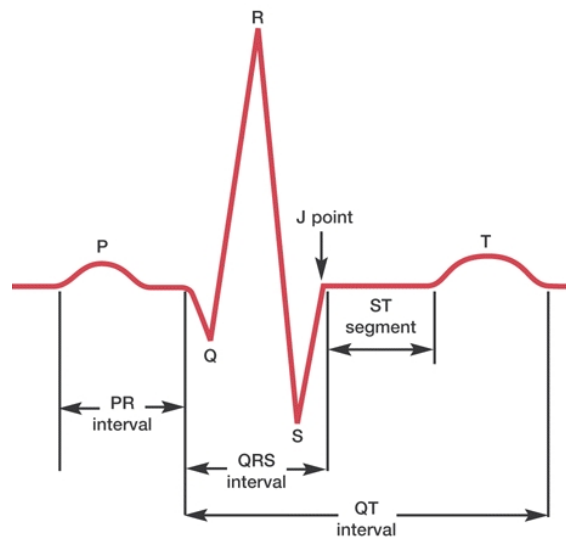


Figure 2.6: Typical ECG signal, the PQRST waveform. Reproduced from Ashley et al. (2004).

The morphologies of the fECG and the adult ECG are rather similar. However, throughout the gestation period and even after birth, the relative amplitudes and time periods of the different waves in the fetal PQRST-complex change quite significantly (Van Leeuwen, Lange, Klein, Geue & Grönemeyer 2004).

2.1.4 Fetal heart rate

The normal fHR varies between 120 to 170 beats-per-minute (bpm) as seen in Figure 2.7. Furthermore, Muro et al. made 24 hour recordings of the fHR on a single subject at 21, 24, 27, 30, 33 and 36 weeks of gestation (Muro, Shono, Shono, Uchiyama & Iwasaka 2004). The calculated mean baseline fHR can be found in Figure 2.8. They found smaller daily variation on the baseline fHR at 21 weeks compared to 36 weeks. The diurnal variation of the fHR is not fully understood. However, it is believed that the maternal influence is the main factor for the fHR variation. Lunshof et al. found that the cortisol and the melatonin concentration in the maternal blood had a very strong correlation with the fHR. They suggested that the fetus's brain and nervous system play an important role by directly controlling the fHR (Lunshof, Boer, Wolf, van Hoffen, Bayram & Mirmiran 1998).

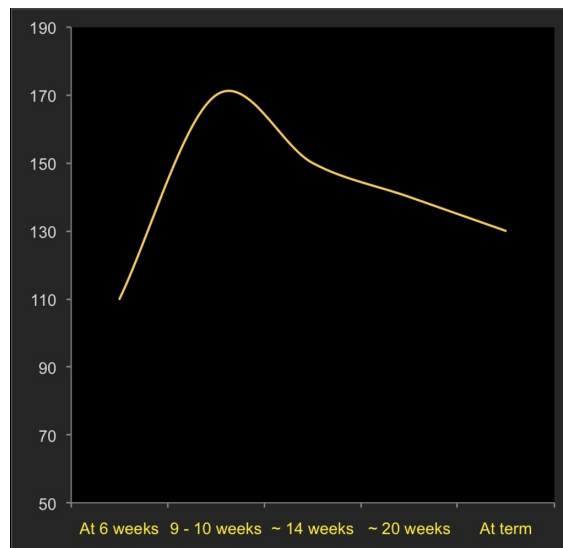


Figure 2.7: Normal fetal heart rate from 6 weeks to full term. Reproduced from Jones et al. (2016).

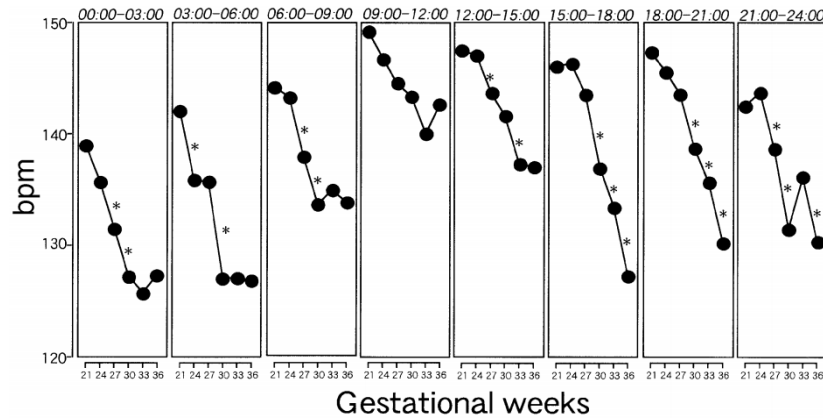


Figure 2.8: Diurnal fHR variation from 21 weeks to 36 weeks of gestation. Maternal influence is believed to be the main factor for the fHR variation. Reproduced from Muro et al. (2004).

2.2 fECG Signal Extraction During Singleton Pregnancies

2.2.1 Brief history

Fetal ECG was firstly observed by Cremer (cited in Sameni et al. 2010) in 1903 and as signal processing techniques improved, it became a more accepted medical diagnostic method (Goodyer, Geiger & Monroe 1942, Lindsley 1942). However, the main issue back then was the interference caused by the maternal cardiac activity (mECG) which resulted in poor fECG (SNR); this is still one of the main issues that the current fECG extraction algorithms need to overcome. In 1960's, invasive extraction methods were trialed for the first time. Intra-uterine electrodes were placed on the wall of the intact membranes of the fetus and the wall of the uterus. This method provided SNR improvement. However, because of the increased danger of an early rupture of membranes, this method did not become mainstream and died away relatively quickly. Hon (cited in Sameni et al. 2010) was the first researcher to obtain fECG readings through an electrode placed directly on the exposed part of the fetus after the rupture of the membranes. In the 1970's and 1980's, the development in the computer science and signal processing techniques enabled progress to be made in cancelling out the mECG signal from the abdominal electrode composite signal. However, this still only provided approximations of the fHR.

2.2.2 Recent work

Many different methods can be found in the literature for extracting fECG signals through non-invasive methods. The common methods found in the literature are:

- Adaptive Methods (AM)
- Template Subtraction (TS)
- Wavelet Transform (WT)
- Blind Source Separation (BSS)
 - Singular Value Decomposition (SVD)
 - Principal Component Analysis (PCA)
 - Independent Component Analysis (ICA)

In the following sections, these methods are discussed in more detail.

2.2.3 Adaptive Methods

AM uses a “learning“ filtration algorithm for subtracting the mECG signal from the composite abdominal signal. Several different types of adaptive algorithms have been used in the literature.

Soleit et al. used an adaptive filter algorithm which used a maternal reference channel for subtracting the mECG signal from the composite signal (Soleit, Gadallah & Salah 2002). The authors were able to extract the fECG signal and estimate the fetus’s heartbeat. However, no consideration was given to the accuracy in which they were able to do this.

Another type of the adaptive filter uses a direct learning algorithm for extracting the fetus QRS complex from the maternal ECG (Park, Lee, Youn, Kim, Kim & Park 1992). Their Moving Averaged Magnitude Difference (MAMD) processor recorded a performance figure of over 90% where the performance figure is calculated using following formula:

$$performance(\%) = \frac{Total\ number\ of\ fetal\ R\ waves - (Number\ of\ misses + Number\ of\ false\ detections)}{Total\ number\ of\ fetal\ R-waves} * 100$$

Wei et al. (Wei, Hongxing & Jianchun 2010) used adaptive filtering in phase space for extracting fECG signal from the maternal abdominal signal. Many other adaptive filtration algorithms assume that the maternal ECG component in the measured abdominal signal has a correlated relationship with the measured reference signal which is often measured from the thorax region of the mother's body. However, this is not often the case. As the mECG signal travels from the mother's heart to the electrode on the mother's abdomen, it encounters non-linear transformation and is time-delayed due to a longer propagation path. Wei tested their algorithm against a "classic" adaptive filter using synthetic and real ECG signals. Their proposed method was able to show improved robustness and fidelity in restoration of the fECG signal. However, their method has a longer time delay before the first results were obtained as this type of algorithm needs a signal of several period durations to implement the local modeling.

2.2.4 Template Subtraction

TS method builds an average mECG cycle (template) by coherently averaging several maternal beats. The method relies on accurate mQRS detection. After the template has been acquired, mQRS complex is adaptively subtracted from the composite signal leaving the residual; fECG and noise.

Di Macro et al. (Di Marco, Marzo & Frangi 2013) used a TS based method for fECG extraction. They used modified Pan Tompkins algorithm to detect mQRS complexes. They then created a median template for each mQRS by finding ten of the best matching mQRS complexes from the same channel. After this, the template was subtracted from the composite signal to obtain the residual signal (the fECG+noise). The fQRS complexes were detected by firstly running the residual signal through a moving average filter and the peaks in the filtered signal, which were assumed to be fQRS complexes, were detected using statistical measures. Figure 2.9 shows an example of the composite signal, the residual signal and the filtered residual signal. Their extraction algorithm was submitted to the Non-Invasive Fetal ECG Physionet Challenge 2013 (Silva, Behar, Sameni, Zhu, Oster, Clifford & Moody 2013) competition and the method achieved 10th and 9th best results in events 4 and 5 respectively.

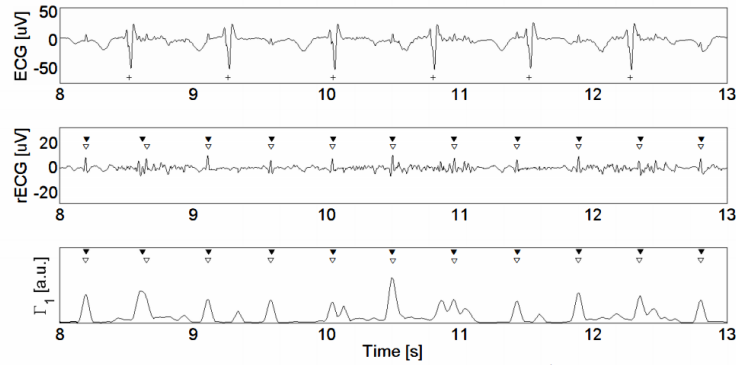


Figure 2.9: Composite signal (top), residual signal (middle) and filtered residual signal (bottom). Black triangles indicate the detected fQRS location and white triangles indicate the actual fQRS location. Reproduced from Di Marco et al. (2013).

2.2.5 Wavelet Transform

The wavelet transform is a linear decomposition method. This method uses a suitable basis function to decompose the signals into different components. The basis function, also called the mother wavelet, is typically selected from the different classes of functions which is in coherence with the time, frequency or scale characteristic of the wanted signal (i.e. ECG signal). Nagarkoti et al. (Nagarkoti, Singh & Kumar 2012) and Hurezeanu et al. (Hurezeanu, Ungureanu, Taralunga, Strungaru, Gussi & Wolf 2014) used Daubechies as the mother wavelet as this is more similar, than other wavelets, to the ECG signals.

Nagarkoti et al. used the wavelet transform to firstly extract the mECG signal from the composite signal and then subtracted that from the composite signal to get the fECG signal. After this, low-pass and band-pass filters were applied to remove additional noise from the signal. In addition, the threshold free detection method was used to find the fetal R peaks and thus the fetal heart rate could be calculated. The method was tested on 20 real world signals; the average Sensitivity (S_e) was 97.88% and the Positive Predictability (+P) was 97.06%.

Hurezeanu et al. used a similar method to Nagarkoti's to extract the fECG signal from the composite signal (i.e. mECG subtraction from the composite signal to obtain fECG signal). However, they were more interested in trying to accurately reconstruct the whole fetal QRS (fQRS) complex rather than just calculate the fetal heart rate. Their method was successful in extracting the fQRS complexes and in theory clinicians would be able to use ECG morphology from their extracted signal for fetal monitoring; not only heart

rate monitoring but also further analysis of the QRS complexes.

Khamene and Negahdaripour introduced a different wavelet based method for fECG extraction (Khamene & Negahdaripour 2000). Their method reconstructs the fECG signal based on the singularities obtained from the composite signal, using the modulus maxima locations in the wavelet domain. The modulus maxima locations in the wavelet domain are used to distinguish between mECG and fECG signals. The mother wavelet of their choice was a quadratic spline wavelet. They tried two different approaches. In the first approach, at least one thoracic signal was used to find the maternal modulus maxima locations and this information was used to discard the maternal modulus maxima locations from the composite signal. The remaining modulus maxima locations were assumed to belong to the fECG signal and thus used to reconstruct the fECG signal. In the second approach, only single abdominal signal was used. This approach firstly detects the maternal R waveform modulus maxima location and uses this information to cancel out the maternal R waveform from the composite signal. After this, fECG signal is reconstructed. Both approaches were tested using synthetic and real world signals. Both approaches were able to extract the fECG signal but for approach two the waveform amplitudes were underestimated. However, as approach two only requires the abdominal signal, it would be a good candidate for fetal heart rate (FHR) detection. Another advantage Khamene and Negahdaripour algorithm has is that no data preprocessing is required (for removing baseline wander, 50Hz noise etc.)

2.2.6 Singular Value Decomposition

SVD can be used to separate a signal in to different components. In our case we are interested in finding the components for mECG and fECG. The SVD method can be considered as being a data driven decomposition method; statistical measures are used to find the basis function from the data rather than using a known basis function. One of the main advantages of SVD is that it only requires one abdominal signal which simplifies the hardware requirements.

Ayat et al. used a combination of SVD and polynomial classifiers to extract fECG from the composite signal (Ayat, Assaleh & Nashash 2008). Their algorithm firstly extracted the mECG from the composite signal and fECG would be obtained by subtracting mECG signal from the composite signal. However, the extracted mCG signal cannot be simply

subtracted from the composite signal due to misalignment of the ECG components between the extracted mECG signal and composite signal. Polynomial classifiers are used to align the extracted mECG with the composite signal. A good estimate of the fECG signal was now obtained. They tested the method on synthetic and real world data. Figure 2.10 shows the extracted fECG signal and the R-peaks which are clearly visible in the fECG waveform.

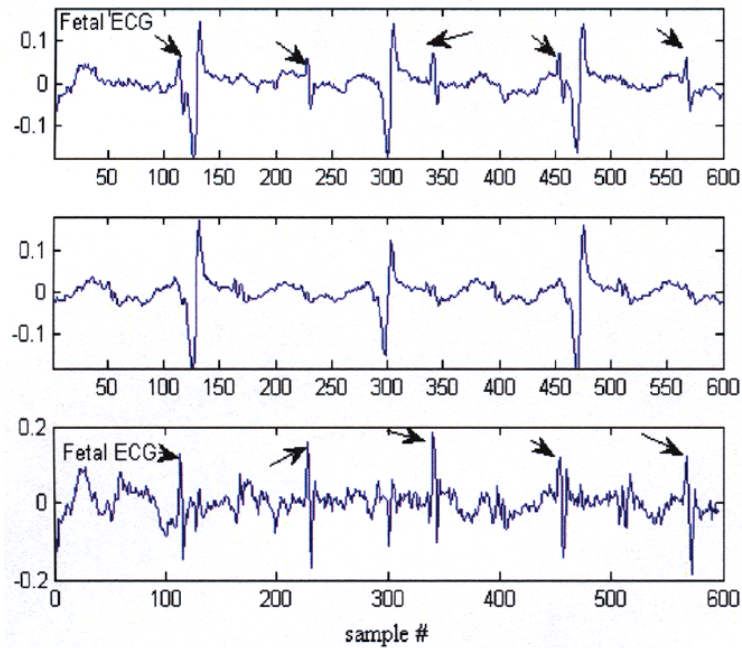


Figure 2.10: Composite signal (top), extracted mECG signal (middle) and extracted fECG signal (bottom). Reproduced from Ayat et al. (2008).

2.2.7 Independent Component Analysis

ICA is a BSS based method. In a BSS based problem, an algorithm is used to recover the original sources from the measured data. For the fECG extraction case, the sources are the mECG, the fECG and the noise. The assumption is that the sources are statistically independent and measured signals from different leads are a linear combination of sources. ICA maximises the statistical interdependencies to find the independent components. ICA requires multiple leads to be used; the higher the number of leads used, the better statistics can be achieved and thus improve the fECG detection.

Some common ICA algorithms which have been used for fECG extraction within the literature are:

- Pearson's algorithm
- Bell and Sejnowski's Infomax algorithm
- Fast ICA algorithm
- Jade algorithm
- Fixed-point algorithm
- Comon's algorithm
- EFICA
- Second Order Blind Identification

Sargam and Sahambi tested Pearson and Bell and Sejnowski's Infomax (Infomax) algorithms for fECG extraction (Sargam & Sahambi 2004). The algorithms were firstly tested on a real world signal set. The signal set was recorded using eight different electrodes; three of them were placed on the thoracic region and five on the abdominal region. Both algorithms were able to extract the fECG signal. However, it was found that the Infomax algorithm took much longer to solve the problem. The algorithms were also tested using synthetic signals. Synthetic signals were produced by mixing mECG, fECG and noise signals together. Two signal sets were produced with varying mECG and fECG amplitude ratios and also a varying amount of noise was added to achieve SNR values from 2 to 10. Signal-to-error ratios (SER) were calculated for different SNR values. Both algorithms returned very similar SER values but again the Infomax algorithm took much longer to solve the problem. From Sargam and Sahambi's work one can conclude that both of these algorithms work well for fECG extraction. However, one might consider using Pearson's algorithm over Infomax algorithm due to lighter computational requirements.

Wan et al. compared Fast ICA and Infomax algorithms (Wan, Liu & Chai 2008). They tested the algorithms on a real world signal set; the signal set was composed from four signals which all contained mECG and fECG signals. Figure 2.11 shows extracted fECG signals for both algorithms. Both algorithms were able to extract the fECG signal; however fastICA algorithm was able to extract the fECG signal significantly faster. No other performance metrics were reported by Wan.

Ananthanag and Sahambi compared four different ICA algorithms for fECG extraction: Jade, Infomax, Fixed-Point and Comon's (Ananthanag & Sahambi 2003). The four algo-

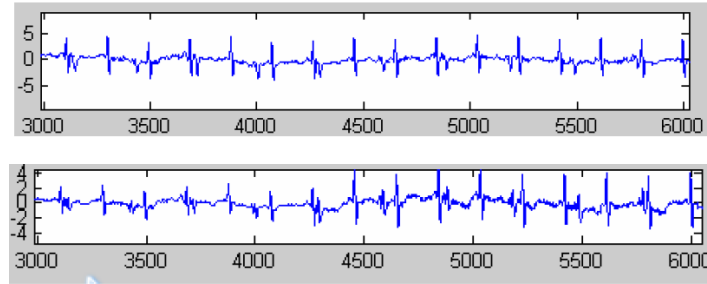


Figure 2.11: Extracted fECG waveform using FastICA algorithm (top) and extracted fECG using Infomax algorithm (bottom). Reproduced from Wan et al. (2008).

gorithms were tested on synthetic signals. SERs were calculated for different SNR values and a number of floating point operations (FLOPS). Table 2.1 shows the results for different SNRs and FLOPS taken to solve the problem. All the algorithms were able to solve the fECG signal from the composite signal. Ananthanag observed that when the SNR value decreased, all the algorithms lost the P and T waves in to the noise but were still able to extract the R wave. This means that the physicians would still be able to use the algorithm for calculating the heart rate. The Jade algorithm took the least FLOPS meaning it was the fastest algorithm to solve the problem. Infomax algorithm took the longest which is in agreement with what Sargam also observed.

Table 2.1: SER values for 5:1 Mat to Fet amplitude ratio (all values are in dB). Reproduced from Ananthang et al. (2003).

	Jade		Infomax		Fixed-Point		Comon's	
SNR	Mat	Fet	Mat	Fet	Mat	Fe1	Mat	Fet
2	2.96	2.63	2.94	2.64	2.96	2.60	2.71	2.23
4	4.67	4.38	4.67	4.37	4.67	4.35	4.35	3.90
6	6.44	6.17	6.43	6.20	6.44	6.11	6.04	5.56
8	8.36	7.97	8.34	8.04	8.35	7.88	7.83	7.17
10	10.29	9.78	10.27	9.67	10.27	9.63	9.57	8.70
FLOPS	193026		316365		17590976		256055	

Taralunga et al. included a pre-filtering step before the ICA algorithm (Taralunga, Ungureanu, Strungaru & Wolf 2011). They used Event Synchronous Cancellor (ESC) algorithm to remove the mECG signal from the composite signal before the ICA algorithm

was run on the data. Their work included testing four different ICA algorithms: FastICA, EFICA (Efficient FastICA), Jade and Second Order Blind Identification (SOBI). Synthetic ECG data was used for testing. Performance metrics included calculating the error between the fECG original signal and the extracted fECG signal. The ICA algorithms were firstly tested without canceling the mECG signal from the composite signal and then on signals where the mECG was filtered out using the ESC algorithm. Combining ESC and ICA provided much improved results. Out of different ICA algorithms, EFICA was the top performing approach.

2.3 fECG Signal Extraction During Multiple Pregnancies

There appears to be somewhat limited literature available for the area of fECG signal extraction during multiple pregnancies. To some degree this makes sense; even though there has been lot of research done for fECG signal extraction during singleton pregnancy, the non-invasive methods have not been able to solve all the signal processing issues and thus the method is not in mainstream use. Multiple pregnancies have the added complexity with two or more fECG signals to be extracted. The main issues are still the same as in the singleton pregnancy case; poor SNR due to mECG signal and other noise sources.

Kam and Cohen investigated fECG extraction during twin pregnancies (Kam & Cohen 2000). They used the BSS method; the ICA JADE algorithm to be more exact. Their initial work included testing with synthetic signals and the first results were very encouraging. However, when the algorithm was tested on real world ECG signals recorded from pregnant women carrying twins or triplets on the 26th-28th week of pregnancy, the algorithm was not able to extract the fECG signals. Further work on synthetic signals with added noise was carried out and it was found that when the SNR was 15dB or more, it was able to extract three ECG signals. The extracted ECG signals can be found from Figure 2.12. When the SNR was less than 15dB, the algorithm was not able to separate between the two fECG signals. In the case of SNR of -20dB, the fECG signals were not exact anymore at all. One of the issues with the work Kam and Cohen did was that they were only simulating a case where only three signal electrodes were used. The JADE algorithm can estimate the same amount of sources as the number of observations points (i.e. input signals). For three signal electrodes, only three sources can be estimated

which is not sufficient if noise is considered as one of the sources. Simulations using more observation points could have improved the results.

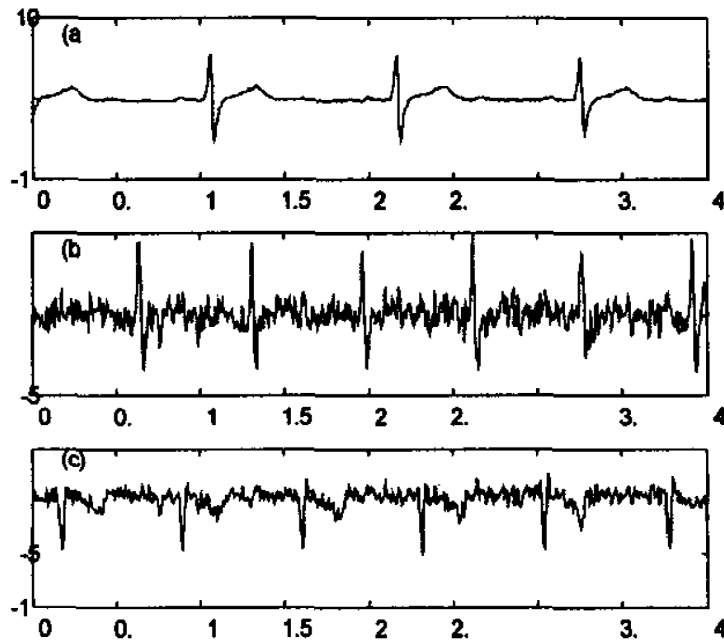


Figure 2.12: Extracted mECG and two fECG signals. Reproduced from Kam et al. (2000).

Fanelli et al. developed a novel algorithm to detect FHR during twin pregnancies (Fanelli, Signorini & Heldt 2012). A synthetic 8-channel signal recording was generated with the assumption that eight electrodes were placed on the mother's abdomen and arranged as vertices of an octagon. This is shown in Figure 2.13. The figure also shows the allowed positions of the fetal signal sources. From the synthetic signal recording, the mECG signal is filtered out from the composite signals using averaging and subtracting processes (Fanelli, Signorini, Ferrario, Perego, Piccini, Andreoni & Magenes 2011). Next the fetal QRS complexes are detected using a template-matching approach and the detected QRS complexes are turned in to a set of binary-time series where 1 represents a converted QRS complex. Figure 2.14 shows an example of the binary series. The separation between different fetuses is based on the assumption that at least one of the electrodes is recording ECG for only one of the fetuses. Figure 2.14 demonstrates that electrodes 6 and 7 are mainly recording ECG for one of the fetuses and that electrodes 2 and 3 are mainly recording ECG for the other fetus. The average sensitivity and accuracy of the algorithm on the synthetic signals were 97.5% and 93.6% respectively. No testing was completed on real world signals. This algorithm can only be used for heart rate detection which is an obvious limitation of the algorithm. Furthermore, the algorithm is not able to recover ECG morphology information.

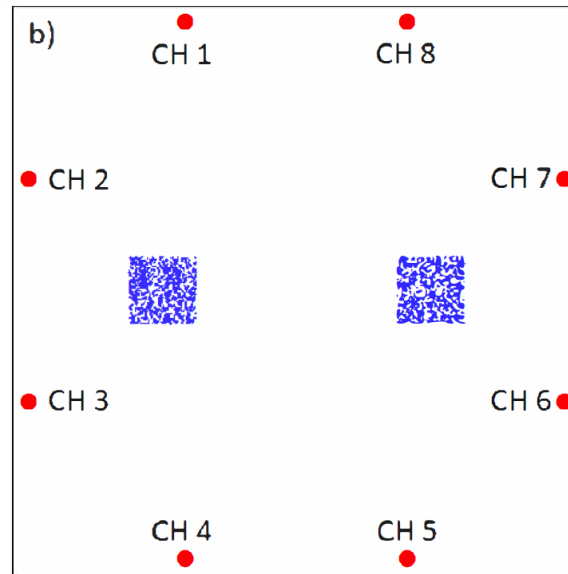


Figure 2.13: Simulated electrode placement and allowed positions of the fetal signal sources. Reproduced from Fanelli et al. (2012).

Sridhar et al. introduced modified FastICA algorithm for fECG signal extraction (Sridhar-Keralapura, Pourfathi & Sirkeci-Mergen 2010). They proposed a new way for obtaining FastICA contrast function by analysing the source data (they called it Data-Centric contrast function). They used synthetic signals to compare their proposed algorithm against typical contrast functions (POW3, Gauss, Tanh, Skew and Pearson) used with FastICA algorithm. They used the Amari distance (PI metric) to evaluate the performance between different contrast functions. Figure 2.15 shows the PI-metric over data acquisition time for different contrast functions where Poly-3, Poly-4, Poly-5 and Poly-6 are the Data-Centric contrast functions. Out of the different Data-Centric contrast functions, the Poly-4 is the best performing one. From the traditional contrast functions, POW3 and Tanh perform very similarly. The algorithm was not tested on real world signals but Sridhar believes that the Data-Centric contrast functions would be more powerful when used in-vivo situations.

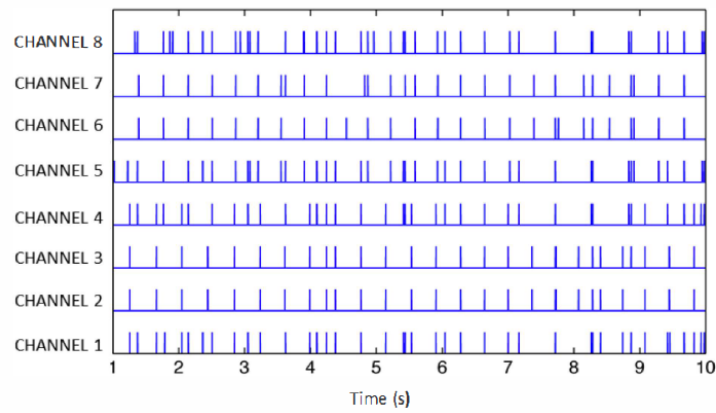


Figure 2.14: Binary series showing detected fetal QRS complexes. Reproduced from Fanelli et al. (2012).

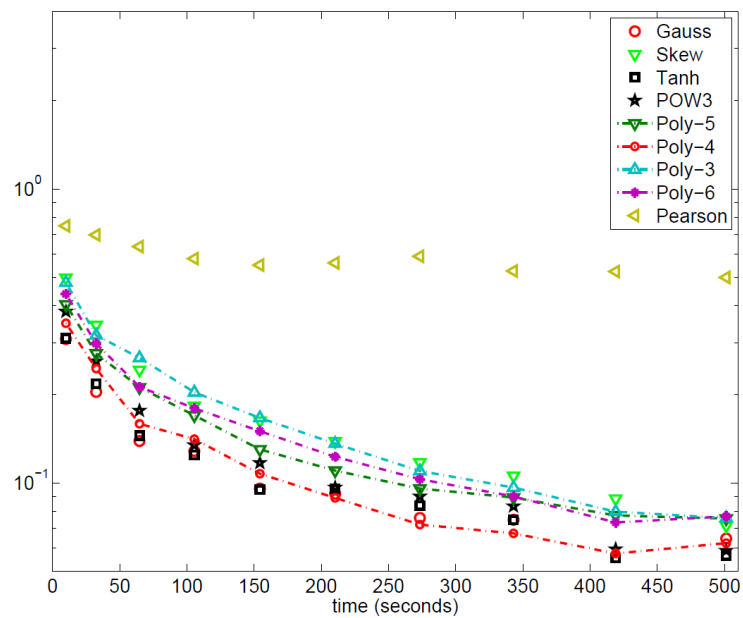


Figure 2.15: PI metric for the different contrast functions. Reproduced from Sridhar et al. (2010).

2.4 fECG Signal Databases

There appears to be at least five fECG signal databases available online. The five databases are:

The DaISy database (De Moor, De Gersem, De Schutter & Favoreel 1997) includes a single 8-channel (five abdominal and three thoracic signals) non-invasive ECG recording. The recording length is 10s using sampling frequency $f_s = 250Hz$

The non-invasive foetal electrocardiogram database (Goldberger, Amaral, Glass, Hausdorff, Ivanov, Mark, Mietus, Moody, Peng & Stanley 2000 (June 13)) available on PhysioNet, includes 55 multichannel (three or four abdominal and two thoracic signals) recordings from a single subject. The recordings were taken at 21-40 weeks gestational age. The recording lengths are variable and sampling frequency is $f_s = 1kHz$.

The abdominal and direct foetal electrocardiogram database (Goldberger et al. 2000 (June 13)) available on PhysioNet, includes recordings from five women in labour (gestational age of 34-41 weeks). The recordings includes four abdominal signals and one signal recorded from the fetus's scalp. The recording lengths are five minutes and sampling frequency is $f_s = 1kHz$.

Noninvasive Fetal ECG: the PhysioNet/Computing in Cardiology Challenge 2013 (Silva et al. 2013) includes 447 one minute recordings from different sources. This dataset was originally put together for a competition run by the PhysioNet to stimulate the development and improvement of non-invasive fECG extraction methods. Even though the competition was run in 2013, the datasets are still available online. The recordings are 4-channel recordings from a mother's abdomen sampled at $f_s = 1kHz$.

Fetal ECG Synthetic Database (Goldberger et al. 2000 (June 13), Andreotti, Behar, Zaunseder, Oster & Clifford 2016) available on PhysioNet, includes 1750 synthetic signals, which equates to 148.5h of data. The simulated recordings have 34 channels (32 abdominal and two mECG signals) with sampling frequency of $f_s = 1kHz$. The recordings include five different noise levels (0, 3, 6, 9 and 12 dB) and also includes simulations of pathophysiological events (fetal movement, change in maternal and fetal heart rate, uterine contraction, ectopic beats and twin pregnancy) dur-

ing pregnancy. The data was generated using *fecgsyn* simulator (Behar, Andreotti, Zaunseder, Li, Oster & Clifford 2014).

Even though there are many real world fECG signal recordings available online, only the Fetal ECG Synthetic Database includes fECG recordings from multiple pregnancies.

2.5 Synthetic fECG Signal Generation Models

The simplest synthetic fECG signals are created by mixing adult ECG signals together. Fanelli et al. used three adult ECG recordings to generate one mECG signal and two fECG signals which were mixed together to generate a synthetic 8-channel abdominal recording (Fanelli et al. 2012). The original ECG signals were sampled at 128Hz. The mECG signal was oversampled to 256Hz and the native sampling frequency was assumed to be 256 Hz; thus the fECG signals had twice the original heart rate. The abdominal signals were generated by putting the three original signals through a mixing matrix which accounts for factors like tissue attenuation and the source distance from the electrode. A similar synthetic fECG signal generation method was used by Kam and Cohen (Kam & Cohen 2000).

Furthermore, the contraction of the myocardium may electrically be considered as a surface of potentials. One of the ways to model this is through the single dipole model. McSharry et al. created a single dipole method to model adult ECG (McSharry, Clifford, Tarassenko & Smith 2003) and Sameni et al. modified McSharry's model to create a method to model fECG signals (Sameni, Clifford, Jutten & Shamsollahi 2007). In Sameni's model, a single dipole per cardiac source can be linearly related to the body surface potentials by a projection matrix that accounts for temporal movements and rotations of the cardiac dipole. Behar et al. updated this model and open sourced it through PhysioNet. Their *fecgsyn* includes a graphical user interface (Alvi, Andreotti, Oster, Zaunseder, Clifford & Behar 2014) and is available at www.physionet.org/physiotools/ipmcode/fecgsyn/.

2.6 Chapter Summary

Several different non-invasive fECG extraction methods for singleton and multiple pregnancies were reviewed in this chapter. Furthermore, this chapter provided necessary information relating to the physiological concepts of fECG required to understand the remainder of this dissertation. The next chapter reviews different ECG data transfer and storage formats. The implementation of the ECG data access MATLAB functions will be discussed and obtained ECG waveforms from the test files will be shown.

Chapter 3

ECG Data Transfer and Storage Formats

One important aspect of fECG signal extraction is the ECG data transfer and storage methods. It appears that there are many different ECG data transfer and storage formats available; this could obstruct the interoperability of ECG between heterogeneous systems and cause critical implementation issues for the healthcare information systems in hospitals and medical organisations.

In this chapter, the four main ECG data storage and transfer formats are introduced. Furthermore, the file structures for the formats which were tested in MATLAB are discussed in detail and the MATLAB implementation and functions required for reading the test files are presented.

3.1 Major Formats

The four main ECG data transfer and storage formats can be found in Table 3.1 as reported by Bond et al., Schlögl and Trigo (Bond, Finlay, Nugent & Moore 2011, Schlögl 2009, Trigo, Alesanco, Martínez & García 2012). These data transfer and storage formats are supported by the Standard Development Organizations (SDOs). There are many other ECG data transfer and storage formats capable of handling ECG data; quasi-standards (EDF/EDF+, GDF, BDF, OpenXDF, VSIR, FEF), XML based (PhililipsXML,

I-Med, ecgML, XML-ECG, ECGaware), databases (WFDB, MIT-BIH, AHA, CSE) etc. In addition, many device manufacturer's have their own proprietary ECG data transfer and storage formats.

Table 3.1: Summary of the most common ECG data transfer and storage formats.

Short Name	Extended name	Standard(s)	References
SCP-ECG / e-SCP-ECG ⁺	Standard Communication Protocol for computer assisted ECG	EN1064:2005, AAMI EC71, ISO 11073-91064:2009	(EN1064:2005+A1:2007 2007, Mandellos et al. 2010)
HL7 aECG	Health Level 7 annotated ECG	ISO/IEEE 11073-10201:2001, ANSI/HL7 V3 ECG, R1-2004 (R2009)	(Brown et al. 2012, Brown & Badilini 2015)
DICOM 30	Digital Imaging and Communication in Medicine Supplement 30	ENV 12052	(<i>DICOM Supplement 30: Waveform Interchange</i> 1999)
MFER	Medical waveform Format Encoding Rules	ISO 92001	(<i>Medical waveform description Format Encoding Rules</i> 2003, ISO22077-1:2015 2015)

It should be mentioned that there are many tools available online that can be used to convert one format to another. These include one way converters:

- SCP-ECG → DICOM (Sakkalis, Chiarugi, Kostomanolakis, Chronaki, Tsiknakis & Orphanoudakis 2003, Ling-Ling, Ni-Ni, Li-Xi & Gang 2006)
- PhilipsXML → HL7 (Helfenbein, Gregg & Zhou 2004)
- BDF → EDF (Biosemi n.d.)
- MIT-BIH → ecgML (Wang, Azuaje, Clifford, Jung & Black 2004)

There are also two-way converters and one-to-many (or many-to-one) converters:

- SCP-ECG \leftrightarrow (GDF) \leftrightarrow HL7 aECG (Schloegl, Chiarugi, Cervesato, Apostolopoulos & Chronaki 2007)
- SCP-ECG \leftrightarrow XML (Jumaa, Fayn & Rubel 2008)
- X73PHD \leftrightarrow SCP-ECG (Trigo, Chiarugi, Alesanco, Martínez-Espronedada, Serrano, Chronaki, Escayola, Martínez & García 2010)
- SCP-ECG + VSIR \rightarrow HL7 aECG (Zywietz, Kraemer, Fischer & Widiger 2004)
- SCP-ECG \rightarrow XML and ASCII (Chiang, Yang, Tzeng, Tseng & Hsieh 2004)
- HL7 aECG and ecgML \rightarrow XML and ASCII (Chiang, Tzeng, Cheng, Lin, Yang, Liang & Lim 2007)
- SCP-ECG, HL7 aECG, MFER, and ECG-9x \leftrightarrow XML-ECG (Lu, Duan & Zheng 2007)

3.2 Detailed Review

The following ECG data transfer and storage formats were tested in MATLAB:

- HL7 aECG
- DICOM supplement 30
- SCP-ECG
- EDF and EDF+
- GDF
- MFER
- ISHNE Holter Standard Output File Format
- WFDB

There are many more ECG data transfer and storage formats available. However, the test files for the formats mentioned earlier were the only ones that could be found online using Google search engine.

3.2.1 HL7 aECG

Health Level-7 Annotated Electrocardiogram (HL7 aECG) data storage format was developed by the not-for-profit standards developing organisation HL7, after the US Food and Drug Administration (FDA) identified a need for a common digital ECG data transfer and storage format. Before the HL7 aECG, FDA received a large number of ECGs in many different formats. Many of them were hard copies of the ECG printout which were manually scanned so that they could be stored digitally. There was also a lack of consistency and accuracy between the different formats when measuring important features (Bond et al. 2011). The HL7 aECG format was accepted as a standard by the ISO/IEEE in 2001 and by the ANSI in 2004.

The HL7 aECG format is encoded in eXtensible Markup Language (XML) (Brown & Badilini 2015). The file markup starts with a root element **AnnotatedECG**. This indicates that the file contains aECG waveforms. The root element is followed by three main elements:

ID - unique identifier (UID) for the particular annotated ECG file.

Code - the **code** has a fixed value of '930000' and the **codeSystem** has a fixed value of '2.16.840.1.113883.6.12'.

effectiveTime - physiological relevant time range assigned to the ECG derived from the findings of the annotated ECG.

An additional **text** element can be used to include supplementary information to the header section of the file. Figure 3.1 shows an example of the HL7 aECG syntax

After the main elements, the aECG file contains information about the clinical trial, patient, trial location, investigator etc. The **series** element contains information about the device used for recording the ECG, the filtering parameters and the ECG waveform. The series element contains the **sequenceSet** element, in which the important ECG

```

<AnnotatedECG>
  <id root="728989ec-b8bc-49cd-9a5a-30be5ade1db5"/>
  <code code="93000" codeSystem="2.16.840.1.113883.6.12"/>
  <text>Annotated ECG for FDA Review</text>
  <effectiveTime>
    <low value="20020510092700"/>
    <high value="20020510092900"/>
  </effectiveTime>
  <confidentialityCode code="B" codeSystem="" displayName="Blinded
to Sponsor and Investigator"/>
  <reasonCode code="PER_PROTOCOL" codeSystem="" />
</AnnotatedECG>

```

Figure 3.1: The HL7 aECG file syntax. Reproduced from Brown et al. (2005).

```

<sequenceSet moodCode="EVN" classCode="OBSCOR">
- <component contextConductionInd="true" typeCode="COMP">
  - <sequence moodCode="EVN" classCode="OBS">
    <code codeSystem="2.16.840.1.113883.6.24" code="TIME_ABSOLUTE"/>
    - <value xsi:type="GLIST_TS">
      <head value="0" unit="s"/>
      <increment value="0.002" unit="s"/>
    </value>
  </sequence>
</component>
- <component contextConductionInd="true" typeCode="COMP">
  - <sequence moodCode="EVN" classCode="OBS">
    <code codeSystemName="MDC" codeSystem="2.16.840.1.113883.6.24" code="MDC_ECG_LEAD_I"/>
    - <value xsi:type="SLIST_PQ">
      <origin value="0" unit="uV"/>
      <scale value="4.76837" unit="uV"/>
      <digits>-6 -7 -7 -7 -6 -6 -6 -6 -7 -8 -12 -21 -27 -33 -37 -38 -33 -24 -12 8 32 66 104 147 192 234 268 :

```

Figure 3.2: The sequenceSet element syntax within the HL7 aECG data storage format.

recording parameters like the sampling frequency (**increment** element; value and unit), the lead name (**code** element), sample offset (**origin** element; value and unit), scaling value (**scale** element; value and unit) are stored. The digitalised sample values (separated by spaces) are also stored within the sequenceSet element (**digits**). The digitalised signal can be converted to actual units (i.e. microvolts) by multiplying the "digits" by the scaling value and adding or subtracting the sample offset. Figure 3.2 shows an example of the sequenceSet part of the HL7 aECG file.

3.2.2 DICOM supplement 30

Initially the Digital Imaging and Communications in Medicine (DICOM) standard was developed as a digital image format for storing, handling and transmitting radiographic images, from medical imaging equipment like Computed Tomography (CT) and Magnetic Resonance Imaging (MRI), and associated metadata between heterogeneous devices like printers, scanners and Picture Archiving and Communication Systems (PACS). DICOM became an European Standard in 1995 (Bond et al. 2011). Even though the DICOM standard was originally developed to only store radiographic images, in the year 1999 DICOM supplement 30 was introduced to support the transfer and storage of raw medical waveforms including blood pressure, audio and ECG signals (*DICOM Supplement 30:*

Waveform Interchange 1999).

DICOM is a binary based storage format. It is also based on an object orientated design principle. What this means is that the information within the DICOM format is categorised into different **Information Objects (IO)**. For example, patient IO would only include information about that object (i.e. patient name, age, gender etc.). Often Entity Relationship (E-R) diagrams are used to guarantee that IOs are designed using the object orientated principles. Figure 3.3 shows an example of the IO relationships within the DICOM format.

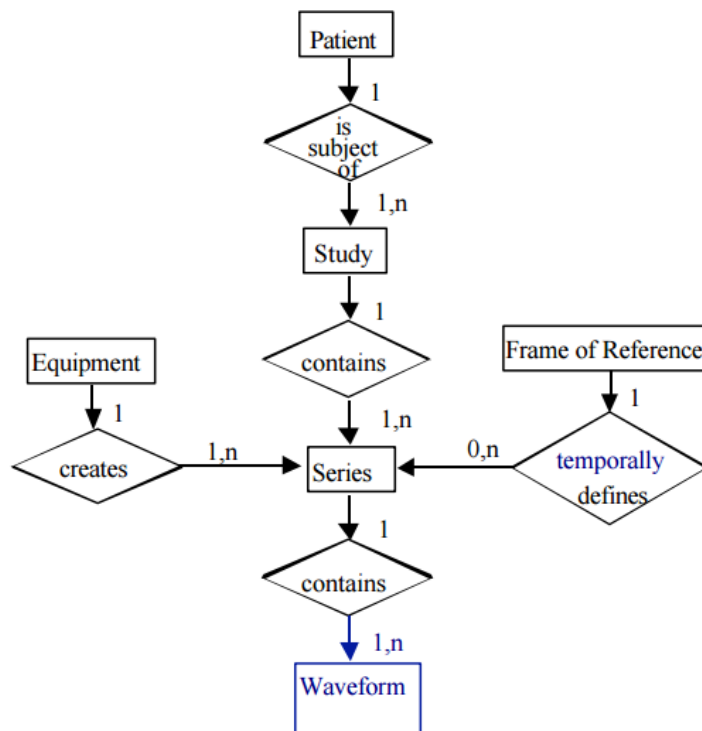


Figure 3.3: Entity Relationship (E-R) diagram for DICOM. The E-R displays the relationships between the different Information Objects (IOs). Reproduced from DICOM supplement 30 (1999).

The Waveform IO includes attributes which are associated with the medical waveform dataset. Furthermore, any particular IO and the attributes within the IO, have a 16-bit unsigned integer tag assigned to them. The tags are stored using hexadecimal notation. Table 3.2 shows the fundamental attributes which are associated with the ECG Waveform IO and the hexadecimal tags associated with the different attributes. The tags are used to access a particular attribute.

Table 3.2: DICOM ECG Waveform IO Attributes, the associated hexadecimal tag and the description for the tag. Adapted from DICOM supplement 30 (1999).

Attribute	Tag	Description
Waveform Sequence	(5400,0100)	Number of waveform items; value between 1 and 5.
Waveform Originality	003A,0004)	Enumerated values; ORIGINAL or DERIVED.
Number of Channels	(003A,0004)	Number of waveform channels included in this recording.
Number of Samples	(003A,0010)	Number of waveform samples per channel.
Sampling Frequency	(003A,001A)	Sampling frequency in Hz.
Waveform Bits Allocated	(5400,1004)	Number of bits used to store one sample; either 8 or 16.
Waveform Sample Interpretation	(5400,1006)	Specifies the data representation of each waveform sample; i.e. SS (signed 16-bit linear).
Waveform Data	(5400,1010)	Encoded waveform samples.

3.2.3 SCP-ECG

Standard communications protocol for computer assisted electrocardiography (SCP-ECG) standard was developed from the early 90s as a collaboration between the international medical community. Manufacturers, physicians and end users from Europe, America and Asia worked together to create a digital standard for sharing ECGs. SPC-ECG became an European standard in 1993 and in 2001 was also accepted by AAMI. In 2002, the openECG project was formed to aid the introduction of the SPC-ECG format to all stakeholders. The openECG community promoted the standard, based on the experience and vision of early adopters, by means of specific proposals like implementation guides, the supply of content and format checking conformance tools and also supply open source SCP-ECG software under the General Public License (GNU). In 2009, SCP-ECG was approved as ISO standard (ISO11073-91064:2009) (Trigo et al. 2012). In 2008, Mandellos et al. suggested enhanced SCP-ECG format called, e-SCP-ECG+ (Mandellos, Koukias & Lymberopoulos 2008). The proposed protocol is able to handle more vital signs and demographic data.

SPC-ECG is a binary based format. The file starts with a two byte checksum to ensure that the file is not corrupted and has been transferred or read correctly. The next four bytes are used to retain the actual size of the entire file in bytes. Next comes 11 sections of which two are mandatory. The exact structure for the SCP-ECG file can be found in Figure 3.4.

The first 16 bytes for each section includes the section header ID. The section header structure is shown in Table 3.3. The Section 0 can be considered as the directory of the file; it includes the starting byte and length in bytes for each of the following sections included in the file. Section 1 has information about the patient and the device used for recording. Section 2 defines how the ECG data has been encoded. Section 3 defines the ECG leads which have been used for recording; each lead is identified using a numbering system, i.e. number 3 represents lead V1. Section 4 stores the QSR locations and Section 5 stores the reference beat data. Section 6 stores the raw ECG data. Section 7 contains ECG measurements like such as QRS axis, P onset, P offset etc. Section 8 includes textual diagnosis that has been produced by the “interpretive” algorithm. Section 9 stores manufacturer specific diagnostic information. Section 10 includes data from the leads like QRS duration, Q wave peak value etc. Section 11 stores universal statement

codes and over reading data. Manufactures can include their own sections as long as they use section numbers from 128 to 1023 (Bond et al. 2011).

Table 3.3: Section header ID for the SCP-ECG file. The section header ID is included in the first 16 bytes of every section. Adapted from Fischer et al. (2006).

Section ID header structure						
CRC	Section ID	Length in bytes	Section version	Protocol version	Reserved	
2 bytes	2 bytes	4 bytes	1 byte	1 byte	6 bytes	

3.2.4 EDF and EDF+

European Data Format Plus (EDF+) is a medical signal transfer and storage format which is based on its predecessor's format, the European Data Format (EDF). The EDF format was developed in the early 90s for the exchange and storages of polygraphic signals (Kemp, Värri, Rosa, Nielsen & Gade 1992). The implementation of the EDF is simple

Mandatory	2 BYTES - CHECKSUM - CRC - CCITT OVER THE ENTIRE RECORD (EXCLUDING THIS WORD)
Mandatory	4 BYTES - (UNSIGNED) SIZE OF THE ENTIRE ECG RECORD (IN BYTES)
Mandatory	(Section 0) POINTERS TO DATA AREAS IN THE RECORD
Mandatory	(Section 1) HEADER INFORMATION - PATIENT DATA/ECG ACQUISITION DATA
Optional	(Section 2) HUFFMAN TABLES USED IN ENCODING OF ECG DATA (IF USED)
Optional	(Section 3) ECG LEAD DEFINITION
Optional	(Section 4) QRS LOCATIONS (IF REFERENCE BEATS ARE ENCODED)
Optional	(Section 5) ENCODED REFERENCE BEAT DATA IF REFERENCE BEATS ARE STORED
Optional	(Section 6) "RESIDUAL SIGNAL" AFTER REFERENCE BEAT SUBTRACTION IF REFERENCE BEATS ARE STORED, OTHERWISE ENCODED RHYTHM DATA
Optional	(Section 7) GLOBAL MEASUREMENTS
Optional	(Section 8) TEXTUAL DIAGNOSIS FROM THE "INTERPRETIVE" DEVICE
Optional	(Section 9) MANUFACTURER SPECIFIC DIAGNOSTIC AND OVERREADING DATA FROM THE "INTERPRETIVE" DEVICE
Optional	(Section 10) LEAD MEASUREMENT RESULTS
Optional	(Section 11) UNIVERSAL STATEMENT CODES RESULTING FROM THE INTERPRETATION

Figure 3.4: The SCP-ECG file structure. Reproduced from Fischer et al. (2006).

and it supports multiple sampling rates and scaling factors. An EDF file consists of a header section followed by a data section. The header section identifies the patient and has important information about the technical aspects of the digitalised recorded signal. The header section consists of 256 bytes of general information like the format version, the patient and the recording identification, time information of the recording, the number of data records and the number of signals in each recording. This is followed by 256 bytes of information for each signal specifying the type of signal (EEG, body temperature etc.), the gain and number of samples in the each data record. Because each signal is separately defined in the header section, this allows the use of different sampling frequencies and gains. The information in the header section is coded using ASCII strings as shown in Figure 3.5a.

In the data section, each signal is a series of 2-byte samples representing digitalised integer values of that signal. The time duration of the recording and the number of samples recorded (i.e. sampling frequency) is specified in the header sections. Figure 3.5b describes the data section of the EDF file.

8 ascii : version of this data format (0)
80 ascii : local patient identification
80 ascii : local recording identification
8 ascii : startdate of recording (dd.mm.yy)
8 ascii : starttime of recording (hh.mm.ss)
8 ascii : number of bytes in header record
44 ascii : reserved
8 ascii : number of data records (-1 if unknown)
8 ascii : duration of a data record, in seconds
4 ascii : number of signals (ns) in data record
ns * 16 ascii : ns * label (e.g. EEG FpzCz or Body temp)
ns * 80 ascii : ns * transducer type (e.g. AgAgCl electrode)
ns * 8 ascii : ns * physical dimension (e.g. μ V or degreeC)
ns * 8 ascii : ns * physical minimum (e.g. -500 or 34)
ns * 8 ascii : ns * physical maximum (e.g. 500 or 40)
ns * 8 ascii : ns * digital minimum (e.g. -2048)
ns * 8 ascii : ns * digital maximum (e.g. 2047)
ns * 80 ascii : ns * prefiltering (e.g. HP:0.1Hz LP:75Hz)
ns * 8 ascii : ns * nr of samples in each data record
ns * 32 ascii : ns * reserved

nr of samples[1] * integer : first signal in the data record
nr of samples[2] * integer : second signal
..
..
nr of samples[ns] * integer : last signal

(a) EDF file header section

(b) EDF file data section

Figure 3.5: The figure shows the EDF file header and data sections. In the header section, the information is coded using ASCII characters. In the data section, the digitalised sample values are stored as a series of 16-bit integers. If the recording consists of multiple signals, the signals are stored in series. Reproduced from Kemp et al. (1992).

The EDF+ was developed to overcome some of the limitations of the EDF; the main ones being that the EDF does not support annotations and non-continuous signals. Quite

often during ElectroNeurography and Evoked Potentials (ENMGEP) studies, there is a requirement to record data discontinuously. The EDF+ allows interrupted recording but keeps all other specifications of the EDF. This way, the EDF+ file can still be read using old EDF software (the discontinuous signal just appears continuous). The EDF+ storage format was published in 2003 by Kemp et al. (Kemp & Olivan 2003).

The header section is used to distinguish between EDF and EDF+ files. More specifically, in the header section of the EDF+ file, the first reserved field (7th field in the header) must start with *EDF+ C* if the recording is uninterrupted and thus having a contiguous recording. If the recording is interrupted (non-contiguous), the first reserved field must start with *EDF+ D*. In the EDF file, the first reserved field can be left blank (filled with ‘spaces’). Another difference between EDF and EDF+ files are the additional header specifications for the EDF+ files. It was found that for the EDF, some of the definitions were rather loose and thus needed clarification.

3.2.5 GDF

General Data Format (GDF) is a biomedical signal transfer and storage format which was developed as part of the BioSig software project (Schlögl & Brunner 2008). The BioSig is an open-source software library of biomedical signal processing tools and currently supports approximately 50 different biomedical data formats. The GDF version 1.00, was released in 2005. The current GDF version is 2.51 (Schlögl 2006, Schlögl 2013).

The GDF was originally developed to overcome some of the limitations in the EDF format; the following limitations were address in the GDF¹:

1. In the EDF, the physical minimum and maximum values of the signal signals are stored in to a 8*ASCII field. This can cause rounding errors, especially with pre-processed data.
2. The EDF uses 16-bit integer to store the sample value. This can cause loss of accuracy, especially with floating point numbers.
3. The EDF does not have automatic overflow detection.

¹it should be mentioned that EDF+ does address some of these limitations.

4. In the EDF header, the year part of the date information is stored using two digits. This can possibly cause issues with the year 2000 (“the Y2K problem”).
5. The maximum number of samples the EDF can store is 31,200 (or 62,400 bytes).
6. The EDF provides no support for the quality management of recorded data.
7. Event information cannot be stored in the EDF.

The GDF file consists of the following five components: fixed header of 256 bytes, channel specific information of 256 bytes per channel, optional header which has variable length, data section and the table of events. The structure is similar to EDF and EDF+ but GDF is more flexible; for example, GDF allows the storage of the biomedical signal in many different data formats (int, uint, float etc.). The full specification can be found from Schlgl 2013.

3.2.6 MFER

Medical waveform description Format Encoding Rules (MFER) was launched in 2002 and became an ISO standard in 2007. The MFER is supported by the Japanese Association of Healthcare Information Systems industry (JAHIS). MFER specialises in encoding the medical waveforms (ECG, EEG and respiratory waveforms) and the MFER standard actually recommends using other formats like, HL7 or DICOM, for encoding the information other than the medical waveforms (Trigo et al. 2012).

MFER is a binary based format and the file format can be broken down to **frames**, **data blocks**, **channels** and **sequences** as described in Figure 3.6. Furthermore, the frame consists of **header** and **waveform data** blocks. The header block describes the sampling conditions (sampling rate, etc.), the frame alignment and other related information. The header block can be further broken down to descriptors and to root definition. The root definition covers all the information for encodings for the relevant channels (*Medical waveform description Format Encoding Rules* 2003). Figure 3.7 shows the breakdown of the frame header.

Figure 3.8 describes the alignment of the the data values within the waveform data block. In this example, one data block consist of five sample data values. If each value is encoded to a 16-bit integer (two bytes), one data block requires 10 bytes of memory. The number

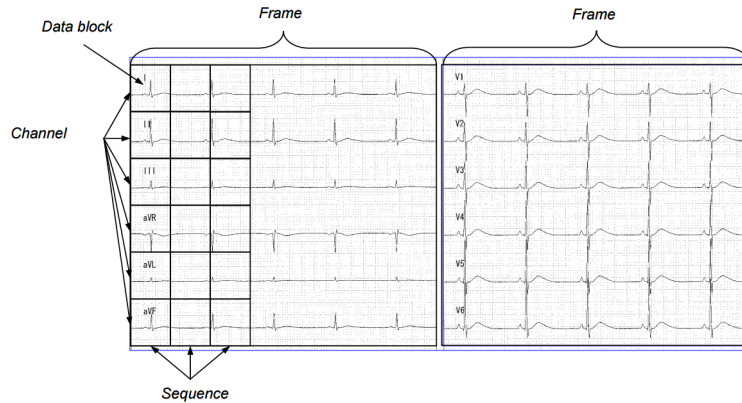


Figure 3.6: The figure shows the MFER frame attributes. Frame is a waveform encoding unit consisting of data blocks, channels and sequences. Reproduced from Medical waveform description Format Encoding Rules (2003).

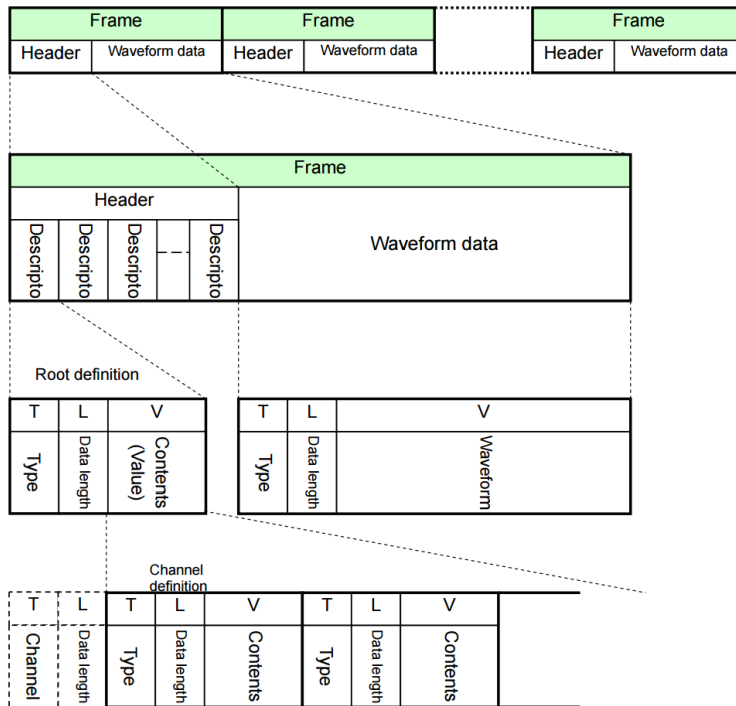


Figure 3.7: MFER frame header breaks down to descriptors which includes the root definitions. A root definitions includes all the encoding rules for the relevant channel. Reproduced from Medical waveform description Format Encoding Rules (2003).

of channels is three and thus, one sequence consists of 10 bytes of data from each channel which equates to 30 bytes in one sequence. The successive sequences come one after another until the end of the frame (as defined in the header section) (*Medical waveform description Format Encoding Rules 2003*).

The information in the header and data blocks are encoded with **TLV** (type, length and

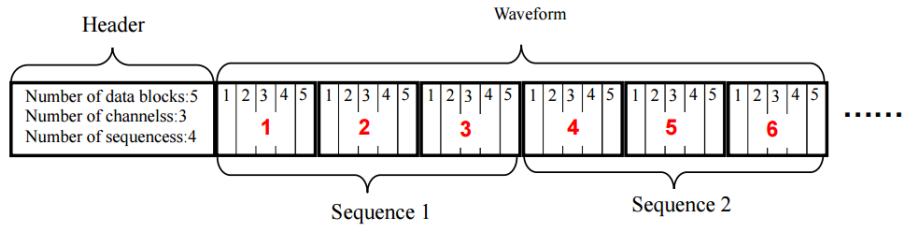


Figure 3.8: MFER data blocks are aligned sequentially by the channel number (channel1, channel2 etc.). The number of sequences within the frame is defined in the header section. Reproduced from Medical waveform description Format Encoding Rules (2003).

value). The type (or the tag) indicates the attributes for the data values and consists of one or more bytes. The length indicates the length of the data values in bytes and the values contains the actual content (i.e. waveform data) of the attribute identified by the tag. The tag structure is shown in Figure 3.9. The two most significant bits define the class or the attributes definition level; either Level 1, Level 2 or Level 3. Level 1 covers the basic definitions (ordinary rules and rules for precise encoding). Level 2 is for supplementary definitions and Level 3 for extended definitions. The primitive/context (P/C) bit is used for channel definition attributes for any particular channel. The root definition can be used to define attributes for all the channels; however channel definitions can be used to override the root definition for a specific channel. The five least significant bits defines the tag number. For example, sampling rate can be defined using tag number 0Bh (01011b) (*Medical waveform description Format Encoding Rules* 2003).

8		7		6		5		4		3		2		1	
Class		P/C		Tag Number											
0	0	0		Level 1											
		1													
0	1	Level 2													
1	0	Level 3													
1	1	Private													

Figure 3.9: MFER information is encoded with TLV (type, length and value). The type, or the tag, definitives the attributes of the data value. The tag is composed of class, primitive/context (P/C) and tag number. Reproduced from Medical waveform description Format Encoding Rules (2003).

3.2.7 ISHNE Holter Standard Output File Format

For decades, Holter devices (portable ECG recorders) used analogue tapes to record the ECG data. The analogue format enabled easy exchange of data between different Holter systems (Zareba, Locati & Blanche 1998). It was found that the early digital Holter systems did not offer a similar sort of flexibility which was seen as a restriction and impeded collaboration between clinical and research groups. In 1997, the International Society of Holter and Noninvasive Electrocadiology (ISHNE) developed the ISHNE Holter Standard Output File Format task force. The task force's main objective was to initiate the standardization of the Holter ECG recordings. The idea was received very well by the Holter manufacturers and many of them joined the task force.

Badilini defined the output file format in 1998 (Badilini et al. 1998). The file format consists of a header block and a data block. The first eight bytes of the file consist of a string of eight characters 'ISHNE1.0'. This allows the verification that the file is in ISHNE format. This is followed by a two byte checksum. The header will start at the 11th byte of the file and consists of a fixed size (512 bytes) header and variable size header. The fixed header defines the main characteristics of the study (patient information, date, time etc.) and the signal(s) (number of leads, sampling frequency etc.). The variable size header consists of a stream of ASCII characters that can be used by the manufacturer according to their needs. The file format does not record beat annotations. The fixed header section is shown in Figure 3.10.

The ECG data is stored as a 16-bit signed integer over two bytes. The two byte samples are stored in little-endian form (least significant byte first). The digital values can range from -32768 to 32767 and the dynamic range can be calculated from the resolution value which is specified in the header section.

3.2.8 WFDB

PhysioNet has a large collection of recorded physiological signals (PhysioBank) and offers open-source software for reading and analysis of these signals (PhysioToolkit) (Goldberger et al. 2000 (June 13)). The signals in the PhysioBank databases are stored in the Waveform Database (WFDB) format which contains two standard categories; European Data Format (EDF) and MIT format.

Size (in bytes) of variable length block	long int	4
Size (in samples) of ECG	long int	4
Offset of variable length block (in bytes from beginning of file, i.e., $8 + 2 + 512 = 522$)	long int	4
Offset of ECG block (in bytes from beginning of file)	long int	4
Version of the file	short int	2
Subject First Name	char[40]	40
Subject Last Name	char[40]	40
Subject ID	char[20]	20
Subject Sex (0: unknown, 1: male, 2: female)	short int	2
Race (0: unknown, 1: Caucasian, 2: Black, 3: Oriental, 4–9 Reserved)	short int	2
Date of Birth (European: day, month, year)	3 short int	6
Date of recording (European)	3 short int	6
Date of creation of Output file (European)	3 short int	6
Start time (European: hour [0–23], min, sec)	3 short int	6
Number of stored leads	short int	2
Lead specification (see included Table)	12 short int	24
Lead quality (see included Table)	12 short int	24
Amplitude resolution in integer no. of nV	12 short int	24
Pacemaker code (see text for description)	short int	2
Type of recorder (either analog or digital)	char[40]	40
Sampling rate (in hertz)	short int	2
Proprietary of ECG (if any)	char[80]	80
Copyright and restriction of diffusion (if any)	char[80]	80
Reserved	char[88]	88

Figure 3.10: ISHNE fixed header defines the important attributes about the file, patient and the recorded ECG signal. Reproduced from Badilini (2008).

The MIT format consists of three files: Header file (.hea), signal file (.dat) and annotations file (.atr). The header file is a text file coded using ASCII characters and includes all the important attributes for the signal file. The different attributes are separated by a space and comments can be included using the ‘hashtag’ (#) character. The header file contains two sections: a record section and a signal specification section. The two different sections are separated by placing them in to different lines using the ASCII linefeed character. The record section (or the record line) includes attributes like the record name, number of signals, sampling frequency etc. In the signal specification section, the different signals are separated in to different lines (signal specification lines). For example, for a 12-lead ECG recording, the signal specification section would have 12 lines of text describing the signal attributes like the file name, the format, ADC gain etc. Figure 3.11 shows an example ECG header file from the MIT-BIH Arrhythmia Database record 100.

```

100 2 360 650000 0:0:0 0/0/0
100.dat 212 200 11 1024 995 -22131 0 MLII
100.dat 212 200 11 1024 1011 20052 0 V5

# 69 M 1085 1629 x1
# Aldomet, Inderal

```

Figure 3.11: Example WFDB header file.

The signal file is a binary file containing the digitised signal samples in the format specified in the header file. The annotations file is a binary file containing the locations of the annotation locations for the specific signal (i.e. ECG signal file could have the corresponding QRS locations in the annotations file).

3.3 MATLAB Implementation

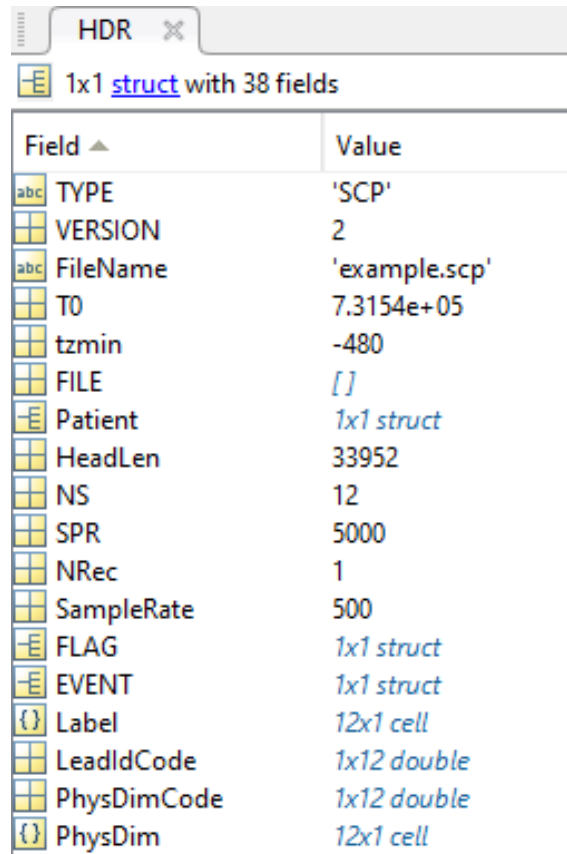
The BIOSIG MATLAB toolbox ² provides necessary functions for accessing most of the different ECG data files; more specifically **mexSOPEN** and **mexSREAD** are the two functions required for reading ECG files. The only exception to the rule is the DICOM ECG files; **mexSOPEN** and **mexSREAD** do not currently support the DICOM ECG files. However, the MATLAB native function **dicominfo** can be used to read DICOM files, including files containing ECG waveforms.

The **mexSOPEN** function call reads the header information from the ECG file. The function call requires two input parameters; file name (i.e. 'aECG.xml') and permissions ('r' for reading from the file or 'w' for writing in to the file). The output from the function call is a structure array which includes all the important information about the patient (i.e. name, sex, age etc.) and the digitalised signal samples (sampling frequency, number of channels etc.). The header structure contains a lot of information. However, for the purpose of creating a waveform plot in MATLAB, the only relevant parameters are **SampleRate**, **NS** (number of signals), **SPR** (number of samples per signal) and **Cal** (multiplier for converting the sample values to physical units as specified in the **PhysDim** field). The relative time array values (starting from zero seconds) can be calculated using the sampling frequency and the number of samples per signal (i.e. $t=0:1/fs:sps/fs$, where fs is sampling frequency and sps is number of samples per signal). The header structure for the SPC-ECG file can be found from Figure 3.12.

mexSREAD function is used to read the actual digitalised sample values. The function call only requires the file name as an input variable and the output is an array matrix of the digitalised signal. Different channels are stored in to different columns (channel 1 samples are stored in to column 1, channel 2 samples are stored in to column 2 etc.).

The **dicominfo** function reads the header information from the DICOM file. The func-

²available: <http://biosig.sourceforge.net/>



Field	Value
TYPE	'SCP'
VERSION	2
FileName	'example.scp'
T0	7.3154e+05
tzmin	-480
FILE	[]
Patient	1x1 struct
HeadLen	33952
NS	12
SPR	5000
NRec	1
SampleRate	500
FLAG	1x1 struct
EVENT	1x1 struct
Label	12x1 cell
LeadIdCode	1x12 double
PhysDimCode	1x12 double
PhysDim	12x1 cell

Figure 3.12: Extracted SPC-ECG file in MATLAB. The header structure contains all the important attributes for creating a meaningful waveform from the digitalised signal.

tion call requires the file name as the only input variable. The output from the function call is a structure array which includes all the important information about the patient (i.e. name, sex, age etc.) and the digitalised signal file (sampling frequency, number of channels etc.). The waveform data and associated attributes are stored in to the WaveformSequence structure. Within the WaveformSequence structure, the digitalised sample values are stored in the WaveformData vector. The WaveformData vector is a continuous stream of sample values (channel 1 followed by channel 2 etc.). The sample values are encoded as specified by the WaveformSampleInterpretation field. For example, if the WaveformSampleInterpretation field has characters **SS**, this would mean the waveform samples are encoded to a right justified signed 16-bit integer. The NumberOfWaveformChannels field specifies how many channels the recording includes and the NumberOfWaveformSamples field specifies how many samples per channel are included in the recording. The NumberOfWaveformChannels and NumberOfWaveformSamples fields can be used to breakdown the WaveformData vector in to individual channels.

The test signals for testing the ECG data transfer and storage methods were sourced

online. Google Search Engine was the main method used for acquiring the test signals. Table 3.4 summarises the test signals and the source they were downloaded from.

Table 3.4: Summary of the test files which were used to test the ECG data access MATLAB functions.

Format	The online source	Hyperlink
HL 7 aECG	Chinese Cardiovascular Disease Database (CCDD)	http://58.210.56.164:88/resource_en.jsp
	National Electrical Manufactures Association (NEMA)	ftp://medical.nema.org/medical/dicom/DataSets/WG02/Enhanced-XA/
SPC-ECG	C# ECG Toolkit	http://en.osdn.jp/frs/g_redirect.php?m=kent&f=%2Fecgtoolkit-cs%2Fecgtoolkit-cs-2_0%2Fexamples.zip
EDF	Physionet	https://physionet.org/physiobank/database/nifecgdb/
GDF	BioSig	http://pub.ist.ac.at/~schloegl/biosig/GDF2.0/gdf2test.gdf
MFER	Medical Waveform Format Encoding Rules	http://www.mfer.org/en/downloads/
ISHNE	University of Rochester Medical Centre	http://thew-project.org/THEWFileFormat.htm
WFDB	Physionet	https://physionet.org/physiobank/database/ecgidb/Person_01/

3.4 Test File ECG Waveforms

Figure 3.13 shows the extracted waveforms from the test signal files. When the test signal had two or more signals available, two signals were displayed. The DICOM test signal file only had one waveform. Furthermore, the DICOM header file did not include the Channel Definition Sequence IO which includes the attributes for converting the digitalised signal into physical values. Thus, the raw sample values were plotted. In addition, the GDF test file did not include actual ECG signal; the file included a synthetic sawtooth waveform.

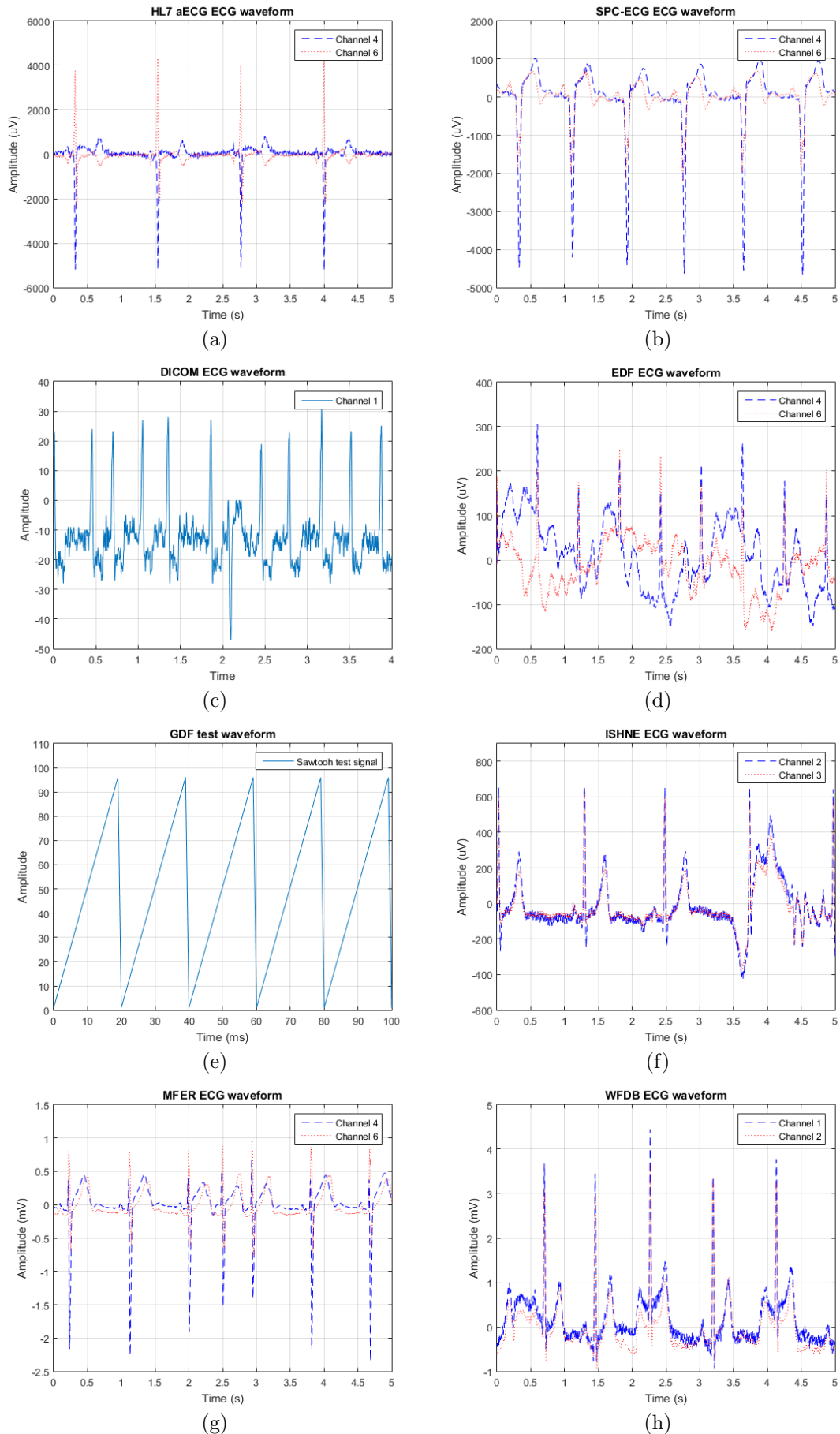


Figure 3.13: Extracted ECG waveforms from the test files: (a) HL7 aECG, (b) SPC-ECG, (c) DICOM, (d) EDF+, (e) GDF, (f) ISHNE, (g) MFER and (h) WFDB.

3.5 Chapter Summary

In this chapter, common ECG data transfer and storage formats were introduced. There are many different formats available and this can cause compatibility issues between different systems in medical organisations. Several different formats are supported by SDOs; these formats are currently the main formats used in the medical industry. The BIOSIG MATLAB Toolbox provides functions for reading many different ECG file formats. Several waveform examples from different ECG file formats were provided in the previous section.

In the next chapter, the different fetal ECG extraction methods and other aspects of fECG extraction used in this dissertation are introduced and discussed in detail.

Chapter 4

Fetal ECG Signal Extraction Methods

In this chapter, the methods and resources used for the fECG signals extraction are discussed in detail. The five main aspects which had to be considered are:

- Test signal
- Preprocessing of the test signals
- Extraction methods
- fQRS detection
- Performance metrics

The items mentioned above are discussed in more detail in the following sections.

4.1 Test Signal

After exhaustive research of the ECG signal databases available online, Physionet's Fetal ECG Synthetic Database (FECGSYNDB)¹ was selected to be used to obtain the composite test signals (Andreotti et al. 2016, Goldberger et al. 2000 (June 13)). This database

¹Available at: <https://physionet.org/physiobank/database/fecgsyndb>

was generated using the FECGSYN fECG signal generator (Behar, Andreotti, Zaunseder, Li, Oster & Clifford 2014).

There are several reasons why the test signals from this online database were selected. Firstly, the FECGSYNDB includes ten different simulated pregnancies and for each pregnancy, seven different physiological events (cases) were simulated. The simulated physiological events can be found in Table 4.1. The physiological cases simulate typical non-stationary events seen on real world fECG signals and thus are critical for evaluating the different fECG extraction methods.

Table 4.1: Simulated physiological events

Case	Description
Baseline	Abdominal mixture (no noise events)
Case 0	Baseline (no events) + noise
Case 1	Foetal movement + noise
Case 2	MHR /FHR acceleration / decelerations + noise
Case 3	Uterine contraction) + noise
Case 4	Ectopic beats (for both foetus and mother) + noise
Case 5	Additional NI-FECG (twin pregnancy) + noise

Furthermore, the recordings include five different fECG SNR levels (0, 3, 6, 9, and 12 dB). Each simulation has been repeated five times. This computes to 1750 synthetic ECG signals. The recording lengths are five minutes with sampling frequency of 250Hz. Each recording includes 34 channels (32 abdominal and two mECG reference channels). Both, the mQRS and fQRS annotation locations are also included. The test signal was arbitrarily selected to be from subject three and repeat three.

To understand how the number of abdominal channels affect the performance of the fECG signal extraction algorithms, each extraction algorithm was tested using 2, 4, 6, 8, 10, 15, 20 and 30 abdominal channels. The abdominal channels were arbitrarily selected, however as the number of channels increased, the channels from the previous tests were maintained. The reason for this was to avoid the results being effected by the quality of the signal of the individual channels. The selected abdominal channels can be found in Table 4.2. Figure 4.1 shows the volume conductor and the electrode configuration in reference to the locations of the maternal and fetal hearts. For AM, channels 33 and 34 were used as reference mECG channels.

Table 4.2: Selected abdominal channel combinations.

No channels	Combination
2	2,29
4	2,6,17,29
6	2,6,11,17,22,29,31
8	2,6,9,11,17,22,29,31
10	2,6,9,11,14,17,22,25,29,31
15	2,4,6,9,11,14,15,17,22,24,25,27,29,30,31
20	2,4,6,8,9,11,13,14,15,16,17,19,22,24,25,27,29,30,31,32
30	1,2,3,4,5,6,7,8,9,11,12,13,14,15,16,17,18,19,20,21,22,23,24,25,26,27,29,30,31,32

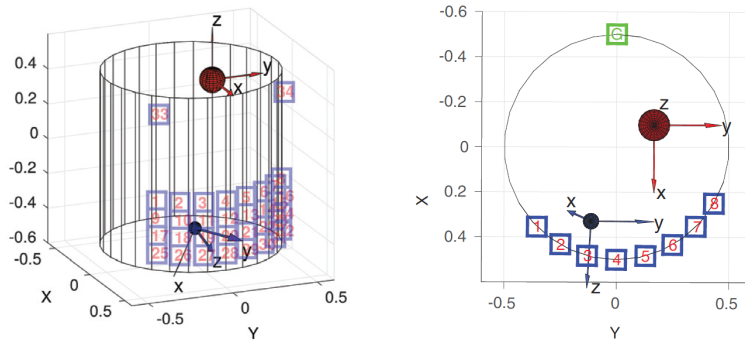


Figure 4.1: Side and upper view of the simulated electrode positions. Positions of fetal (blue sphere) and maternal (red sphere) hearts are also shown. Reproduced from Behar et al. (2014).

The FECGSYNDB provides the maternal, fetal and noise signals as separate sources (i.e. the database provides separate waveform files for each signal source). Thus, to create the required composite signal, the different source signals need to be mixed together.

4.2 Test Signal Preprocessing

The test signal was preprocessed through low pass and high pass filters so that the high frequency noise and the baseline wander were removed from the composite signal. The 3rd and 5th order Butterworth filters were used as the high pass and low pass filters respectively. The MATLAB native function Zero-phase digital filter (`filtfilt.m`) was used for filtering the signal.

Figure 4.2 shows the power spectrum for typical ECG signal components in the frequency domain. The fetal QRS band is roughly in range of 10 Hz-15 Hz. Furthermore, Behar et al. completed a comprehensive study on how the different filter cut-off frequencies affect the fECG extraction algorithm performance (Behar, Oster & Clifford 2014). They found low frequency and high frequency cut-off frequencies of 10Hz and 99Hz respectively provided the best results. These values were adapted for this project as well. It should be mentioned that, when low frequency cut-off of 10Hz is used, the mECG and the fECG P and T waves are suppressed. For this project this is not an issue, however if morphological analysis was of interest, lower high pass filter cut-off frequency would need to be used to preserve the fetal P and T waves. Kligfield et al. recommends using cut-off frequency in the range of 0.05 Hz - 0.67 Hz in order to preserve the P and T waves (Kligfield, Gettes, Bailey, Childers, Deal, Hancock, van Herpen, Kors, Macfarlane, Mirvis et al. 2007). Figure 4.3 shows the effect of the different low frequency cut-off values.

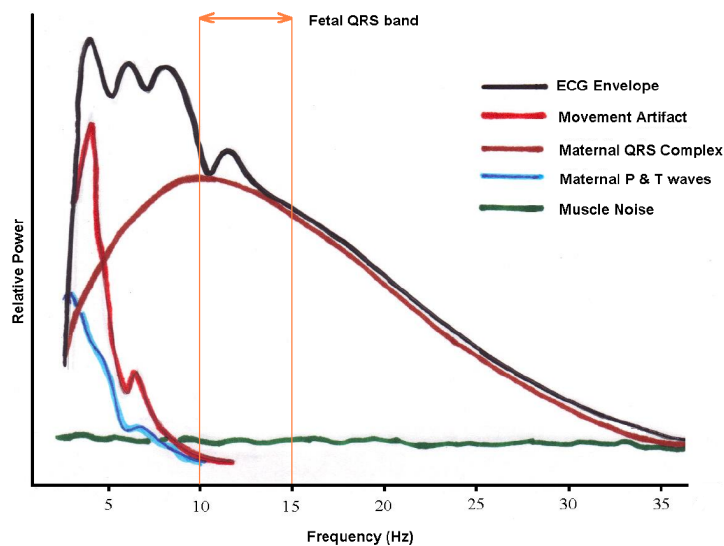


Figure 4.2: The relative power spectrum of the typical ECG signal components presented in the frequency domain. The fQRS frequency band largely overlaps with the mQRS frequency band. Reproduced from Sameni et al. (2010).

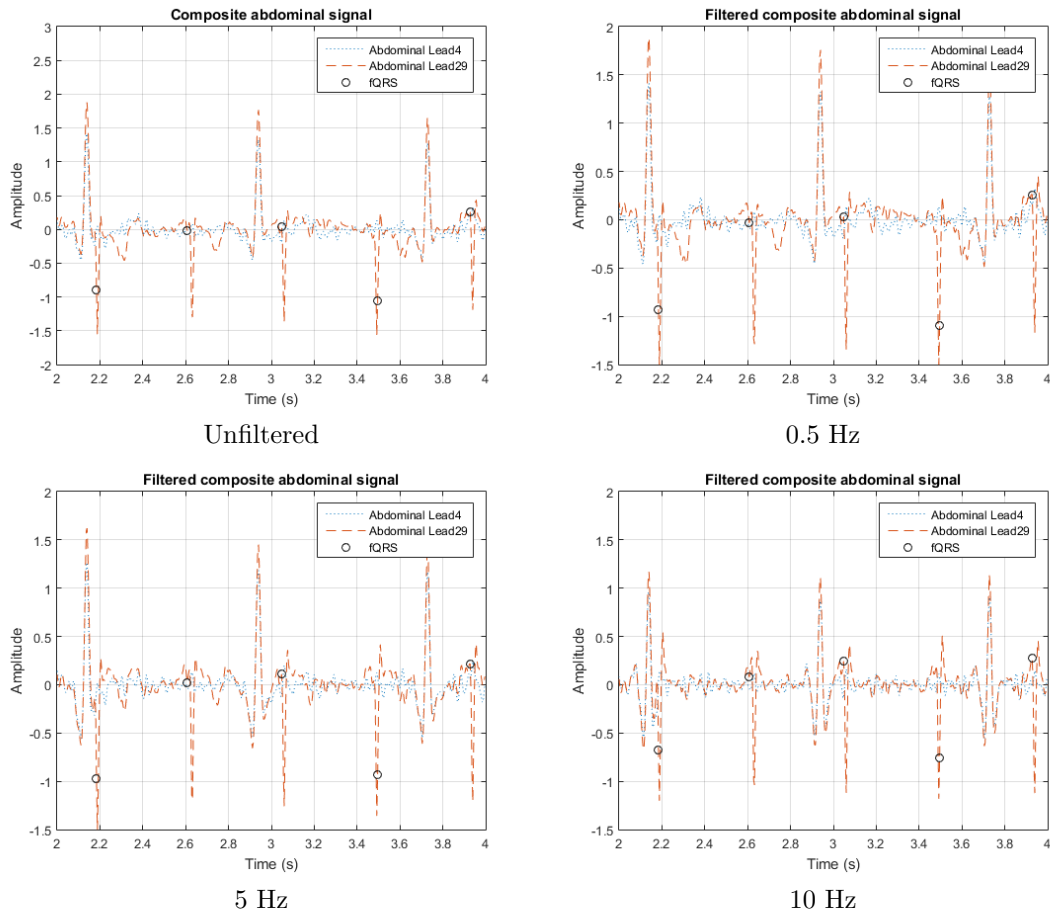


Figure 4.3: The figure shows unfiltered composite abdominal signal (top left) and processed abdominal signals which have been filtered using high pass filter with cut-off frequencies 0.5 Hz (top right), 5 Hz (bottom left) and 10 Hz (bottom right). From the signal at the bottom right, the maternal and fetal the P and T waves are removed from the signal.

4.3 fECG Extraction Methods

The following fECG signal extraction methods are evaluated using the MATLAB software:

- Blind Source Separation (BSS)
- Template Subtraction (TS)
- Adaptive Methods(AM)

There are many fECG extraction methods which have been used in the literature for fECG extraction. However, in some of the recent published work, the algorithms mentioned above have been most extensively researched and provided the most promising results.

For example, over 50 teams participated in the 2013 PhysioNet/Computing in Cardiology Challenge and most of the fECG extraction methods submitted were based on BSS, TS, AM or combination of these methods (Silva et al. 2013). Top scoring methods were ICA (Varanini, Tartarisco, Billeci, Macerata, Pioggia & Balocchi 2013), AM (Podziemski & Gieraltowski 2013) and a hybrid method; Behar et al. used a method which combined PCA, ICA and TS methods (Behar, Oster & Clifford 2013).

AM and TS based methods are single channel methods; only one abdominal channel is required for fECG extraction (TS based methods also require a reference mECG channel). The BSS based methods are multi-channel methods; at least two abdominal channels are required for fECG extraction. For fair comparison between the single channel methods and BSS based methods, single channel methods applied fECG extraction to all the available channels.

In the following sections, the implementation of the selected methods in to MATLAB will be discussed in more detail.

4.3.1 Blind Source Separation

Three different BSS based fECG extraction methods were tested. More specifically, the performance of FastICA, JADE and PCA algorithms for fECG signal extraction were evaluated.

FastICA algorithm was developed by Aapo Hyvarinen at the Helsinki University of Technology (Hyvarinen 1999). For the FastICA method, hyperbolic tangent non-linearity contrast function was used and both deflationary and symmetric approaches were tested. A maximum number of iterations was set to 20000.

The JADE algorithm was originally developed by Cardoso and Souloumiac (Cardoso & Souloumiac 1993). The algorithm was initially developed for telecommunications application but has been quite used in literature for other applications as well; including fECG signal extraction. Default parameters were used for the JADE algorithm.

PCA is a simple, non-parametric method used for data analysis in many applications; from neuroscience to computer graphics. One of the advantages of the PCA methods is that it does not require the user to set any parameters. It works like a black box; data

goes in and different data comes out. Consequently, this is one of the disadvantages for the PCA method as well.

One of the issues with the ICA based methods is that, for best performance, they require optimal number of sources (or input channels). This is due to the fact that when the number of input channels exceeds the number of underlying sources, the ICA assumption of square mixing of the underlying sources does not hold any more. This issue is referred as a model order problem (Roberts & Everson 2001, James & Hesse 2004). PCA can be used to workaround this issue; more specifically, PCA can be used to analyse the principal components in the data set, and by disregarding components with small eigenvalues, the sources used for the ICA calculation step can be optimised. From the early test work, it was found that the dimension reduction step would provide significant improvement on the detection accuracy and also reduced the convergence time for the ICA algorithms. As such, PCA dimension reduction step was applied for the ICA algorithms in the final testing phase.

The MATLAB functions for the BSS algorithms were obtained from the ECGSYN MATLAB toolbox (Behar, Andreotti, Zaunseder, Li, Oster & Clifford 2014). The ECGSYN toolbox includes `FECGSYN_bss_extraction.m` function. This function requires following input variables

- data - fECG composite signal
- method - string containing method name i.e. "PCA", "JADE" etc.
- blen- the input signal is divided in to segments of blen length (in seconds)
- fs - sampling frequency
- defl - boolean, if 1, the PCA dimension reduction step is applied

The segment length was chosen to be 45 seconds. Sampling frequency was 250 Hz.

The output from the function is extracted principle components.

4.3.2 Template Subtraction

TS based methods use an algorithm to build an average mECG template which is extracted from the composite signal. In this project, five different TS based fECG extraction methods were tested. The methods were obtained through the ECGSYN MATLAB toolbox.

The first method is a simple TS method where the mQRS beats were directly subtracted from the abdominal channels without any other signal processing steps. The second method uses a scalar gain to adapt the template to each mQRS beat (Cerutti, Baselli, Civardi, Ferrazzi, Marconi, Pagani & Pardi 1986). In the third method, a scaling procedure was performed to create templates for maternal P, QRS and T waves independently (Martens, Rabotti, Mischi & Sluijter 2007). The fourth method created the template by weighting the former cycles, where the weights selected minimised the mean square error (MSE) (Vullings, Peters, Sluijter, Mischi, Oei & Bergmans 2009). The fifth method stacks the composite signal, uses PCA method to find principal components and then back propagation step takes place on beat-to-beat basis to produce mECG template (Kanjilal, Palit & Saha 1997).

The MATLAB TS algorithms are included in function `FECGSYN_ts_extraction.m` from ECGSYN MATLAB toolbox. The function call requires following input variables:

- peaks - mQRS position markers
- ecg - fECG composite signal
- method - string containing the method name i.e. "TS", "TS-PCA" etc.
- nbCycles - number of cycles used to build the mECG template
- nbPC - number of principal components used for PCA
- fs - sampling frequency

For this dissertation, 20 cycles were used for template creation and for the PCA method, two principal components were used. The sampling frequency was 250Hz.

The output from the function is the extracted fECG signal from each composite channel.

4.3.3 Adaptive Methods

AM use one or more reference mECG signals for filtering the mECG from the abdomen composite signal. As the name suggests, AM is able to "learn" and recursively update the filter parameters. For this dissertation, three different AM were evaluated.

The first method uses the least mean square (LMS) method to find optimal filter coefficients to minimise the MSE between desired signal (mECG reference signal) and the output signal (composite signal) (Widrow, Glover, McCool, Kaunitz, Williams, Hearn, Zeidler, Dong & Goodlin 1975). The second AM uses recursive least square (RLS) method. RLS algorithm aims to minimise the total squared error; the algorithm not only uses the current data point but also historic data points to update the filter coefficients (Behar, Johnson, Clifford & Oster 2014). The third method uses Recurrent Neural Network (RNN) approach; more specifically Echo State Neural Network (ESN) method was used for optimising the filter parameters (Behar, Johnson, Clifford & Oster 2014). Visualisation of an ESN based fECG extraction algorithm is shown in Figure 4.4.

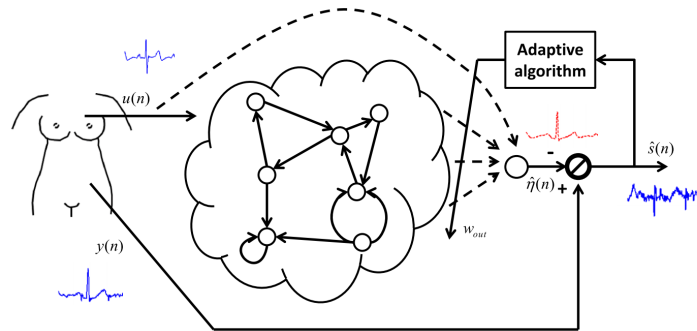


Figure 4.4: The ESN based fECG extraction algorithm showing the relationship between the reference signal $u(n)$, predicted signal $\hat{r}(n)$, composite signal $y(n)$, and the extracted fECG $\hat{s}(n)$. Dashed lines represent adaptive weights. Reproduced from Behar et al. (2014).

LMS and RLS methods assume a linear relationship between the reference signal and the projected MECCG, whereas the ESN based method can handle non-linearities.

The AM for MATLAB are included in the `FECGSYN_adaptfilt_extraction.m` function from the `FECGSYN` MATLAB toolbox. The function call requires the following input variables:

- `ecg_target` - composite ECG signal

- `ecg_ref` - reference mECG signal
- `method` - string containing the method name i.e. "LMS", "RMS" or "ESN"
- `debug` - boolean, if 1, debug information provided
- `fs` - sampling frequency

The signal was processed through the AM extraction algorithms in segments of 30s and the sampling frequency was 250 Hz. The output from the function is the residuals (fECG) for each signal channel.

4.4 fQRS Detection

A modified version of the Pan&Tompkins QRS energy detector algorithm was used for detecting the fQRS complexes. The original Pan&Tompkins QRS detector was developed to detect adult QRS complexes as explained in detail in Pan et al. (Pan & Tompkins 1985). To count for the higher heart rates of fetuses, the refractory period option for the detector was set to 130ms (normal setting being 250ms for adults or mQRS) and the energy threshold was set to 0.3. The refractory period and energy threshold value were adopted from Behar et al. 2014.

The modified version of the Pan&Tompkins QRS energy detector is implemented in to the MATLAB function `qrs_detect` (`qrs_detect.m`) and it was obtained through the FECCSYN MATLAB toolbox. The input variables for the function call are:

- `ecg` - extracted fECG signal
- `THRES` - energy threshold for the detector
- `REF_PERIOD` - refractory period in seconds between two R-peaks
- `fs` - sampling frequency

The output from the `qrs_detect` function is an array with the detected QRS locations (in samples).

4.5 Performance Metrics

Many different extraction algorithm performance metrics have been used in the literature. In this dissertation, the fQRS detection is the greatest interest as this can be used for calculating the fHR. Thus, the selected performance metrics only consider the extraction algorithms ability to detect fQRS complexes. For this reason, the selected performance metrics are:

- Sensitivity (SE)
- Positive Predictive Value (PPV)
- F_1 accuracy measure (F_1)
- Mean Absolute Error (MAE)

The above performance metrics are widely used in the literature (Silva, Moody, Behar, Johnson, Oster, Clifford & Moody 2015, Behar, Oster & Clifford 2014) and using the selected performance metrics simplifies the comparison of the results from this project to the ones found from the literature.

In accordance with American National Standards Institute (ANSI) EC57:2012 standard - *Testing and reporting performance results of cardiac rhythm and ST segment measurement algorithms* (ANSI/AAMIEC57:2012 2012), the SE and PPV are defined as:

$$SE = \frac{TP}{TP + FN} \quad PPV = \frac{TP}{TP + FP}$$

,

where TP is the number of true positives (detected fQRS), FN is the number of false negatives (missed fQRS detection) and FP is the number of false positives (false detected fQRS).

F_1 accuracy score is used to understand the overall accuracy of the extraction algorithm. The F_1 is defined as:

$$F_1 = 2 * \frac{PPV * SE}{PPV + SE} = \frac{2 * TP}{2 * TP + FP + FN}$$

As the equation for the F_1 score shows, the F_1 value is symmetrically affected by both the PPV and the SE values; in other words for the extraction algorithm to obtain a good F_1 score, it needs to minimise both the number of false detections and the number of missed detections. The F_1 value is an harmonic mean measure (an average of the PPV and SE values) and it provides a good summary metric when an average of rates is desired (Sasaki et al. 2007).

SE, PPV and F_1 metrics do not give any indication of the difference in time between the detected fQRS and reference fQRS. This is why MAE metric is also used for performance evaluation. MAE is calculated only for the TP detections as this will make the MAE calculation independent of the detection accuracy. MAE is defined as:

$$MAE = \frac{1}{TP} * \sum_{i=1}^{TP} |d_i - \hat{d}_i|,$$

where the d_i is reference fQRS annotation and \hat{d}_i is detected fQRS annotation.

The MATLAB function `bxm_compare` (`bxm_compare.m`) from the FECGSYN MATLAB toolbox was used to calculate the performance metrics. The reference fQRS locations were provided by the FECGSYNDB database. The required input variables are

- Reference fQRS locations (array containing the fQRS locations in samples)
- Detected fQRS locations (array containing the fQRS locations in samples)
- Acceptance interval

For adult QRS detection, the acceptance interval is 150ms as defined in the ANSI EC57:2012 standard. However, as suggested in the literature (Andreotti, Riedl, Himmelsbach, Wedekind, Wessel, Stepan, Schmieder, Jank, Malberg & Zaunseder 2014, Zaunseder, Andreotti, Cruz, Stepan, Schmieder, Malberg, Jank & Wessel 2012), acceptance interval of 50ms is more appropriate for fQRS detection as this accounts for the higher fHR. The function calculates the performance metrics for each detected fQRS array. The result from the channel which gave the best F_1 score, was kept as the result from any given fECG extraction iteration.

4.6 MATLAB Implementation

In this section, the MATLAB implementation of the fECG extraction methods will be discussed. Figures 4.5 and 4.6 show a simplified flowchart of the main program. Different MATLAB programs were created for the different input signal SNR levels and the fECG extraction methods (AM, TS and BSS). However, the MATLAB program flow for the different methods are very similar and thus the same flowchart can be used to describe each one.

The program starts by checking if the signal's .mat file (sub03_SNRdb_l3.mat) is already present in the program folder and if not, the signals are downloaded from the Physionet server and stored in to a .mat file. WFDB MATLAB Toolbox provides a function **rdsamp** which can be used to read signals from the Physionet servers. The FECGSYNDB database provides separate waveforms files for the different abdominal signal components (mECG, fECG and noise). This is the reason, the fECG and mECG waveforms can be plotted as a reference.

The composite abdominal signal is created for the particular physiological case by adding the different signal components together; the program stores the composite abdominal signal to a variable **comp_s**. The different physiological cases are run one after another using a **for loop**.

Next, the composite abdominal signal is plotted and after this, it is run through the prefiltering function which removes low frequency and high frequency noise from the composite abdominal signal. A plot of the filter composite abdominal signal is created. The different fECG extraction methods can now be run; the methods are run sequentially using a for loop. Within this for loop, there is another for loop to run the different abdominal channel combinations. The signals from the particular channel combination are loaded in to a variable **y**.

The variable **y** is used as an input to the fECG extraction methods functions. Other input variables are specific parameters for the particular fECG extraction method. The output from the fECG extraction function is a matrix containing the extract fECG waveforms for each input channel (i.e. for two input abdominal channels, the output consists of two fECG waveforms etc). The fECG waveform matrix is used as the input to the fQRS detection function. The fQRS detection function output is a matrix with the

detected fQRS locations reported in samples for each fECG waveform. This matrix and the reference fQRS locations array are used as inputs to the benchmarking function. The benchmarking function calculates the performance metrics (F_1 , MAE, TP, FN, FP, SE and PPV). The performance metrics are stored in to a **results** variable.

The fECG waveform which provided the best F_1 score is plotted and stored in to a png file. After the last abdominal channel combination (30 channels) has been run, the results variable is stored in to a csv file.

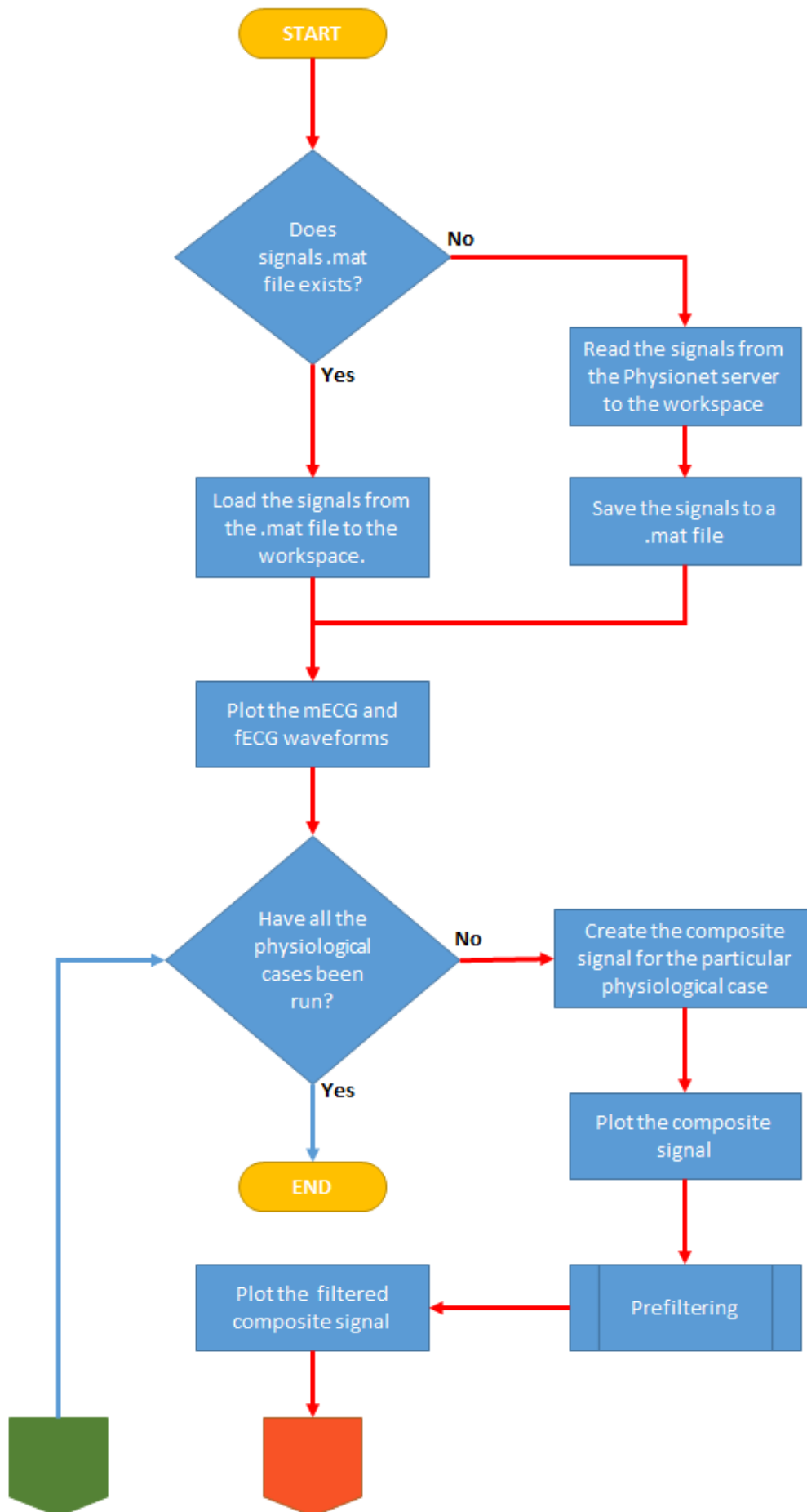


Figure 4.5: Simplified flowchart for the fECG extraction MATLAB program. Page 1 of 2.

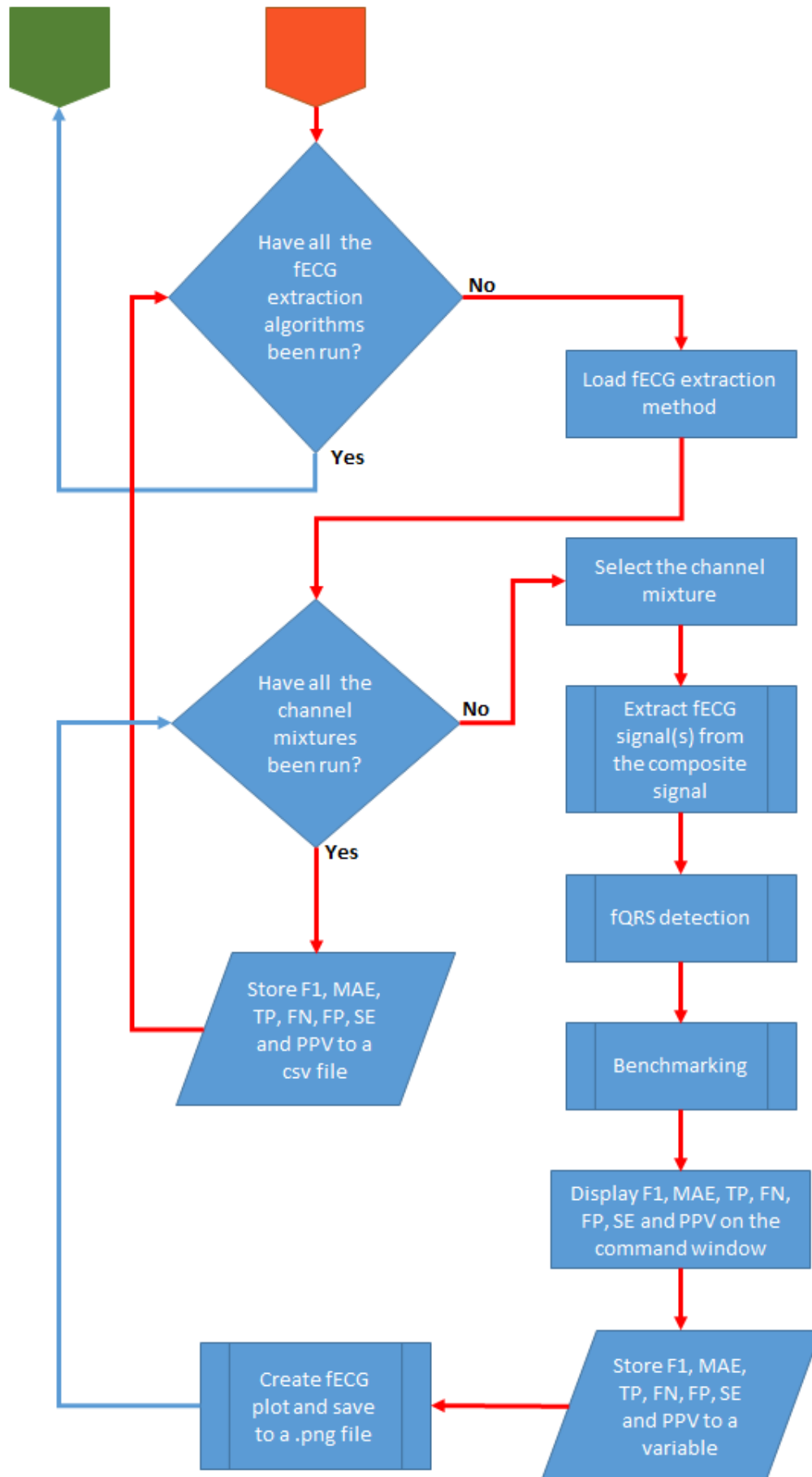


Figure 4.6: Simplified flowchart for the fECG extraction MATLAB program. Page 2 of 2.

4.7 Chapter Summary

The main aspects of the fECG extraction, which had to be considered for this project, were discussed in this chapter. The three fECG extraction method categories which were adopted for the project are AM, TS and BSS. Each category includes several different fECG extraction approaches (or algorithms) and as such, 11 different extraction methods were implemented in to MATLAB and their respective fECG extraction performances were evaluated. The next chapter presents the results for the different fECG extraction methods.

Chapter 5

fECG Signal Extraction Results and Performance Comparison

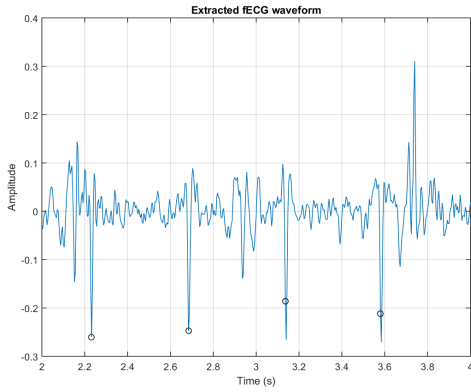
In this chapter, the results for the different fECG signal extraction methods will be shown and discussed. Several fECG waveform examples are shown. Furthermore, the results for the F_1 score and MAE are presented using box plots. The box plots show the results for each physiological case (C0, C1, C2, C3, C4 and C5) and the overall fECG signal extraction performance is also shown.

Box plots are used to show the interquartile range (IQR) and the median value of distribution. The IQR indicates where the middle proportion of the distribution is and where the median value sits in the IQR. The whiskers show the minimum and maximum values; this indicates whether there are any outliers in the dataset. The statistics are calculated from the F_1 and MAE values across the different noise levels in the particular physiological case.

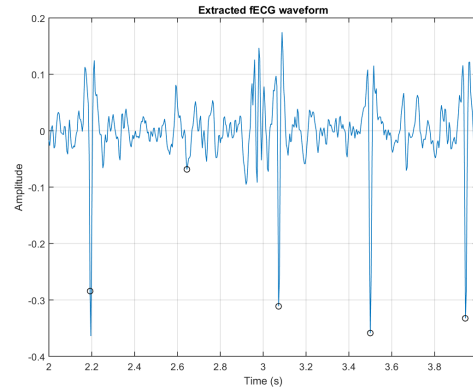
5.1 Single Pregnancy Case

Figure 5.1 displays two second segment examples of the extracted fECG waveforms for the extraction methods AM-ESN, TS-PCA and BSS-JADE for the single fetus physiological cases 2 and 4 (C2 and C4). The methods mentioned earlier were the best performing methods in their respective method category (AM, TS and BSS). Visually, the BSS-

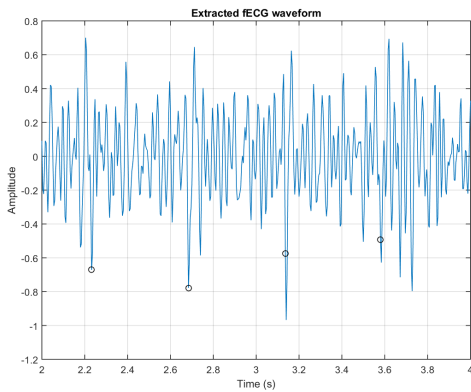
JADE method produces the cleanest looking fECG waveform; the waveform has the least amount of background noise and the peak-to-background ratio is the highest as well. TS-PCA produces the noisiest fECG waveform.



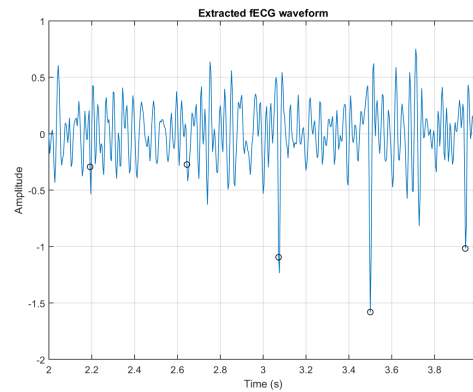
Case 2: AM-ESN



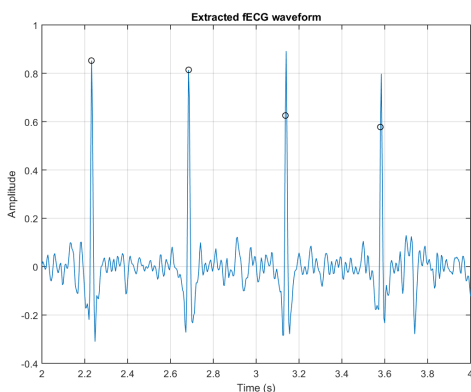
Case 4: AM-ESN



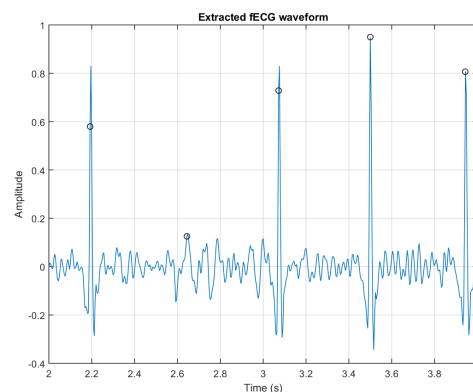
Case 2: TS-PCA



Case 4: TS-PCA



Case 2: BSS-JADE



Case 4: BSS-JADE

Figure 5.1: Two second segments of the extracted fECG waveforms for the single fetus physiological cases 2 and 4 for the AM-ESN, TS-PCA and BSS-JADE fECG signal extraction methods are shown. The black circles indicate the reference fQRS locations. Visually, the BSS-JADE method produces the “cleanest” fECG waveform in both of the cases.

The F_1 score for the single fetus cases are shown in figures 5.2, 5.4, 5.6, 5.8 and 5.10.

Significant deviation in the median F_1 score can be seen between the different methods over the different physiological cases. The number abdominal channels used as inputs to the fECG extraction methods also affect the F_1 score. For the AM and TS based methods, the F_1 score typically improves as the number of abdominal channels used for the fECG extraction is increased. This makes sense as the number of abdominal channels is increased, the better the chance of having a stronger fECG signal in the abdominal mixture. For the BSS based methods, there is no clear trend showing how the number of abdominal channels used for the fECG extraction affects the F_1 score. JADE algorithm tends to perform best when 2, 4 or 6 abdominal signals are used. PCA tends to get a better F_1 score as number of abdominal channels are increased and FastICA algorithm (both deflationary and symmetric approaches) has a somewhat random response when the number of abdominal channels are increased.

BSS based methods out-performed the AM and TS based methods on the baseline case (C0). For the fetal movement (C1) and mHR and fHR acceleration / deceleration (C2) cases, all the methods received a very similar median F_1 score. All the methods received similar but lower average F_1 score for the uterine contraction (C3) and ectopic beats (C4) cases.

The fECG SNR level of the abdominal signal has a significant effect on the F_1 score on the TS and AM based methods. In the box plots this can be seen as a wider IQR range. BSS based methods are not affected as much by the fECG SNR level.

The MAE results for the single fetus cases are shown in figures 5.3, 5.5, 5.7, 5.9 and 5.11. For the AM and TS based methods, median MAE result does not tend to be affected significantly by the abdominal channels used for the fECG extraction. However, the BSS methods get varying MAE result for the different abdominal channels.

Figure 5.12 shows the overall median F_1 score over the different physiological cases. Table 5.1 shows the best performing methods in their respective categories. BSS-JADE received the best median F_1 score of 99.85 % for four abdominal channels.

The overall MAE result is shown in Figure 5.13. All the methods received a similar median MAE result except the FastICA algorithm which performed significantly poorer than the other methods. JADE achieved the best MAE result of 0.49 ms for four abdominal channels.

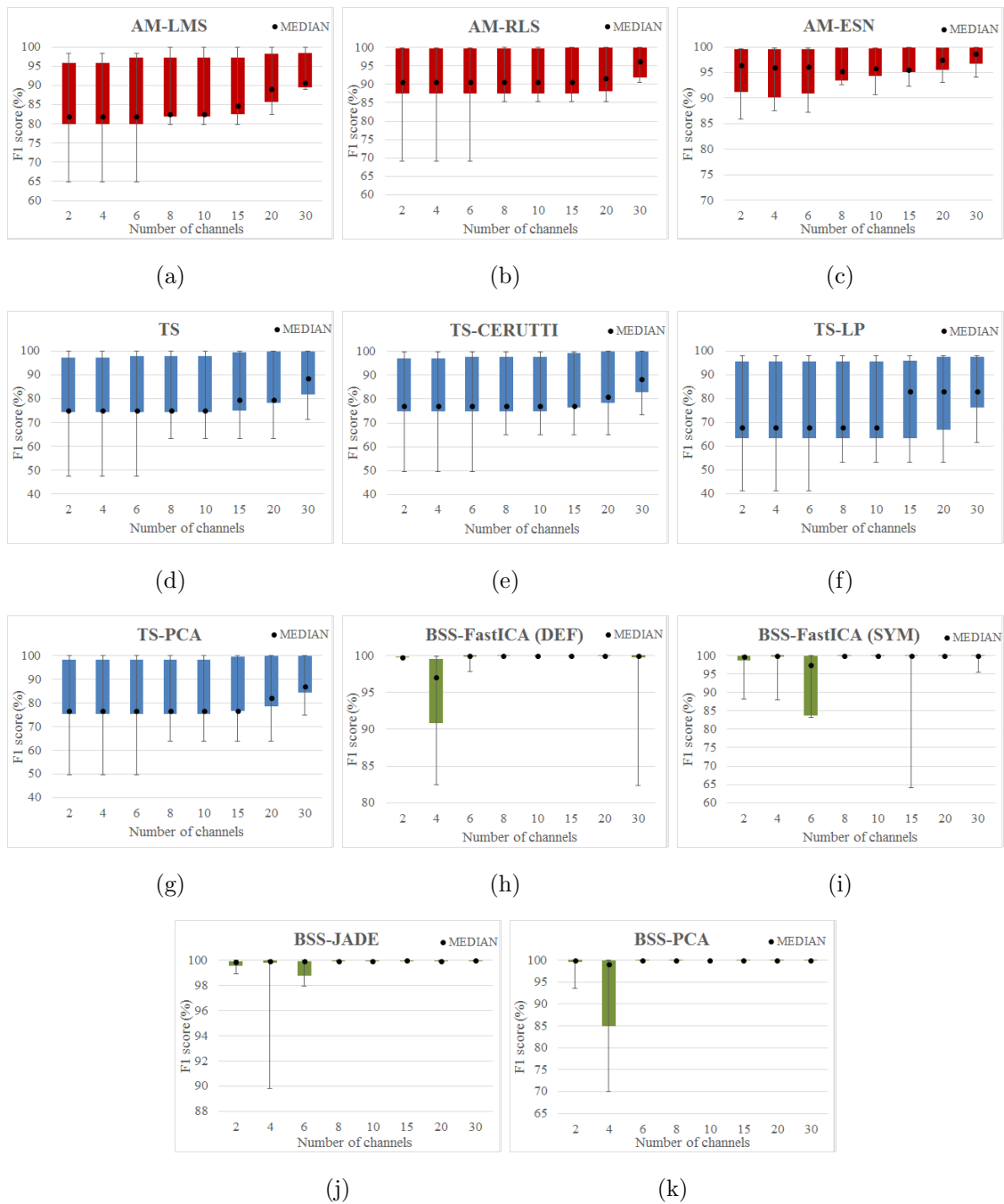


Figure 5.2: F_1 score for the different fECG signal extraction methods for the **Case 0 - Baseline + noise**: (a) AM-LMS, (b) AM-RLS, (c) AM-ESN, (d) TS, (e) TS-CERUTTI, (f) TS-LP, (g) TS-PCA, (h) BSS-FastICA (DEF), (i) BSS-FastICA (SYM), (j) BSS-JADE and (k) BSS-PCA.

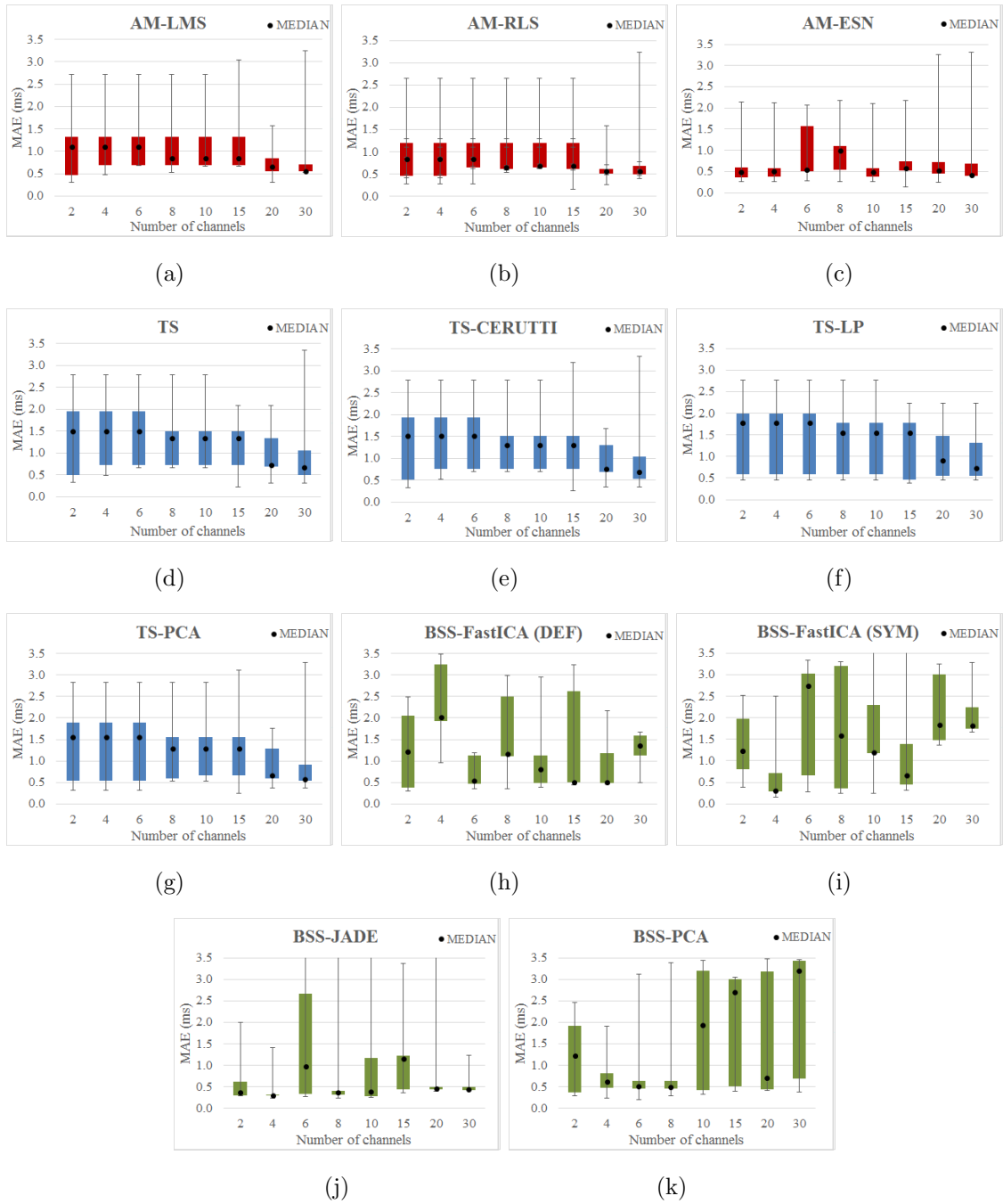


Figure 5.3: MAE result for the different fECG signal extraction methods for the **Case 0 - Baseline + noise**: (a) AM-LMS, (b) AM-RLS, (c) AM-ESN, (d) TS, (e) TS-CERUTTI, (f) TS-LP, (g) TS-PCA, (h) BSS-FastICA (DEF), (i) BSS-FastICA (SYM), (j) BSS-JADE and (k) BSS-PCA.

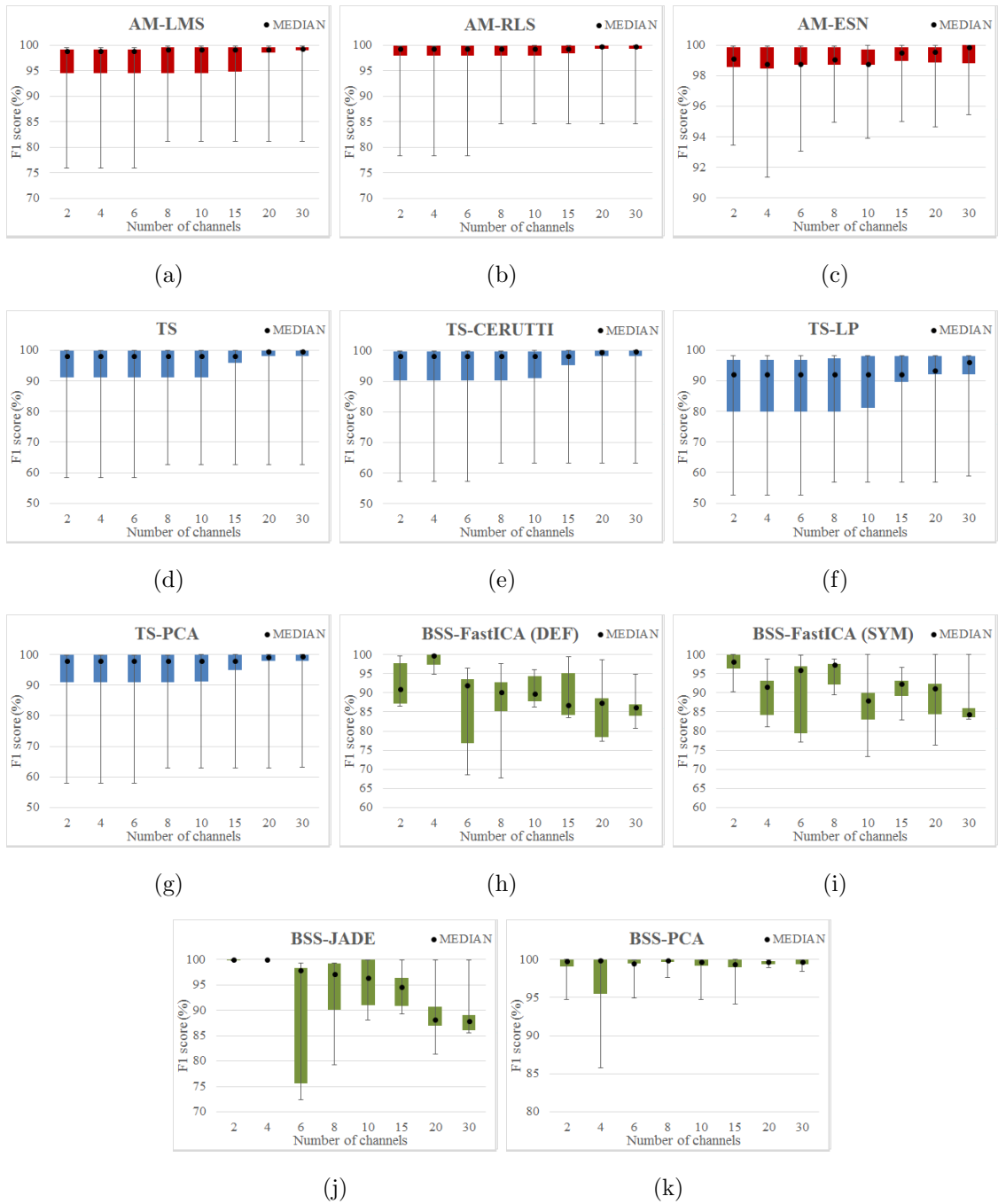


Figure 5.4: F_1 score for the different fECG signal extraction methods for the **Case 1 - Fetal movement + noise**: (a) AM-LMS, (b) AM-RLS, (c) AM-ESN, (d) TS, (e) TS-CERUTTI, (f) TS-LP, (g) TS-PCA, (h) BSS-FastICA (DEF), (i) BSS-FastICA (SYM), (j) BSS-JADE and (k) BSS-PCA.

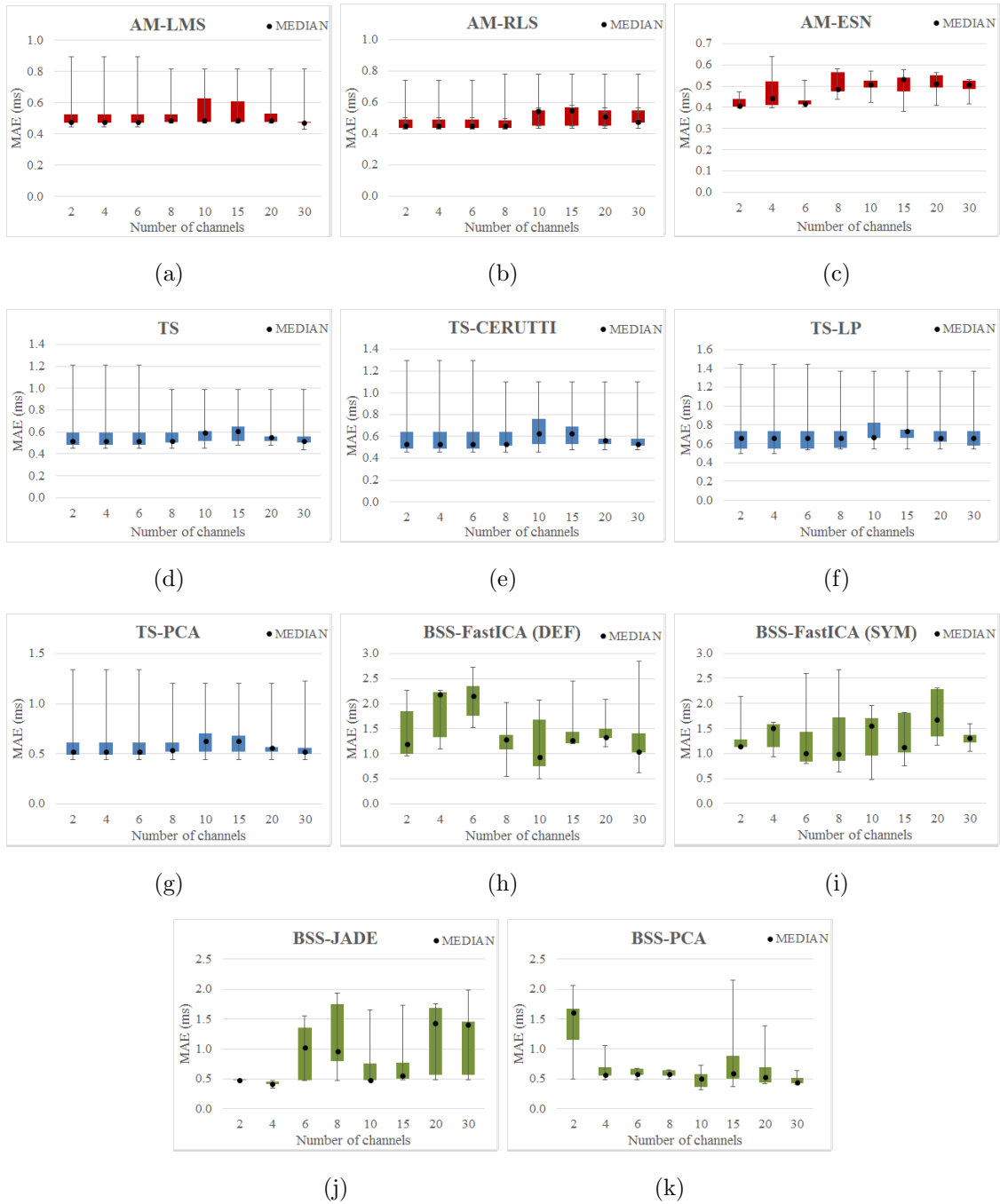


Figure 5.5: MAE score for the different fECG signal extraction methods for the **Case 1 - Fetal movement + noise**: (a) AM-LMS, (b) AM-RLS, (c) AM-ESN, (d) TS, (e) TS-CERUTTI, (f) TS-LP, (g) TS-PCA, (h) BSS-FastICA (DEF), (i) BSS-FastICA (SYM), (j) BSS-JADE and (k) BSS-PCA.

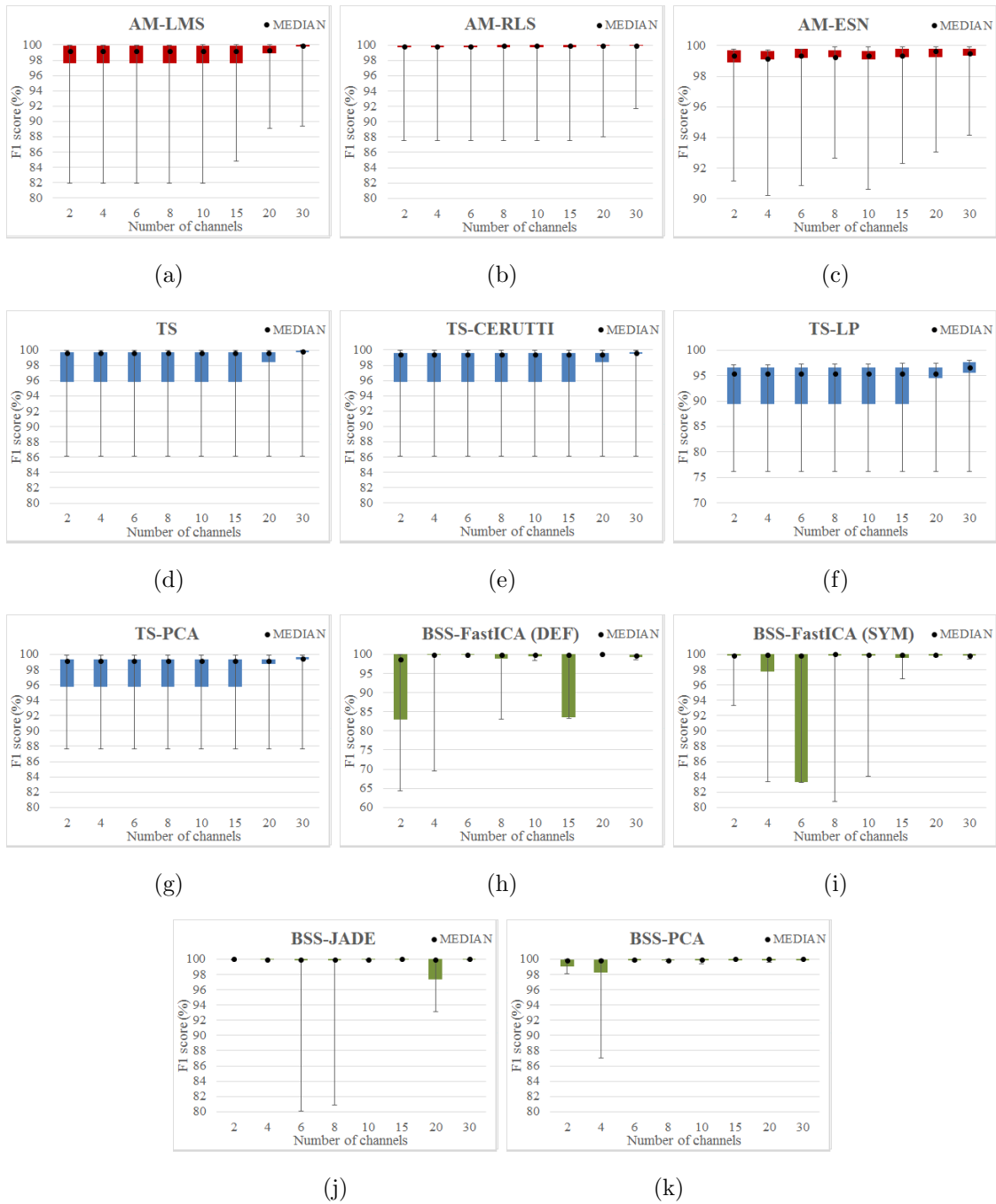


Figure 5.6: F_1 score for the different fECG signal extraction methods for the **Case 2 - mHR and fHR acceleration/deceleration + noise**: (a) AM-LMS, (b) AM-RLS, (c) AM-ESN, (d) TS, (e) TS-CERUTTI, (f) TS-LP, (g) TS-PCA, (h) BSS-FastICA (DEF), (i) BSS-FastICA (SYM), (j) BSS-JADE and (k) BSS-PCA.

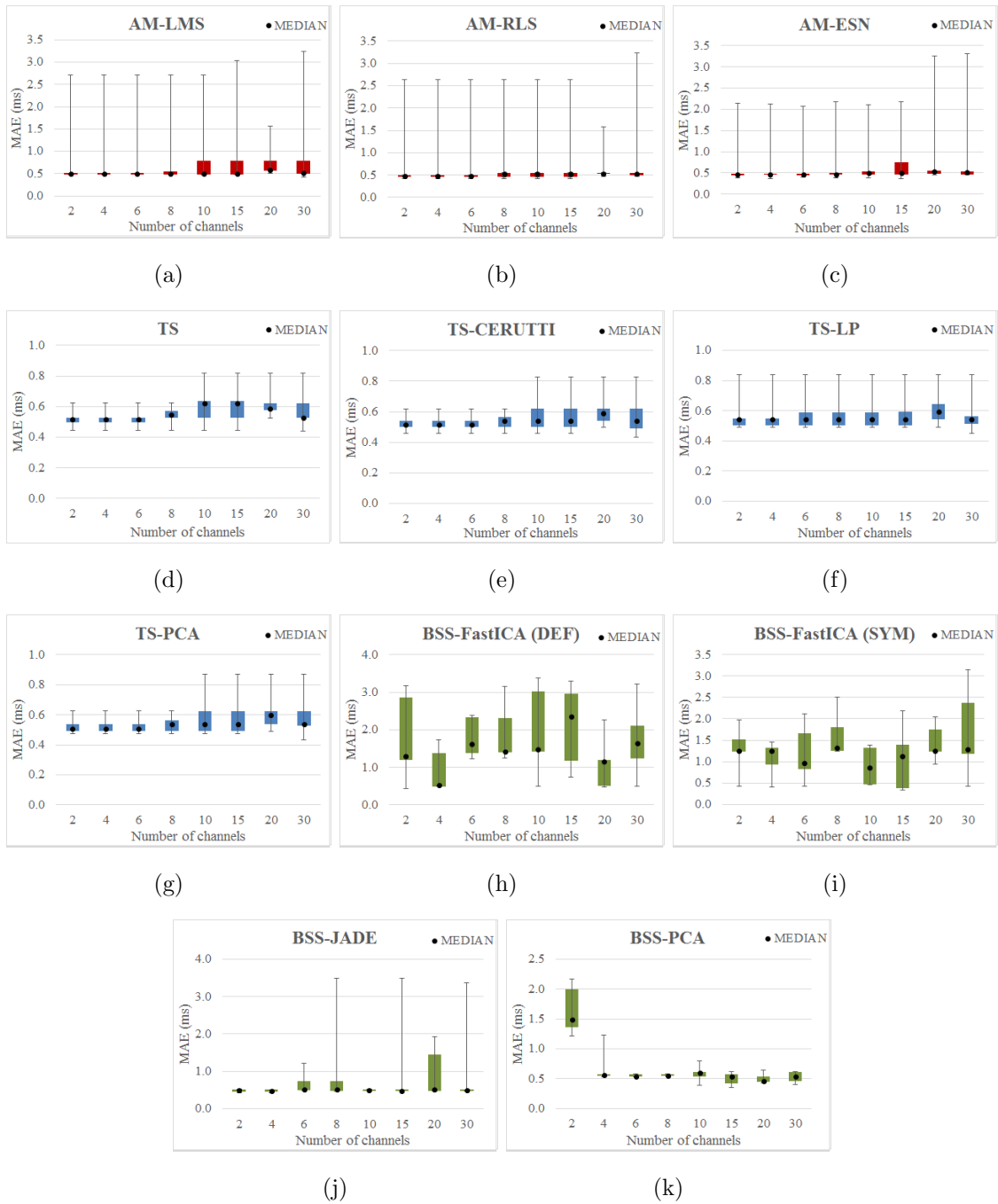


Figure 5.7: MAE score for the different fECG signal extraction methods for the **Case 2 - mHR and fHR acceleration/deceleration + noise**: (a) AM-LMS, (b) AM-RLS, (c) AM-ESN, (d) TS, (e) TS-CERUTTI, (f) TS-LP, (g) TS-PCA, (h) BSS-FastICA (DEF), (i) BSS-FastICA (SYM), (j) BSS-JADE and (k) BSS-PCA.

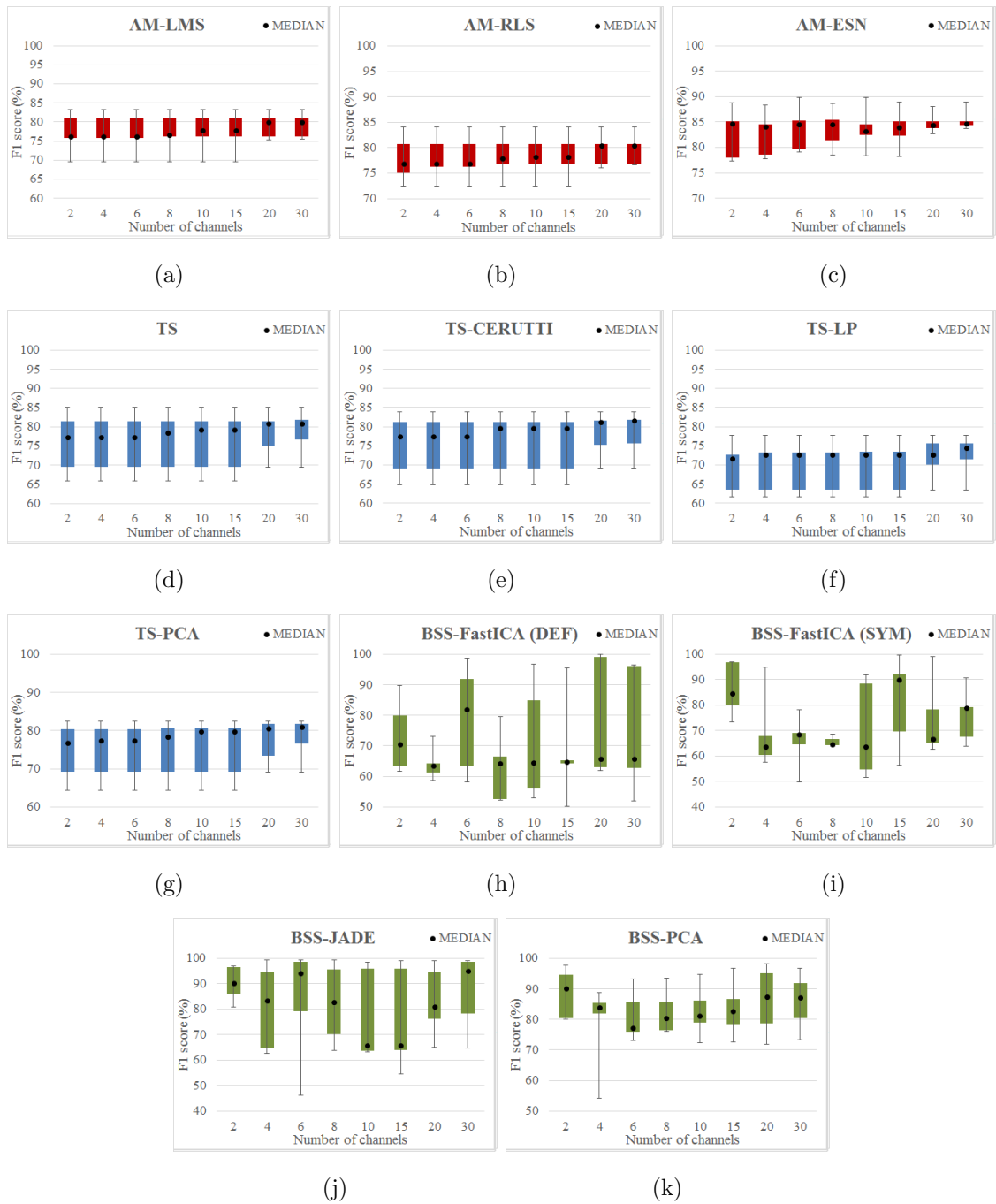


Figure 5.8: F_1 score for the different fECG signal extraction methods for the **Case 3 - Uterine contraction + noise**: (a) AM-LMS, (b) AM-RLS, (c) AM-ESN, (d) TS, (e) TS-CERUTTI, (f) TS-LP, (g) TS-PCA, (h) BSS-FastICA (DEF), (i) BSS-FastICA (SYM), (j) BSS-JADE and (k) BSS-PCA.

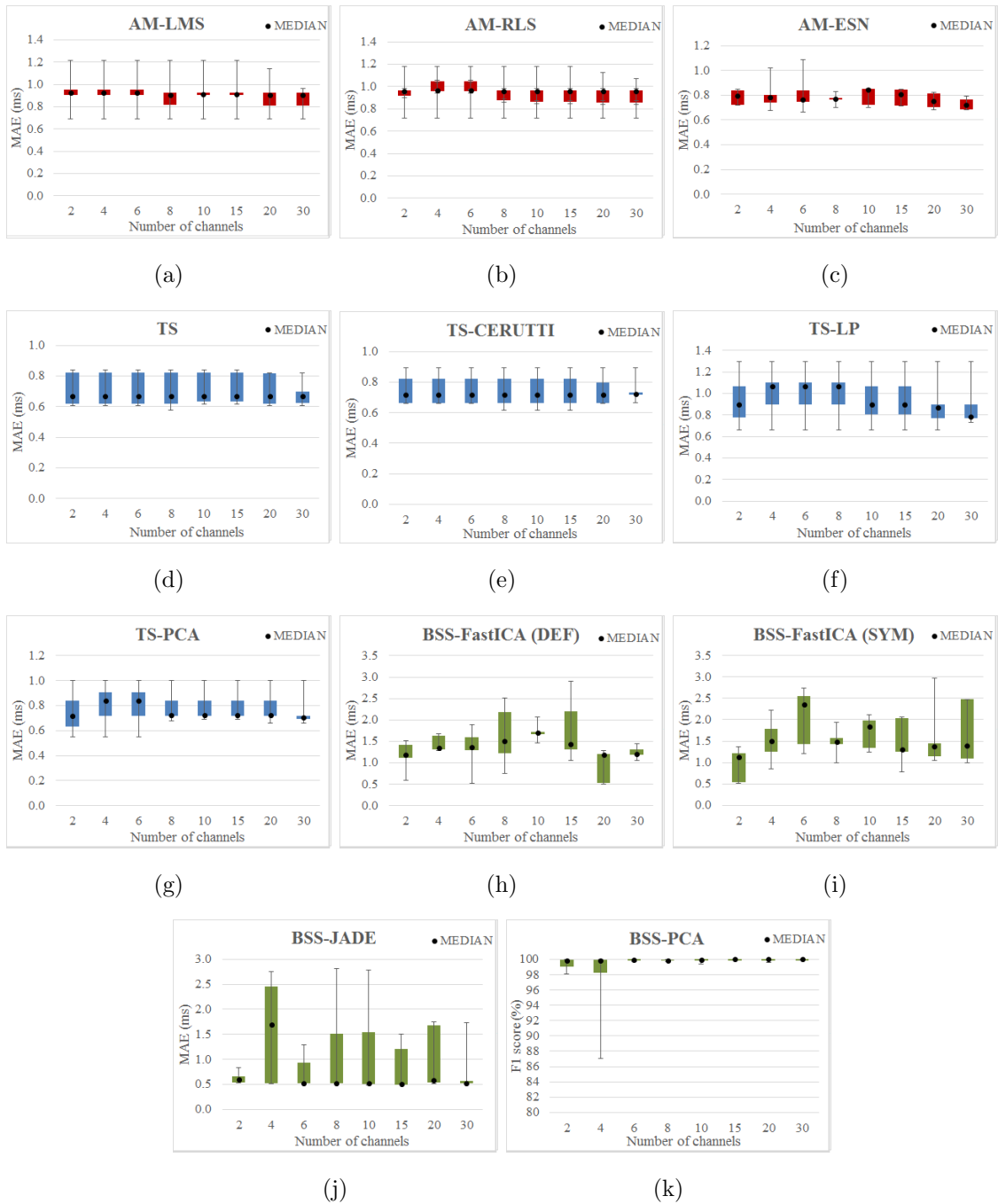


Figure 5.9: MAE score for the different fECG signal extraction methods for the **Case 3 - Uterine contraction + noise**: (a) AM-LMS, (b) AM-RLS, (c) AM-ESN, (d) TS, (e) TS-CERUTTI, (f) TS-LP, (g) TS-PCA, (h) BSS-FastICA (DEF), (i) BSS-FastICA (SYM), (j) BSS-JADE and (k) BSS-PCA.

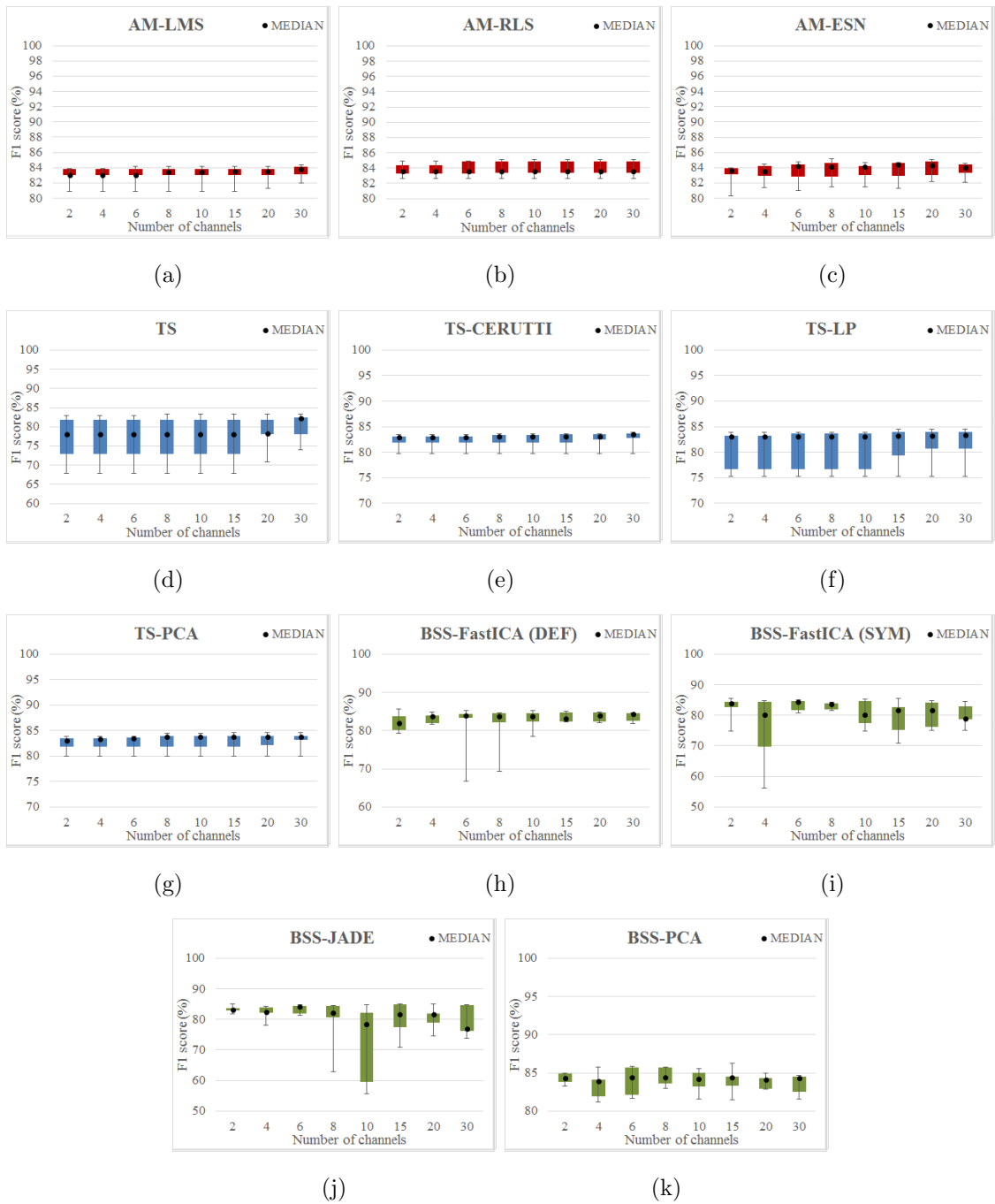


Figure 5.10: F_1 score for the different fECG signal extraction methods for the **Case 4 - Ectopic beats + noise**: (a) AM-LMS, (b) AM-RLS, (c) AM-ESN, (d) TS, (e) TS-CERUTTI, (f) TS-LP, (g) TS-PCA, (h) BSS-FastICA (DEF), (i) BSS-FastICA (SYM), (j) BSS-JADE and (k) BSS-PCA.

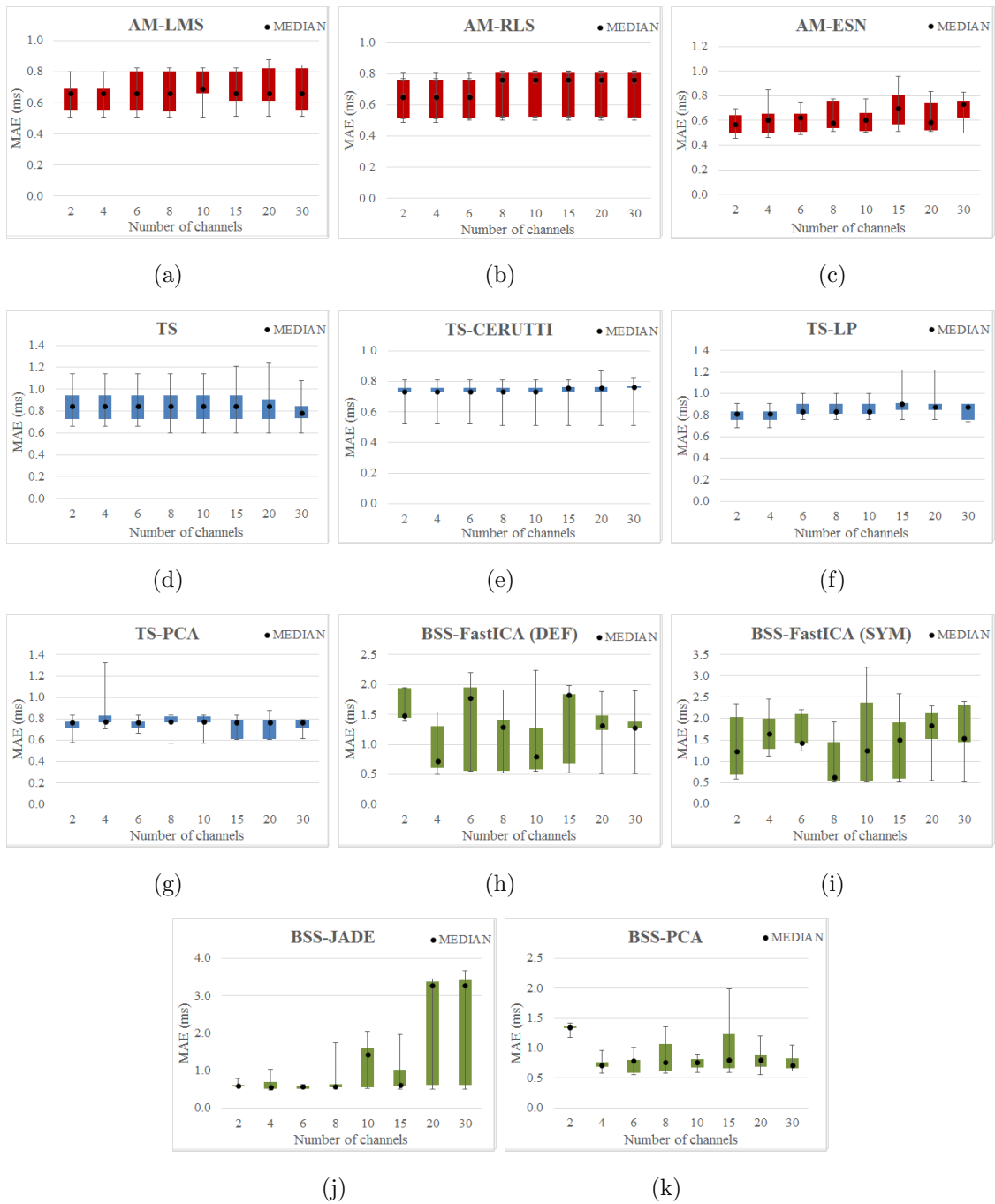


Figure 5.11: MAE score for the different fECG signal extraction methods for the **Case 4 - Ectopic beats + noise**: (a) AM-LMS, (b) AM-RLS, (c) AM-ESN, (d) TS, (e) TS-CERUTTI, (f) TS-LP, (g) TS-PCA, (h) BSS-FastICA (DEF), (i) BSS-FastICA (SYM), (j) BSS-JADE and (k) BSS-PCA.

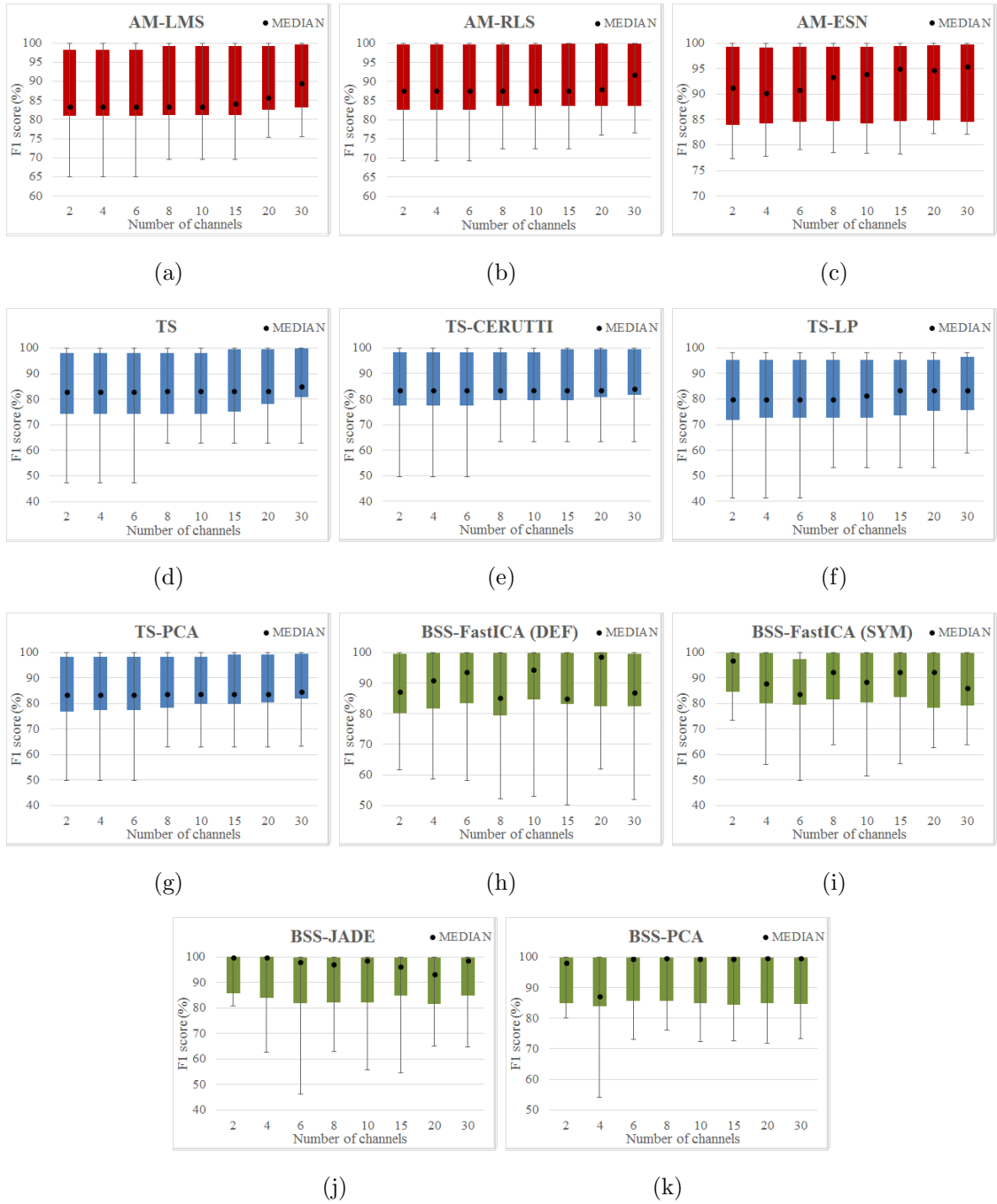


Figure 5.12: Overall F_1 score for the different fECG signal extraction methods: (a) AM-LMS, (b) AM-RLS, (c) AM-ESN, (d) TS, (e) TS-CERUTTI, (f) TS-LP, (g) TS-PCA, (h) BSS-FastICA (DEF), (i) BSS-FastICA (SYM), (j) BSS-JADE and (k) BSS-PCA.

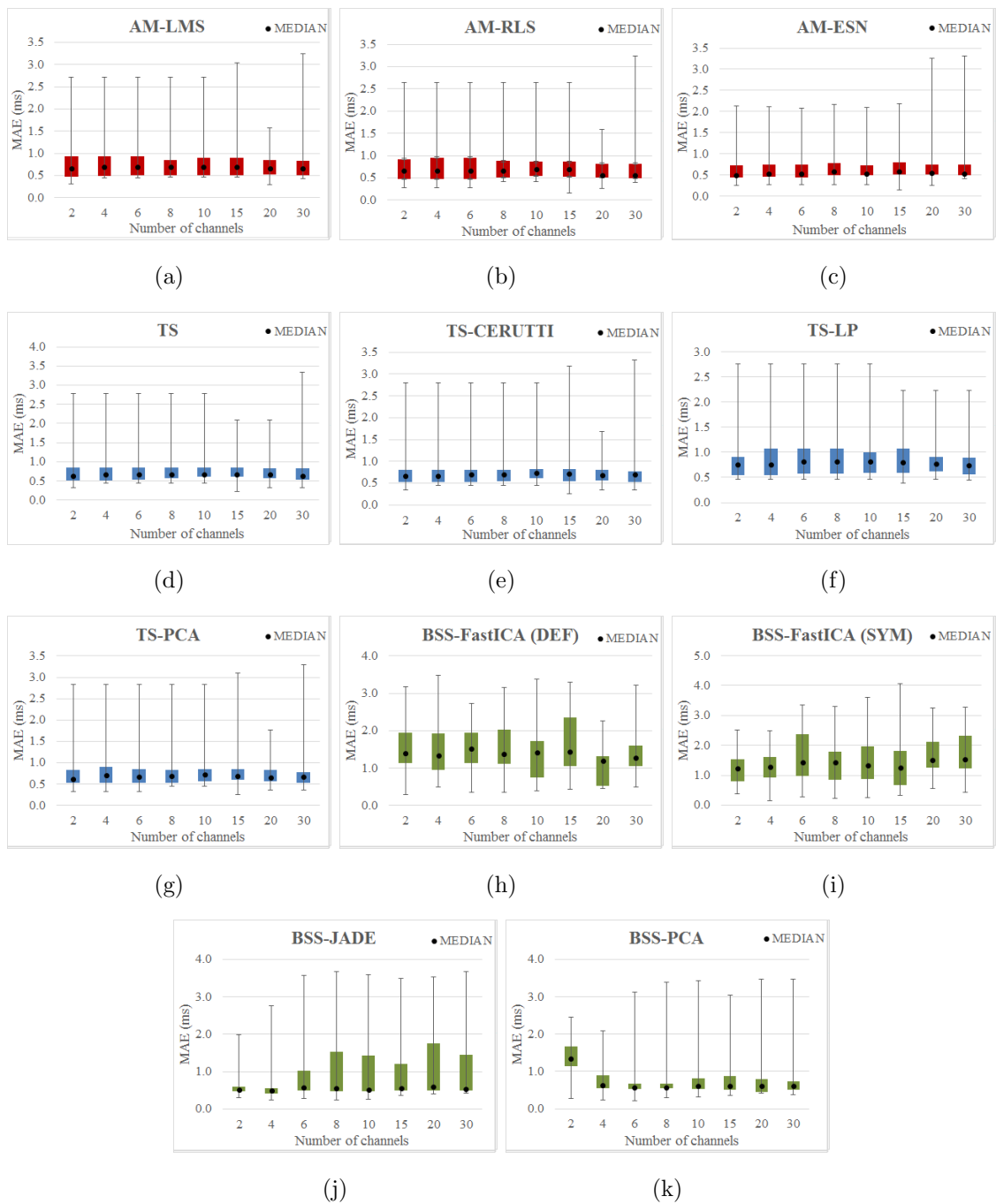


Figure 5.13: Overall MAE results for the different fECG signal extraction methods: (a) AM-LMS, (b) AM-RLS, (c) AM-ESN, (d) TS, (e) TS-CERUTTI, (f) TS-LP, (g) TS-PCA, (h) BSS-FastICA (DEF), (i) BSS-FastICA (SYM), (j) BSS-JADE and (k) BSS-PCA.

Table 5.1: The top performing fECG extraction methods in each method category (AM, TS and BSS). JADE algorithm was the overall best performing method achieving median F_1 score of 99.85 %.

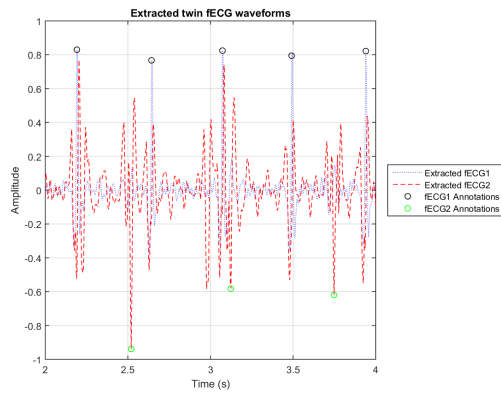
Method	F_1 (IQR)
AM-ESN	95.44 % (15.18 %)
TS-PCA	84.63 % (17.64 %)
BSS-JADE	99.85 % (14.07 %)

5.2 Twin Pregnancy Case

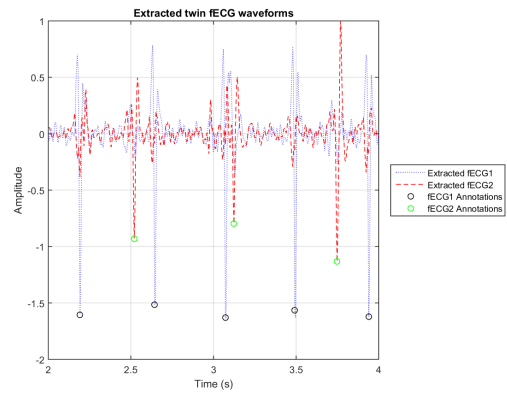
Figure 5.14 shows two second segments of the extracted fECG waveforms for the twin pregnancy case for the BSS based extraction methods. All the algorithms were able to extract the fetal signal components from the composite abdominal signal. The JADE algorithm provided the cleanest looking waveform.

Figure 5.15 presents the F_1 score and MAE results for the twin pregnancy case. All the BSS algorithms performed poorly when only two abdominal channels were used for fECG extraction. However, as the number of abdominal channels increased, the extraction performance improved as well. For example, for the JADE algorithm, increasing the number of abdominal channels from two to four, provided a substantial improvement in the median F_1 score (from 63.24 % to 98.27 %). However, the deviation from the mean is still quite large as shown by the box plot (Figure 5.15c). The FastICA algorithm using symmetric approach provided the best overall median F_1 score of 99.89 % when 15 abdominal signals were used.

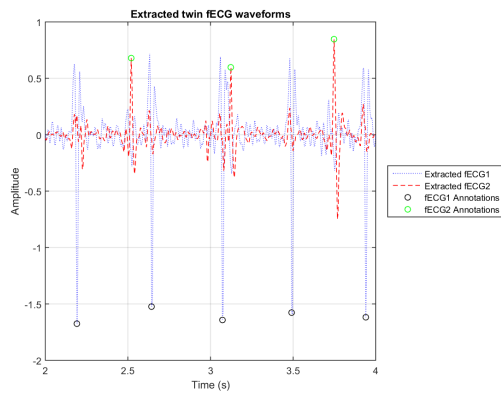
The MAE result follows similar trend; the MAE results improved as the number of abdominal signals increased. The PCA algorithm provided the best MAE result of 0.46 ms for 15 abdominal signals.



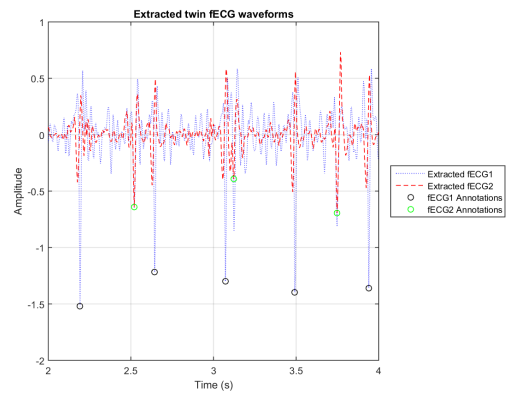
(a) FastICA (DEF)



(b) FastICA (SYM)



(c) JADE



(d) PCA

Figure 5.14: Extracted fECG waveforms for the twin pregnancy case for the BSS based extraction methods. Black and green circles indicate the reference fQRS location for the fetus one and fetus two respectively.

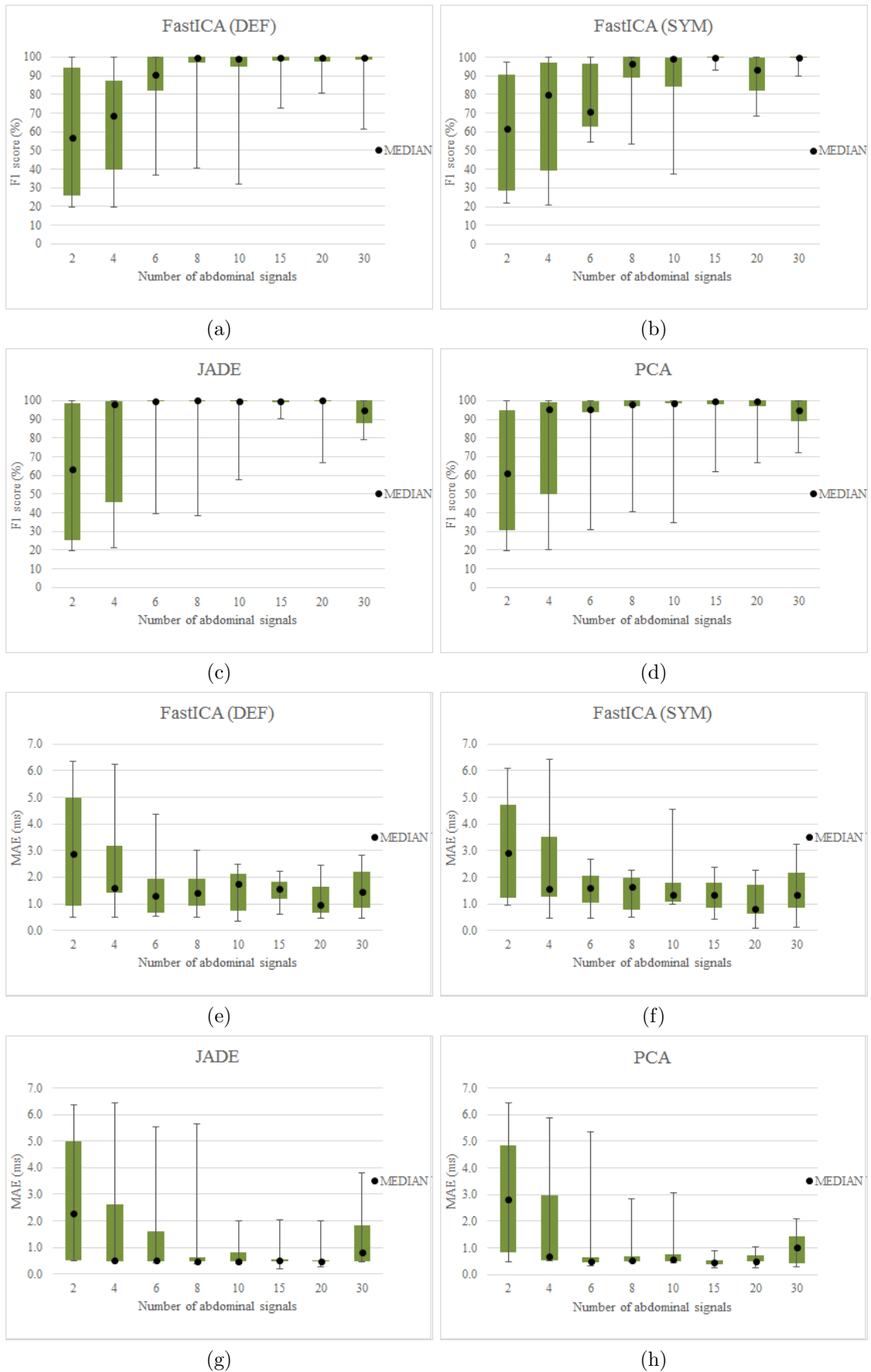


Figure 5.15: Overall F_1 scores (a, b, c and d) and the MAE results (e, f, g and h) for the fECG signal extraction methods for the **Case 5 - Twin pregnancy + noise** using the BSS based methods.

5.3 Comparison of Results

Table 5.2 shows Andreotti and his team's median F_1 score and what they were able to achieve using the same fECG extraction methods as that which has been used in this project (Andreotti et al. 2016). In addition, the test signal they used was also sourced from the FECGSYNDB database which means a fair comparison can be made between the results from this project and Andreotti and his team's work. Andreotti and his team used eight abdominal channels. Thus, Table 5.3 was constructed from the results from this project for the same abdominal channel configuration.

Tables 5.2 and 5.3 demonstrate that the results are quite similar. There are two exceptions to the rule; the Case 0 and the overall result. The median F_1 scores from this project in these two cases, for the AM and TS based methods, are significantly lower when compared to the results Andreotti and his team achieved. The BSS methods achieved similar scores in all the cases.

One possible explanation for Andreotti and his team achieving better results is that they calculated the statistics for the F_1 score in one minute epochs from the channel which provided the highest F_1 score. In this project, the F_1 score was calculated from the total five minute length of any given recording. Furthermore, Andreotti and his team used the entire FECGSYN database (1750 signals) in their work whereas in this project, 35 signals were used. It is quite possible that better statistics would be achieved, which could improve the results, if further testing was done on the signals from the FECGSYNDB.

Overall, the results show similar trend; the BSS based methods were the best performing methods followed by AM and TS based methods.

Table 5.2: Median F_1 score for the fECG signal extraction from work completed by Androetti et al. (2016). The corresponding IQRs are show inside the parentheses.

Method	Case 0	Case 1	Case 2	Case 3	Case 4	Overall
BSS-JADE	100 (0.1)	99.7 (3.9)	100 (0.1)	89.4 (23.2)	87.1 (6.6)	99.9 (6.4)
BSS-PCA	99.9 (1.1)	99.3 (4.8)	99.8 (1.4)	94.5 (7.2)	86.4 (7.7)	98.7 (7.9)
TS-CER	97.7 (13.3)	99.0 (8.5)	98.5 (9.6)	77.4 (11.1)	87.8 (11.0)	95.0 (18.8)
TS-PCA	98.3 (11.8)	99.2 (7.6)	98.7 (9.3)	77.5 (10.2)	88.4 (10.8)	96.0 (18.5)
AM-LMS	99.1 (6.9)	99.5 (8.2)	99.5 (3.7)	80.2 (10.6)	87.1 (9.8)	97.1 (15.0)
MA-RLS	99.2 (6.0)	99.6 (4.2)	99.6 (3.4)	80.6 (11.1)	87.6 (9.4)	97.3 (14.6)
AM-ESN	99.6 (2.9)	99.7 (2.7)	99.6 (2.0)	82.5 (8.8)	87.4 (8.3)	97.9 (12.5)

Table 5.3: The median F_1 score for the fECG signal extraction methods using eight abdominal channels. The corresponding IQRs are show inside the parentheses.

Method	Case 0	Case 1	Case 2	Case 3	Case 4	Overall
BSS-JADE	99.9 (0.1)	97.2 (9.1)	99.9 (0.1)	82.7 (25.4)	82.1 (3.7)	97.2 (17.8)
BSS-PCA	99.9 (0.1)	99.9 (0.2)	99.9 (0.1)	80.5 (9.2)	84.4 (2.1)	99.7 (14.3)
TS-CER	77.0 (22.7)	98.3 (9.5)	99.4 (3.8)	79.7 (12.1)	83.1 (1.5)	83.6 (18.6)
TS-PCA	76.5 (23.1)	98.0 (8.9)	99.2 (3.6)	78.4 (11.3)	83.8 (2.1)	83.8 (19.9)
AM-LMS	82.5 (15.4)	99.2 (5.1)	99.2 (2.4)	76.7 (5.0)	83.4 (0.8)	83.4 (18.1)
MA-RLS	90.6 (12.2)	99.3 (1.9)	99.9 (0.1)	77.9 (3.9)	83.6 (1.5)	87.6 (16.1)
AM-ESN	95.2 (6.5)	99.1 (1.2)	99.3 (0.4)	84.6 (3.9)	84.2 (1.8)	93.4 (14.6)

5.4 Chapter Summary

The results for the different fECG extraction methods were presented in this chapter. All the methods were able to extract the fECG signal from the abdominal signal. However, depending on the signal quality and the physiological events affecting the abdominal signals, the extraction performance between the different methods varied significantly. Overall, the BSS methods outperformed the AM and TS based methods; the BSS-JADE algorithm achieved the top overall median F_1 score.

Furthermore, the BSS based methods were able to extract both fECG signals in the twin pregnancy case. However, the composite abdominal signal did not include any other

simulated physiological events so the question arises, how representative this synthetic signal is when compared to the real world twin pregnancy abdominal signals. Thus, more testing is required on a real world signal set to understand the true robustness and suitability of the BSS based fECG extraction methods for twin pregnancy cases.

The next chapter concludes this dissertation and includes notes about related future work for further research.

Chapter 6

Conclusion and Future Work

6.1 Dissertation Summary

This dissertation focused on researching novel methods for fECG extraction from a set of abdominal signals (non-invasive fECG). In addition, the most common ECG data storage and transfer formats were also covered.

The non-invasive fetal ECG measurement offers many advantages over the alternative fetal monitoring methods; clinically relevant information (i.e. fHR) can be extracted quickly, accurately and easily. There is also possibility for morphological analysis of the fetal ECG which provides a range of possibilities for antenatal safety monitoring.

The first two chapters covered background information on the fECG physiology and current extraction methods found in the literature. The ECG data transfer and storage formats, including implementation of ECG data accesses functions in to MATLAB, were discussed in chapter 3. Chapters 4 and 5 covered ECG extraction implementation to MATLAB and the results / performance comparison for the different fECG extraction methods.

A series of different non-invasive fetal ECG extraction methods were benchmarked in this dissertation; a total number of 11 different approaches were implemented in MATLAB and evaluated using synthetic abdominal test signals. The extraction methods were based on Adaptive Methods (AM), Template Subtraction (TS) or Blind Source Separation (BSS). The two main benchmarking performance metrics were F_1 score and Mean

Absolute Error (MAE), where the F_1 score measures the methods ability to detect the fetal QRS (fQRS) location and MAE provides a statistical measure for the difference in time between the detected fQRS and reference fQRS locations. The test signals provided 32 abdominal channels and all the methods were evaluated using a different number of abdominal channels (2, 4, 6, 9, 10, 15, 20 and 30 channels).

All the methods were able to extract fECG signal from the abdominal signal. However, SNR of the abdominal signal did have a significant affect on the performance of the extraction method; especially the TS and AM based methods seem to suffer more from noisy abdominal signal in comparison to the BSS methods. Furthermore, the abdominal channels selection can also have a substantial affect on the extraction performance. Especially, the BSS-ICA based methods are known to struggle when the number of input channels exceeds the number of underlying sources. The workaround for this is to use PCA dimension reduction to optimise the number of sources for the ICA calculation step. The results for AM and TS based methods generally improved as the the number of abdominal channels were increased. As these methods are single channel methods, this indicates that the ideal channel selection is important for best performance; the ideal abdominal signal includes high fECG SNR. The BSS based methods would generally achieve the best performance when a relatively low number of abdominal channels was used (2, 4 and 6).

The BSS JADE algorithm was the best performing method, for the single fetus case, achieving overall median F_1 score of 99.85 %. TS-PCA and AM-ESN were the best performing methods in their respective method categories achieving median F_1 score of 84.63 % and 95.44 % respectively.

The BSS based methods were evaluated for the twin pregnancy case. All the algorithms performed poorly when only two abdominal channels were used but the extraction performance improved significantly as the number of abdominal channels used was increased. FastICA algorithm using symmetric approach was the best performing method achieving median F_1 score of 99.89 % when 15 abdominal signals were used for the fECG extraction.

6.2 Future Work

Continuing on from this research, there are a number of different avenues that can be explored further in the field of non-invasive fECG extraction. Testing the extraction methods on real world signals would be one of the most obvious next steps. Testing the methods on synthetically generated signals is a good starting point; however, the simulated signals can only provide an approximate of the behaviour of real world signals.

The Physionet has several fECG databases available. However, the available databases are low in number of recordings, individuals and abdominal channels available. Only a few of the recordings have reference annotations available. Furthermore, currently there is no real world fECG signal database available for the multiple pregnancy case. As such, there is a need for an open-source fECG signal database which would ideally have multichannel abdominal ECG recordings (including mECG reference signal) from different subjects at different gestational ages. The database should include recordings from multiple pregnancies and include annotations as well.

For this dissertation, no consideration was given for parameter optimisation; the parameters for the prefilteration, fECG extraction and fQRS detection steps were adopted from the literature. As such, more research should go in to optimising the different parameters to achieve better fECG extraction performance.

Another interesting aspect for future research would be to combine two or more fECG extraction methods. The assumption is that different methods have their strengths and weaknesses, and that combining different methods might lead to a better outcome. For example, implementation of a hybrid method which would firstly remove the mECG component from the abdominal signal using either AM or TS based method and then use BSS based method to extract the fECG signal from the residuals. It should be mentioned that Behar et al. received the top score in the Phyionet 2013 challenge by using Fuse method which would selectively combine ICA-TS, ICA-TS-ICA, TS-ICA, ICA and TS methods (Silva et al. 2013, Behar et al. 2013).

The abdominal signal quality would be another area for further research. In addition, the AM based methods use mECG reference signal so depending on the extraction method, consideration should be given to the quality of both the abdominal and reference mECG signals. Obviously noisy and non-representative signals should not be used for fECG

extraction.

One quite specific area of further research would be to study the affect of the vernix caseosa layer on the fECG signal extraction. As reported in the literature, the very low conductivity vernix caseosa layer forms around 28th-32nd weeks and dissolves at 37th-38th weeks in normal pregnancies and this should limit the success of abdominal fECG recordings during this time period. However, there appears to be very limited information available in the literature to what extent the vernix caseosa layer influences the abdominal fECG extraction and as such, should be further quantified.

Lastly, from the literature, it appears that there are not many non-invasive fECG signal extraction apparatuses commercially available. Especially, there are no portable devices available fECG signal extraction so perhaps this is another area of further research in this field. The device should be small and easy to use. Also, to make the device comfortable to use for the end user and to simplify the design, a low number of abdominal electrodes should be used for the recording of the signal. However, this would probably mean that the signal processing issues mentioned in this dissertation would need to be addressed first.

References

AHA (2008), ‘Congenital Heart Defects in Children Fact Sheet’, online. [Accessed April 18, 2016; American Heart Association].

URL: *<http://www.americanheart.org/children>*

Alvi, M. S., Andreotti, F., Oster, J., Zaunseder, S., Clifford, G. D. & Behar, J. (2014), fecgsyngui: A gui interface to fecgsyn for simulation of maternal-foetal activity mixtures on abdominal electrocardiogram recordings, *in* ‘Computing in Cardiology Conference (CinC), 2014’, IEEE, pp. 541–544.

Ananthanag, K. & Sahambi, J. (2003), Investigation of blind source separation methods for extraction of fetal ecg, *in* ‘Electrical and Computer Engineering, 2003. IEEE CCECE 2003. Canadian Conference on’, Vol. 3, IEEE, pp. 2021–2024.

Andreotti, F., Behar, J., Zaunseder, S., Oster, J. & Clifford, G. D. (2016), ‘An open-source framework for stress-testing non-invasive foetal ecg extraction algorithms’, *Physiological Measurement* **37**(5), 627.

Andreotti, F., Riedl, M., Himmelsbach, T., Wedekind, D., Wessel, N., Stepan, H., Schmieder, C., Jank, A., Malberg, H. & Zaunseder, S. (2014), ‘Robust fetal ecg extraction and detection from abdominal leads’, *Physiological measurement* **35**(8), 1551.

ANSI/AAMIEC57:2012 (2012), Testing and reporting performance results of cardiac rhythm and st segment measurement algorithms, Standard, American National Standards Institute.

Ashley, E. A. & Niebauer, J. (2004), ‘Conquering the ecg’.

Australian regulatory guidelines for medical devices (ARGMD) (2011), Technical report, Department of Health and Aging - Therapeutic Goods Administration.

- URL:** <https://www.tga.gov.au/sites/default/files/devices-argmd-p1-01.pdf>
- Ayat, M., Assaleh, K. & Nashash, H. (2008), Fetal ecg extraction from a single abdominal ecg signal using svd and polynomial classifiers, *in* 'Machine Learning for Signal Processing, 2008. MLSP 2008. IEEE Workshop on', IEEE, pp. 250–254.
- Badilini, F. et al. (1998), 'The ishne holter standard output file format', *Annals of non-invasive electrocardiology* **3**, 263–266.
- Barnett, S. & Maulik, D. (2001), 'Guidelines and recommendations for safe use of doppler ultrasound in perinatal applications', *Journal of Maternal-Fetal Medicine* **10**(2), 75–84.
- Bass, G. & Shouldice, R. (2002), 'From bench to bedside', *The Engineers Journal* pp. 47–49.
- Behar, J., Andreotti, F., Zaunseder, S., Li, Q., Oster, J. & Clifford, G. D. (2014), 'An ecg simulator for generating maternal-foetal activity mixtures on abdominal ecg recordings', *Physiological measurement* **35**(8), 1537.
- Behar, J., Johnson, A., Clifford, G. D. & Oster, J. (2014), 'A comparison of single channel fetal ecg extraction methods', *Annals of biomedical engineering* **42**(6), 1340–1353.
- Behar, J., Oster, J. & Clifford, G. D. (2013), Non-invasive fecg extraction from a set of abdominal sensors, *in* 'Computing in Cardiology 2013', IEEE, pp. 297–300.
- Behar, J., Oster, J. & Clifford, G. D. (2014), 'Combining and benchmarking methods of foetal ecg extraction without maternal or scalp electrode data', *Physiological measurement* **35**(8), 1569.
- Biosemi (n.d.), 'Bdftoedf converter'.
URL: <http://www.biosemi.com/download/ToolsForRuntimeEngine861/Converter86.zip>
- Bond, R. R., Finlay, D. D., Nugent, C. D. & Moore, G. (2011), 'A review of ecg storage formats', *International journal of medical informatics* **80**(10), 681–697.
- Brown, B. & Badilini, F. (2015), *HL7 aECG Implementation Guide*.
URL: https://www.hl7.org/documentcenter/public_temp_5B305E0D-1C23-BA17-0C75E0EF4F029C8C/wg/rcrim/annecg/aECG%20Implementation%20Guide%202005-03-21%20final%203.pdf

- Brown, B., Kohls, M. & Stockbridge, N. (2012), *FDA XML Data Format Design Specification*.
URL: <http://xml.coverpages.org/FDA-EGC-XMLDataFormat-C.pdf>
- Cardoso, J.-F. & Souloumiac, A. (1993), Blind beamforming for non-gaussian signals, in 'IEE Proceedings F-Radar and Signal Processing', Vol. 140, IET, pp. 362–370.
- Cerutti, S., Baselli, G., Civardi, S., Ferrazzi, E., Marconi, A. M., Pagani, M. & Pardi, G. (1986), 'Variability analysis of fetal heart rate signals as obtained from abdominal electrocardiographic recordings', *Journal of Perinatal Medicine-Official Journal of the WAPM* **14**(6), 445–452.
- Chiang, C.-C., Tzeng, W.-C., Cheng, H.-C., Lin, C.-T., Yang, Y.-C., Liang, S.-F. & Lim, S.-B. (2007), 'Construction and application of an electronic ecg management system', *J. Inf. Technol. Appl* **2**(3), 135–140.
- Chiang, C., Yang, Y., Tzeng, W., Tseng, W. & Hsieh, J. (2004), An scp compatible 12-lead electrocardiogram database for signal transmission, storage, and analysis, in 'Computers in Cardiology, 2004', IEEE, pp. 621–624.
- Complications In A Multiples Pregnancy* (2015), online. [Accessed June 12, 2016, American Pregnancy Association].
URL: <http://americanpregnancy.org/multiples/complications>
- De Moor, B., De Gersem, P., De Schutter, B. & Favoreel, W. (1997), 'Daisy: A database for identification of systems', *JOURNAL A* **38**, 4–5.
- Di Marco, L. Y., Marzo, A. & Frangi, A. (2013), Multichannel foetal heartbeat detection by combining source cancellation with expectation-weighted estimation of fiducial points, in 'Computing in Cardiology 2013', IEEE, pp. 329–332.
- DICOM Supplement 30: Waveform Interchange* (1999).
URL: http://dicom.nema.org/Dicom/supps/sup30_lb.pdf
- EN1064:2005+A1:2007 (2007), Health informatics - standard communication protocol - computer-assisted electrocardiography, Standard, European Committee for Standardization, Brussels, Belgium.
- Fanelli, A., Signorini, M., Ferrario, M., Perego, P., Piccini, L., Andreoni, G. & Magenes, G. (2011), Telefetalcare: a first prototype of a wearable fetal electrocardiograph, in

- 'Engineering in Medicine and Biology Society, EMBC, 2011 Annual International Conference of the IEEE', IEEE, pp. 6899–6902.
- Fanelli, A., Signorini, M. & Heldt, T. (2012), Extraction of fetal heart rate from maternal surface ecg with provisions for multiple pregnancies, *in* 'Engineering in Medicine and Biology Society (EMBC), 2012 Annual International Conference of the IEEE', IEEE, pp. 6165–6168.
- Fischer, R., Chiarugi, F. & Zywiets, T. (2006), Enhanced integrated format and content checking for processing of scp ecg records, *in* '2006 Computers in Cardiology', IEEE, pp. 413–416.
- Goldberger, A. L., Amaral, L. A. N., Glass, L., Hausdorff, J. M., Ivanov, P. C., Mark, R. G., Mietus, J. E., Moody, G. B., Peng, C.-K. & Stanley, H. E. (2000 (June 13)), 'PhysioBank, PhysioToolkit, and PhysioNet: Components of a new research resource for complex physiologic signals', *Circulation* **101**(23), e215–e220. *Circulation Electronic Pages*: <http://circ.ahajournals.org/cgi/content/full/101/23/e215> PMID:1085218; doi: 10.1161/01.CIR.101.23.e215.
- Goodyer, A., Geiger, A. & Monroe, W. (1942), 'Clinical Fetal Electrocardiography', *Yale Journal of Biology and Medicine* .
- Helfenbein, E., Gregg, R. & Zhou, S. (2004), Philips medical systems support for open ecg and standardization efforts, *in* 'Computers in Cardiology, 2004', IEEE, pp. 393–396.
- Hilbel, T., Brown, B., De Bie, J., Lux, R. & Katus, H. (2007*a*), Innovation and advantage of the dicom ecg standard for viewing, interchange and permanent archiving of the diagnostic electrocardiogram, *in* '2007 Computers in Cardiology', IEEE, pp. 633–636.
- Hilbel, T., Brown, B., De Bie, J., Lux, R. & Katus, H. (2007*b*), Innovation and advantage of the dicom ecg standard for viewing, interchange and permanent archiving of the diagnostic electrocardiogram, *in* '2007 Computers in Cardiology', IEEE, pp. 633–636.
- Hill, M. (2016), 'Embryology Australian Statistics', online. [Accessed April 18, 2016].
URL: https://embryology.med.unsw.edu.au/embryology/index.php/Australian_Statistics
- Hurezeanu, B., Ungureanu, G. M., Taralunga, D. D., Strungaru, R., Gussi, I. & Wolf, W. (2014), Fecg delineation from abdominal signals using wavelet transform, *in* 'Elec-

- trical and Power Engineering (EPE), 2014 International Conference and Exposition on', IEEE, pp. 518–521.
- Hurst, J. W. (1998), 'Naming of the waves in the ecg, with a brief account of their genesis', *Circulation* **98**(18), 1937–1942.
- Hyvarinen, A. (1999), 'Fast and robust fixed-point algorithms for independent component analysis', *IEEE transactions on Neural Networks* **10**(3), 626–634.
- ISO (2007), Health informatics – medical waveform format – part 92001: Encoding rules, Standard, International Organization for Standardization, Geneva, CH.
- ISO22077-1:2015 (2015), Health informatics - medical waveform format - part 1: Encoding rules, Standard, International Organization for Standardization.
- James, C. J. & Hesse, C. W. (2004), 'Independent component analysis for biomedical signals', *Physiological measurement* **26**(1), R15.
- Jones, J. & Weerakkody, Y. (2016), 'Fetal heart rate', online. [Accessed August 18, 2016].
URL: <http://radiopaedia.org/articles/fetal-heart-rate>
- Jumaa, H., Fayn, J. & Rubel, P. (2008), Xml based mediation for automating the storage of scp-ecg data into relational databases, in 'Computers in Cardiology, 2008', IEEE, pp. 445–448.
- Kam, A. & Cohen, A. (2000), Separation of twins fetal ecg by means of blind source separation (bss), in 'Electrical and electronic engineers in israel, 2000. the 21st ieee convention of the', IEEE, pp. 342–345.
- Kanjilal, P. P., Palit, S. & Saha, G. (1997), 'Fetal ecg extraction from single-channel maternal ecg using singular value decomposition', *IEEE Transactions on Biomedical Engineering* **44**(1), 51–59.
- Kemp, B. & Oliven, J. (2003), 'European data format plus (EDF+), an edf alike standard format for the exchange of physiological data', *Clinical Neurophysiology* **114**(9), 1755–1761.
- Kemp, B., Värri, A., Rosa, A. C., Nielsen, K. D. & Gade, J. (1992), 'A simple format for exchange of digitized polygraphic recordings', *Electroencephalography and clinical neurophysiology* **82**(5), 391–393.

- Khamene, A. & Negahdaripour, S. (2000), 'A new method for the extraction of fetal ecg from the composite abdominal signal', *Biomedical Engineering, IEEE Transactions on* **47**(4), 507–516.
- Kimura, E., Norihiko, T. & Ishihara, K. (2006), Development mfer (medical waveform format encoding rules) parser, *in* 'AMIA annual symposium proceedings', Vol. 2006, American Medical Informatics Association, p. 985.
- Kligfield, P., Gettes, L. S., Bailey, J. J., Childers, R., Deal, B. J., Hancock, E. W., van Herpen, G., Kors, J. A., Macfarlane, P., Mirvis, D. M. et al. (2007), 'Recommendations for the standardization and interpretation of the electrocardiogram: part i: the electrocardiogram and its technology a scientific statement from the american heart association electrocardiography and arrhythmias committee, council on clinical cardiology; the american college of cardiology foundation; and the heart rhythm society endorsed by the international society for computerized electrocardiology', *Journal of the American College of Cardiology* **49**(10), 1109–1127.
- Kovács, F., Horváth, C., Balogh, Á. T. & Hosszú, G. (2011), 'Fetal phonocardiography past and future possibilities', *Computer methods and programs in biomedicine* **104**(1), 19–25.
- Lindsley, D. B. (1942), 'Heart and brain potentials of human fetuses in utero', *The American Journal of Psychology* **55**(3), 412–416.
- Ling-Ling, W., Ni-Ni, R., Li-Xi, P. & Gang, W. (2006), Developing a dicom middleware to implement ecg conversion and viewing, *in* 'Engineering in Medicine and Biology Society, 2005. IEEE-EMBS 2005. 27th Annual International Conference of the', IEEE, pp. 6953–6956.
- Lu, X., Duan, H. & Zheng, H. (2007), Xml-ecg: An xml-based ecg presentation for data exchanging, *in* 'Bioinformatics and Biomedical Engineering, 2007. ICBBE 2007. The 1st International Conference on', IEEE, pp. 1141–1144.
- Lunshof, S., Boer, K., Wolf, H., van Hoffen, G., Bayram, N. & Mirmiran, M. (1998), 'Fetal and maternal diurnal rhythms during the third trimester of normal pregnancy: Outcomes of computerized analysis of continuous twenty-fourhour fetal heart rate recordings', *American journal of obstetrics and gynecology* **178**(2), 247–254.

- Mandellos, G. J., Koukias, M. N. & Lymberopoulos, D. K. (2008), Structuring the e-scp-ecg+ protocol for multi vital-sign handling, *in* 'BioInformatics and BioEngineering, 2008. BIBE 2008. 8th IEEE International Conference on', IEEE, pp. 1–6.
- Mandellos, G. J., Koukias, M. N., Styliadis, I. S. & Lymberopoulos, D. K. (2010), 'e-scp-ecg+ protocol: An expansion on scp-ecg protocol for health telemonitoring pilot implementation', *International journal of telemedicine and applications* **2010**, 1.
- Martens, S. M., Rabotti, C., Mischi, M. & Sluijter, R. J. (2007), 'A robust fetal ecg detection method for abdominal recordings', *Physiological measurement* **28**(4), 373.
- McSharry, P. E., Clifford, G. D., Tarassenko, L. & Smith, L. A. (2003), 'A dynamical model for generating synthetic electrocardiogram signals', *Biomedical Engineering, IEEE Transactions on* **50**(3), 289–294.
- Medical waveform description Format Encoding Rules* (2003). Available: <http://ecg.heart.or.jp/En/MFER101E-2003.pdf>.
- Muro, M., Shono, H., Shono, M., Uchiyama, A. & Iwasaka, T. (2004), 'Changes in diurnal variations in the fetal heart rate baseline with advancing gestational age', *Sleep and Biological Rhythms* **2**, 83–85.
- Nagarkoti, S. K., Singh, B. & Kumar, M. (2012), An algorithm for fetal heart rate detection using wavelet transform, *in* 'Recent Advances in Information Technology (RAIT), 2012 1st International Conference on', IEEE, pp. 838–840.
- NEALS (2008), 'Understanding the basic anatomy and physiology of the human body - the cardiovascular system', online. [Accessed 16-August-2016; State of New South Wales, Department of Education and Training].
URL: http://lrrpublic.cli.det.nsw.edu.au/lrrSecure/Sites/LRRView/7700/documents/5657/5657/5657_02.htm
- Neilson, D. R., Freeman, R. K. & Mangan, S. (2008), 'Signal ambiguity resulting in unexpected outcome with external fetal heart rate monitoring', *American journal of obstetrics and gynecology* **198**(6), 717–724.
- Oostendorp, T., Van Oosterom, A. & Jongasma, H. (1989), 'Electrical properties of tissues involved in the conduction of foetal ecg', *Medical and Biological Engineering and Computing* **27**(3), 322–324.

- Pagano, R. R. (2012), *Understanding statistics in the behavioral sciences*, Cengage Learning.
- Pan, J. & Tompkins, W. J. (1985), 'A real-time qrs detection algorithm', *IEEE transactions on biomedical engineering* (3), 230–236.
- Park, Y., Lee, K., Youn, D., Kim, N., Kim, W. & Park, S. (1992), 'On detecting the presence of fetal r-wave using the moving averaged magnitude difference algorithm', *IEEE transactions on biomedical engineering* .
- Peters, M., Crowe, J., Piéri, J.-F., Quartero, H., Hayes-Gill, B., James, D., Stinstra, J. & Shakespeare, S. (2001), 'Monitoring the fetal heart non-invasively: a review of methods', *Journal of perinatal medicine* **29**(5), 408–416.
- Podziemski, P. & Gieraltowski, J. (2013), Fetal heart rate discovery: algorithm for detection of fetal heart rate from noisy, noninvasive fetal ecg recordings, in 'Computing in Cardiology 2013', IEEE, pp. 333–336.
- Pope, J. & Latson, L. (2011), 'Fetal blood flow', online. [Accessed 16-August-2016; Healthwise Inc.].
URL: <http://www.uofmhealth.org/health-library/hw255772>
- Pregnant with twins: potential complications* (2012), online. [Accessed June 12, 2016; Babycenter Australia].
URL: <http://www.babycenter.com.au/a3584/pregnant-with-twins-potential-complications>
- Rajesh, A. & Ganesan, R. (2014), 'Comprehensive study on fetal ecg extraction'. [2014 International Conference on Control, Instrumentation, Communication and Computational Technologies (ICCICCT)].
- Roberts, S. & Everson, R. (2001), *Independent component analysis: principles and practice*, Cambridge University Press.
- Sakkalis, V., Chiarugi, F., Kostomanolakis, S., Chronaki, C., Tsiknakis, M. & Orphanoudakis, S. (2003), A gateway between the scp-ecg and the dicom supplement 30 waveform standard, in 'Computers in Cardiology, 2003', IEEE, pp. 25–28.
- Sameni, R. & Clifford, G. D. (2010), 'A review of fetal ecg signal processing; issues and promising directions', *The open pacing, electrophysiology & therapy journal* **3**, 4.

- Sameni, R., Clifford, G. D., Jutten, C. & Shamsollahi, M. B. (2007), ‘Multichannel ecg and noise modeling: application to maternal and fetal ecg signals’, *EURASIP Journal on Applied Signal Processing* **2007**(1), 94–94.
- Sargam, D. P. & Sahambi, J. (2004), A comparative survey on removal of mecg artifacts from fecg using ica algorithms, in ‘Intelligent Sensing and Information Processing, 2004. Proceedings of International Conference on’, IEEE, pp. 88–91.
- Sasaki, Y. et al. (2007), ‘The truth of the f-measure’, *Teach Tutor mater* pp. 1–5.
- Schloegl, A., Chiarugi, F., Cervesato, E., Apostolopoulos, E. & Chronaki, C. (2007), Two-way converter between the hl7 aecg and scp-ecg data formats using biosig, in ‘Computers in Cardiology, 2007’, IEEE, pp. 253–256.
- Schlögl, A. (2006), ‘Gdf-a general dataformat for biosignals’, *arXiv preprint cs/0608052*.
- Schlögl, A. (2009), An overview on data formats for biomedical signals, in ‘World Congress on Medical Physics and Biomedical Engineering, September 7-12, 2009, Munich, Germany’, Springer, pp. 1557–1560.
- Schlögl, A. (2013), ‘Gdf-a general dataformat for biosignals v2.51’, *arXiv preprint cs/0608052*.
- Schlögl, A. & Brunner, C. (2008), ‘Biosig: a free and open source software library for bci research’, *Computer* **41**(10), 44–50.
- Silva, I., Behar, J., Sameni, R., Zhu, T., Oster, J., Clifford, G. D. & Moody, G. B. (2013), Noninvasive fetal ecg: the physionet/computing in cardiology challenge 2013, in ‘Computing in Cardiology Conference (CinC), 2013’, IEEE, pp. 149–152.
- Silva, I., Moody, B., Behar, J., Johnson, A., Oster, J., Clifford, G. D. & Moody, G. B. (2015), ‘Robust detection of heart beats in multimodal data’, *Physiological measurement* **36**(8), 1629.
- Soleit, E., Gadallah, M. & Salah, A. (2002), Adaptive Detection of the Fetus ECG Signal, in ‘Nineteenth National Radio Science’.
- Sridhar-Keralapura, M., Pourfathi, M. & Sirkeci-Mergen, B. (2010), Independent component analysis with data-centric contrast functions for separating maternal and twin fetal ecg, in ‘Proceedings of the World Congress on Engineering and Computer Science’, Vol. 2, Citeseer.

- Stinstra, J. G. (2001), The reliability of the fetal magnetocardiogram, Ph.d. dissertation, University of Twente. Available: <http://doc.utwente.nl/35964/>.
- Taralunga, D., Ungureanu, M., Strungaru, R. & Wolf, W. (2011), Performance comparison of four ica algorithms applied for fecg extraction from transabdominal recordings, in 'Signals, Circuits and Systems (ISSCS), 2011 10th International Symposium on', IEEE, pp. 1–4.
- Trigo, J. D., Alesanco, Á., Martínez, I. & García, J. (2012), 'A review on digital ecg formats and the relationships between them', *Information Technology in Biomedicine, IEEE Transactions on* **16**(3), 432–444.
- Trigo, J. D., Chiarugi, F., Alesanco, Á., Martínez-Espronedada, M., Serrano, L., Chronaki, C. E., Escayola, J., Martínez, I. & García, J. (2010), 'Interoperability in digital electrocardiography: harmonization of iso/ieee x73-phd and scp-ecg', *Information Technology in Biomedicine, IEEE Transactions on* **14**(6), 1303–1317.
- URMC (2016), 'Complications of multiple pregnancy', online. [Online; accessed June 12, 2016; University of Rochester Medical Center].
URL: <https://www.urmc.rochester.edu/Encyclopedia/Content.aspx?ContentTypeID=85&ContentID=P08021>
- Van Leeuwen, P., Lange, S., Klein, A., Geue, D. & Grönemeyer, D. H. (2004), 'Dependency of magnetocardiographically determined fetal cardiac time intervals on gestational age, gender and postnatal biometrics in healthy pregnancies', *BMC pregnancy and childbirth* **4**(1), 1.
- Van Oosterom, A. (1989), 'Lead systems for the abdominal fetal electrocardiogram', *Clinical Physics and Physiological Measurement* **10**(4B), 21.
- Varanini, M., Tartarisco, G., Billeci, L., Macerata, A., Pioggia, G. & Balocchi, R. (2013), A multi-step approach for non-invasive fetal ecg analysis, in 'Computing in Cardiology 2013', IEEE, pp. 281–284.
- VIC DHHS (2012), 'Summary of ten most frequently reported birth defects in victoria', online. [Accessed April 18, 2016; Victoria Department of Health & Human Services].
URL: <https://www2.health.vic.gov.au/about/publications/researchandreports/Summary%20of%20ten%20most%20frequently%20reported%20birth%20defects%20in%20Victoria%202003-2004>

- Vullings, R., Peters, C., Sluijter, R., Mischi, M., Oei, S. & Bergmans, J. (2009), 'Dynamic segmentation and linear prediction for maternal ecg removal in antenatal abdominal recordings', *Physiological measurement* **30**(3), 291.
- Wan, H., Liu, Q. & Chai, J. (2008), A method for extracting fecg based on ica algorithm, *in* 'Signal Processing, 2008. ICSP 2008. 9th International Conference on', IEEE, pp. 2761–2764.
- Wang, H., Azuaje, F., Clifford, G., Jung, B. & Black, N. (2004), Methods and tools for generating and managing ecgml-based information, *in* 'Computers in Cardiology, 2004', IEEE, pp. 573–576.
- Wei, Z., Hongxing, L. & Jianchun, C. (2010), 'Adaptive filtering in phase space for foetal electrocardiogram estimation from an abdominal electrocardiogram signal and a thoracic electrocardiogram signal', *IET Signal Processing Journal* .
- Widrow, B., Glover, J. R., McCool, J. M., Kaunitz, J., Williams, C. S., Hearn, R. H., Zeidler, J. R., Dong, J. E. & Goodlin, R. C. (1975), 'Adaptive noise cancelling: Principles and applications', *Proceedings of the IEEE* **63**(12), 1692–1716.
- Zareba, W., Locati, E. H. & Blanche, P. M. (1998), 'The ishne holter standard output file format: a step toward compatibility of holter systems', *Annals of noninvasive electrocardiology* **3**(3), 261–262.
- Zaunseder, S., Andreotti, F., Cruz, M., Stepan, H., Schmieder, C., Malberg, H., Jank, A. & Wessel, N. (2012), Fetal qrs detection by means of kalman filtering and using the event synchronous canceller, *in* '7th international workshop on biosignal interpretation'.
- Zhang, J.-w., Wang, L.-p., Liu, X., Zhu, H.-h. & Dong, J. (2010), Chinese cardiovascular disease database (ccdd) and its management tool, *in* 'BioInformatics and BioEngineering (BIBE), 2010 IEEE International Conference on', IEEE, pp. 66–72.
- Zywietz, C. & Fischer, R. (2004), Integrated content and format checking for processing of scp ecg records, *in* 'Computers in Cardiology, 2004', IEEE, pp. 37–40.
- Zywietz, C., Kraemer, M., Fischer, R. & Widiger, B. (2004), 'Integrating the ecg enterprise: Hes-ecg with the built-in vital signs information nomenclature', *Computers in Cardiology* **31**(1), 41–44.

Appendix A

Project Specification

ENG 4111/2 Research Project

Project Specification

For: **Jarkko Jarvinen**
Topic: Extraction of ECGs for Twin Pregnancies
Supervisor: John Leis
Sponsorship: Faculty of Health, Engineering & Sciences

Project Aim: To research and develop methods for fetal ECG (fECG) signal extraction during twin pregnancies.

Program:

1. Research the current methods for fECG signal extraction during singleton and twin/multiple pregnancies.
2. Critically examine the different fECG signal extraction methods found during the literature research.
3. Investigate ECG data storage formats, and obtain MATLABTM data access functions if they exist. If none are publically available, then implement and test suitable MATLAB ECG data access functions based on available specifications.
4. Implement selected methods, which were found during the literature research, to evaluate their performance.
5. Search online biomedical signal databases for suitable ECG signal(s) to be used for testing. If suitable ECG signal(s) are not found, create a synthetic test signal.
6. Code the selected methods using MATLAB.
7. Test the program and critically examine the results. Compare the test results against the results found during the literature research.

As time and resources permit:

1. Propose methods for improving the performance of the methods already investigated.
2. Implement, test and critically evaluate the proposals.

Agreed:

Student Name: Jarkko Jarvinen
Date: 16/02/2016

Supervisor Name: John Leis
Date: 16/02/2016

Appendix B

fECG Extraction Raw Results

This appendix presents the raw results for the different fECG extraction methods. The reported results are F_1 , MAE, TP, FN, FP, SE and PPV.

B.1 Case 0 - Baseline + Noise

Table B.1: Extracted fECG raw results for the Case 0 (SNR 0 dB)

0db																	
	No. Leads	F_1	MAE	TP	FN	FP	SE	PPV		No. Leads	F_1	MAE	TP	FN	FP	SE	PPV
AF-LMS	2	64.90	1.10	416	269	181	60.73	69.68	TS-PCA	2	49.80	1.89	316	369	268	46.13	54.11
	4	64.90	1.10	416	269	181	60.73	69.68		4	49.80	1.89	316	369	268	46.13	54.11
	6	64.90	1.10	416	269	181	60.73	69.68		6	49.80	1.89	316	369	268	46.13	54.11
	8	82.50	0.84	547	138	94	79.85	85.34		8	63.92	1.30	411	274	190	60.00	68.39
	10	82.50	0.84	547	138	94	79.85	85.34		10	63.92	1.30	411	274	190	60.00	68.39
	15	82.50	0.84	547	138	94	79.85	85.34		15	63.92	1.30	411	274	190	60.00	68.39
	20	82.50	0.84	547	138	94	79.85	85.34		20	63.92	1.30	411	274	190	60.00	68.39
	30	88.94	0.55	599	86	63	87.45	90.48		30	74.85	0.91	491	194	136	71.68	78.31
AF-RLS	2	69.21	0.85	453	232	171	66.13	72.60	FASTICA-DEF	2	99.56	0.38	682	3	3	99.56	99.56
	4	69.21	0.85	453	232	171	66.13	72.60		4	99.93	1.93	684	1	0	99.85	100
	6	69.21	0.85	453	232	171	66.13	72.60		6	97.87	1.14	666	19	10	97.23	98.52
	8	85.33	0.61	570	115	81	83.21	87.56		8	100	0.36	685	0	0	100	100
	10	85.33	0.61	570	115	81	83.21	87.56		10	100	0.39	685	0	0	100	100
	15	85.33	0.61	570	115	81	83.21	87.56		15	100	0.44	685	0	0	100	100
	20	85.33	0.61	570	115	81	83.21	87.56		20	100	0.45	685	0	0	100	100
	30	90.48	0.49	613	72	57	89.49	91.49		30	99.78	1.36	683	2	1	99.71	99.85
AF-ENS	2	85.95	0.49	575	110	78	83.94	88.06	FASTICA-SYM	2	99.85	0.38	684	1	1	99.85	99.85
	4	87.52	0.51	589	96	72	85.99	89.11		4	100	0.29	685	0	0	100	100
	6	87.25	0.51	585	100	71	85.40	89.18		6	83.14	0.67	562	123	105	82.04	84.26
	8	93.36	0.54	633	52	38	92.41	94.34		8	100	0.36	685	0	0	100	100
	10	94.33	0.49	641	44	33	93.58	95.10		10	99.85	1.19	684	1	1	99.85	99.85
	15	95.01	0.52	647	38	30	94.45	95.57		15	64.06	4.07	393	292	149	57.37	72.51
	20	95.52	0.46	650	35	26	94.89	96.15		20	100	1.83	685	0	0	100	100
	30	96.70	0.41	659	26	19	96.20	97.20		30	100	2.25	685	0	0	100	100
TS	2	47.46	1.95	299	386	276	43.65	52.00	JADE	2	99.56	0.38	682	3	3	99.56	99.56
	4	47.46	1.95	299	386	276	43.65	52.00		4	100	0.30	685	0	0	100	100
	6	47.46	1.95	299	386	276	43.65	52.00		6	100	0.28	685	0	0	100	100
	8	63.34	1.34	412	273	204	60.15	66.88		8	100	0.36	685	0	0	100	100
	10	63.34	1.34	412	273	204	60.15	66.88		10	100	0.39	685	0	0	100	100
	15	63.34	1.34	412	273	204	60.15	66.88		15	100	0.44	685	0	0	100	100
	20	63.34	1.34	412	273	204	60.15	66.88		20	100	0.45	685	0	0	100	100
	30	71.20	1.06	466	219	158	68.03	74.68		30	100	0.43	685	0	0	100	100
TS-CERUTTI	2	49.64	1.93	312	373	260	45.55	54.55	PCA	2	99.85	0.37	684	1	1	99.85	99.85
	4	49.64	1.93	312	373	260	45.55	54.55		4	98.98	0.24	676	9	5	98.69	99.27
	6	49.64	1.93	312	373	260	45.55	54.55		6	100	0.21	685	0	0	100	100
	8	64.86	1.31	418	267	186	61.02	69.21		8	100	0.30	685	0	0	100	100
	10	64.86	1.31	418	267	186	61.02	69.21		10	100	0.32	685	0	0	100	100
	15	64.86	1.31	418	267	186	61.02	69.21		15	100	0.39	685	0	0	100	100
	20	64.86	1.31	418	267	186	61.02	69.21		20	100	0.42	685	0	0	100	100
	30	73.30	1.04	479	206	143	69.93	77.01		30	100	0.37	685	0	0	100	100
TS-LP	2	41.19	1.99	257	428	306	37.52	45.65		2	41.19	1.99	257	428	306	37.52	45.65
	4	41.19	1.99	257	428	306	37.52	45.65		4	41.19	1.99	257	428	306	37.52	45.65
	6	41.19	1.99	257	428	306	37.52	45.65		6	41.19	1.99	257	428	306	37.52	45.65
	8	53.11	1.54	337	348	247	49.20	57.71		8	53.11	1.54	337	348	247	49.20	57.71
	10	53.11	1.54	337	348	247	49.20	57.71		10	53.11	1.54	337	348	247	49.20	57.71
	15	53.11	1.54	337	348	247	49.20	57.71		15	53.11	1.54	337	348	247	49.20	57.71
	20	53.21	1.48	336	349	242	49.05	58.13		20	53.21	1.48	336	349	242	49.05	58.13
	30	61.54	1.31	392	293	197	57.23	66.55		30	61.54	1.31	392	293	197	57.23	66.55

Table B.2: Extracted fECG raw results for the Case 0 (SNR 3 dB)

3db																	
	No. Leads	F ₁	MAE	TP	FN	FP	SE	PPV		No. Leads	F ₁	MAE	TP	FN	FP	SE	PPV
AF-LMS	2	81.93	2.72	544	141	99	79.42	84.60	TS-PCA	2	75.19	2.83	500	185	145	72.99	77.52
	4	81.93	2.72	544	141	99	79.42	84.60		4	75.19	2.83	500	185	145	72.99	77.52
	6	81.93	2.72	544	141	99	79.42	84.60		6	75.19	2.83	500	185	145	72.99	77.52
	8	81.93	2.72	544	141	99	79.42	84.60		8	75.19	2.83	500	185	145	72.99	77.52
	10	81.93	2.72	544	141	99	79.42	84.60		10	75.19	2.83	500	185	145	72.99	77.52
	15	84.77	3.03	562	123	79	82.04	87.68		15	76.52	3.11	502	183	125	73.29	80.06
	20	89.09	1.57	600	85	62	87.59	90.63		20	82.24	1.76	544	141	94	79.42	85.27
30	89.42	3.24	600	85	57	87.59	91.32	30	84.40	3.29	560	125	82	81.75	87.23		
AF-RLS	2	87.56	2.65	584	101	65	85.26	89.99	FASTICA-DEF	2	99.78	2.49	684	1	2	99.85	99.71
	4	87.56	2.65	584	101	65	85.26	89.99		4	99.56	3.24	682	3	3	99.56	99.56
	6	87.56	2.65	584	101	65	85.26	89.99		6	99.85	1.18	685	0	2	100	99.71
	8	87.56	2.65	584	101	65	85.26	89.99		8	99.85	1.11	685	0	2	100	99.71
	10	87.56	2.65	584	101	65	85.26	89.99		10	99.93	0.81	684	1	0	99.85	100
	15	87.56	2.65	584	101	65	85.26	89.99		15	100	2.63	685	0	0	100	100
	20	88.04	1.58	589	96	64	85.99	90.20		20	99.93	2.18	684	1	0	99.85	100
30	91.72	3.23	615	70	41	89.78	93.75	30	100	1.67	685	0	0	100	100		
AF-ENS	2	91.18	2.13	615	70	49	89.78	92.62	FASTICA-SYM	2	99.78	2.52	684	1	2	99.85	99.71
	4	90.19	2.12	611	74	59	89.20	91.19		4	99.78	0.30	684	1	2	99.85	99.71
	6	90.84	2.07	615	70	54	89.78	91.93		6	83.65	3.02	560	125	94	81.75	85.63
	8	92.63	2.17	628	57	43	91.68	93.59		8	99.85	0.24	685	0	2	100	99.71
	10	90.61	2.10	613	72	55	89.49	91.77		10	99.85	2.29	685	0	2	100	99.71
	15	92.32	2.18	625	60	44	91.24	93.42		15	99.85	1.39	685	0	2	100	99.71
	20	93.07	3.25	631	54	40	92.12	94.04		20	99.85	1.37	685	0	2	100	99.71
30	94.13	3.31	641	44	36	93.58	94.68	30	100	1.67	685	0	0	100	100		
TS	2	74.39	2.78	491	194	144	71.68	77.32	JADE	2	99.85	0.31	685	0	2	100	99.71
	4	74.39	2.78	491	194	144	71.68	77.32		4	99.78	0.30	684	1	2	99.85	99.71
	6	74.39	2.78	491	194	144	71.68	77.32		6	97.95	0.98	669	16	12	97.66	98.24
	8	74.39	2.78	491	194	144	71.68	77.32		8	99.85	0.24	685	0	2	100	99.71
	10	74.39	2.78	491	194	144	71.68	77.32		10	99.85	0.25	685	0	2	100	99.71
	15	79.52	2.09	526	159	112	76.79	82.45		15	100	1.23	685	0	0	100	100
	20	79.52	2.09	526	159	112	76.79	82.45		20	99.85	0.4	685	0	2	100	99.71
30	81.78	3.34	541	144	97	78.98	84.80	30	100	1.2321	685	0	0	100	100		
TS-CERUTTI	2	74.91	2.79	494	191	140	72.12	77.92	PCA	2	99.64	2.46	683	2	3	99.71	99.56
	4	74.91	2.79	494	191	140	72.12	77.92		4	70.00	1.92	462	223	173	67.45	72.76
	6	74.91	2.79	494	191	140	72.12	77.92		6	99.85	0.46	685	0	2	100	99.71
	8	74.91	2.79	494	191	140	72.12	77.92		8	99.85	0.46	685	0	2	100	99.71
	10	74.91	2.79	494	191	140	72.12	77.92		10	100	3.19	685	0	0	100	100
	15	76.57	3.19	505	180	129	73.72	79.65		15	99.93	3.00	685	0	1	100	99.85
	20	80.91	1.69	534	151	101	77.96	84.09		20	99.93	3.17	685	0	1	100	99.85
30	83.03	3.32	548	137	87	80.00	86.30	30	99.93	3.20	685	0	1	100	99.85		
TS-LP	2	67.74	2.77	440	245	174	64.23	71.66		2	67.74	2.77	440	245	174	64.23	71.66
	4	67.74	2.77	440	245	174	64.23	71.66		4	67.74	2.77	440	245	174	64.23	71.66
	6	67.74	2.77	440	245	174	64.23	71.66		6	67.74	2.77	440	245	174	64.23	71.66
	8	67.74	2.77	440	245	174	64.23	71.66		8	67.74	2.77	440	245	174	64.23	71.66
	10	67.74	2.77	440	245	174	64.23	71.66		10	67.74	2.77	440	245	174	64.23	71.66
	15	82.89	2.23	550	135	92	80.29	85.67		15	82.89	2.23	550	135	92	80.29	85.67
	20	82.89	2.23	550	135	92	80.29	85.67		20	82.89	2.23	550	135	92	80.29	85.67
30	82.89	2.23	550	135	92	80.29	85.67	30	82.89	2.23	550	135	92	80.29	85.67		

Table B.4: Extracted fECG raw results for the Case 0 (SNR 9 dB)

9db																	
	No. Leads	F ₁	MAE	TP	FN	FP	SE	PPV		No. Leads	F ₁	MAE	TP	FN	FP	SE	PPV
AF-LMS	2	95.82	0.47	653	33	24	95.19	96.46	TS-PCA	2	98.32	0.54	672	14	9	97.96	98.68
	4	95.82	0.47	653	33	24	95.19	96.46		4	98.32	0.54	672	14	9	97.96	98.68
	6	97.29	0.70	664	22	15	96.79	97.79		6	98.32	0.54	672	14	9	97.96	98.68
	8	97.29	0.70	664	22	15	96.79	97.79		8	98.32	0.54	672	14	9	97.96	98.68
	10	97.29	0.70	664	22	15	96.79	97.79		10	98.32	0.54	672	14	9	97.96	98.68
	15	97.29	0.70	664	22	15	96.79	97.79		15	99.42	0.25	681	5	3	99.27	99.56
	20	98.25	0.30	673	13	11	98.11	98.39		20	99.78	0.37	684	2	1	99.71	99.85
	30	98.39	0.71	674	12	10	98.25	98.54		30	99.78	0.37	684	2	1	99.71	99.85
AF-RLS	2	99.64	0.45	682	4	1	99.42	99.85	FASTICA-DEF	2	99.71	2.06	682	4	0	99.42	100
	4	99.64	0.45	682	4	1	99.42	99.85		4	90.79	3.49	611	75	49	89.07	92.58
	6	99.78	0.65	684	2	1	99.71	99.85		6	100	0.48	686	0	0	100	100
	8	99.78	0.65	684	2	1	99.71	99.85		8	100	2.50	686	0	0	100	100
	10	99.78	0.65	684	2	1	99.71	99.85		10	100	0.48	686	0	0	100	100
	15	99.85	0.16	685	1	1	99.85	99.85		15	100	0.51	686	0	0	100	100
	20	100	0.27	686	0	0	100	100		20	100	0.51	686	0	0	100	100
	30	100	0.68	686	0	0	100	100		30	100	1.60	686	0	0	100	100
AF-ENS	2	99.56	0.37	683	3	3	99.56	99.56	FASTICA-SYM	2	98.76	1.98	675	11	6	98.40	99.12
	4	99.56	0.38	683	3	3	99.56	99.56		4	87.92	2.49	593	93	70	86.44	89.44
	6	99.56	1.57	682	4	2	99.42	99.71		6	97.44	3.34	666	20	15	97.09	97.80
	8	99.85	1.10	685	1	1	99.85	99.85		8	100	1.58	686	0	0	100	100
	10	99.71	0.38	684	2	2	99.71	99.71		10	100	1.18	686	0	0	100	100
	15	99.85	0.14	685	1	1	99.85	99.85		15	100	0.44	686	0	0	100	100
	20	99.85	0.24	685	1	1	99.85	99.85		20	100	1.47	686	0	0	100	100
	30	99.85	0.42	685	1	1	99.85	99.85		30	100	1.75	686	0	0	100	100
TS	2	97.36	0.49	663	23	13	96.65	98.08	JADE	2	98.90	1.99	677	9	6	98.69	99.12
	4	97.36	0.49	663	23	13	96.65	98.08		4	100	0.33	686	0	0	100	100
	6	97.95	0.67	668	18	10	97.38	98.53		6	98.76	2.66	676	10	7	98.54	98.98
	8	97.95	0.67	668	18	10	97.38	98.53		8	100	0.41	686	0	0	100	100
	10	97.95	0.67	668	18	10	97.38	98.53		10	100	1.18	686	0	0	100	100
	15	99.64	0.23	683	3	2	99.56	99.71		15	100	1.16	686	0	0	100	100
	20	100	0.32	686	0	0	100	100		20	100	0.50	686	0	0	100	100
	30	100	0.32	686	0	0	100	100		30	100	0.50	686	0	0	100	100
TS-CERUTTI	2	97.14	0.52	663	23	16	96.65	97.64	PCA	2	93.56	1.92	632	54	33	92.13	95.04
	4	97.14	0.52	663	23	16	96.65	97.64		4	100	0.48	686	0	0	100	100
	6	97.65	0.70	666	20	12	97.09	98.23		6	100	0.51	686	0	0	100	100
	8	97.65	0.70	666	20	12	97.09	98.23		8	100	0.50	686	0	0	100	100
	10	97.65	0.70	666	20	12	97.09	98.23		10	100	0.42	686	0	0	100	100
	15	99.49	0.26	682	4	3	99.42	99.56		15	100	0.51	686	0	0	100	100
	20	100	0.35	686	0	0	100	100		20	100	0.45	686	0	0	100	100
	30	100	0.35	686	0	0	100	100		30	100	3.42	686	0	0	100	100
TS-LP	2	95.50	0.58	647	39	22	94.32	96.71									
	4	95.50	0.58	647	39	22	94.32	96.71									
	6	95.50	0.58	647	39	22	94.32	96.71									
	8	95.50	0.58	647	39	22	94.32	96.71									
	10	95.50	0.58	647	39	22	94.32	96.71									
	15	95.79	0.38	649	37	20	94.61	97.01									
	20	97.42	0.55	661	25	10	96.36	98.51									
	30	97.42	0.55	661	25	10	96.36	98.51									

B.2 Case 1 - Fetal Movement + Noise

Table B.6: Extracted fECG raw results for the Case 1 (SNR 0 dB)

odb																	
	No. Leads	F ₁	MAE	TP	FN	FP	SE	PPV		No. Leads	F ₁	MAE	TP	FN	FP	SE	PPV
AF-LMS	2	75.91	0.89	501	185	133	73.03	79.02	TS-PCA	2	58.05	1.34	377	309	236	54.96	61.50
	4	75.91	0.89	501	185	133	73.03	79.02		4	58.05	1.34	377	309	236	54.96	61.50
	6	75.91	0.89	501	185	133	73.03	79.02		6	58.05	1.34	377	309	236	54.96	61.50
	8	81.12	0.81	537	149	101	78.28	84.17		8	62.95	1.20	406	280	198	59.18	67.22
	10	81.12	0.81	537	149	101	78.28	84.17		10	62.95	1.20	406	280	198	59.18	67.22
	15	81.12	0.81	537	149	101	78.28	84.17		15	62.95	1.20	406	280	198	59.18	67.22
	20	81.12	0.81	537	149	101	78.28	84.17		20	62.95	1.20	406	280	198	59.18	67.22
30	81.12	0.81	537	149	101	78.28	84.17	30	63.23	1.23	411	275	203	59.91	66.94		
AF-RLS	2	78.31	0.74	520	166	122	75.80	81.00	FASTICA-DEF	2	90.98	1.19	615	71	51	89.65	92.34
	4	78.31	0.74	520	166	122	75.80	81.00		4	99.78	2.26	684	2	1	99.71	99.85
	6	78.31	0.74	520	166	122	75.80	81.00		6	68.51	2.35	434	252	147	63.27	74.70
	8	84.65	0.78	568	118	88	82.80	86.59		8	67.72	1.37	429	257	152	62.54	73.84
	10	84.65	0.78	568	118	88	82.80	86.59		10	95.99	0.93	634	52	1	92.42	99.84
	15	84.65	0.78	568	118	88	82.80	86.59		15	86.82	1.28	527	159	1	76.82	99.81
	20	84.65	0.78	568	118	88	82.80	86.59		20	78.51	2.09	464	222	32	67.64	93.55
30	84.65	0.78	568	118	88	82.80	86.59	30	83.97	1.05	529	157	45	77.11	92.16		
AF-ENS	2	93.44	0.47	634	52	37	92.42	94.49	FASTICA-SYM	2	90.36	1.12	609	77	53	88.78	91.99
	4	91.34	0.52	617	69	48	89.94	92.78		4	93.07	1.62	598	88	1	87.17	99.83
	6	93.04	0.53	628	58	36	91.55	94.58		6	97.01	1.00	648	38	2	94.46	99.69
	8	94.93	0.56	646	40	29	94.17	95.70		8	97.39	0.99	653	33	2	95.19	99.70
	10	93.88	0.57	637	49	34	92.86	94.93		10	73.27	1.70	488	198	158	71.14	75.54
	15	95.02	0.58	648	38	30	94.46	95.58		15	96.64	1.13	661	25	21	96.36	96.92
	20	94.63	0.56	643	43	30	93.73	95.54		20	84.38	1.34	516	170	21	75.22	96.09
30	95.44	0.53	649	37	25	94.61	96.29	30	86.05	1.31	543	143	33	79.16	94.27		
TS	2	58.40	1.21	377	309	228	54.96	62.31	JADE	2	99.78	0.47	685	1	2	99.85	99.71
	4	58.40	1.21	377	309	228	54.96	62.31		4	99.93	0.42	686	0	1	100	99.85
	6	58.40	1.21	377	309	228	54.96	62.31		6	99.34	0.48	680	6	3	99.13	99.56
	8	62.72	0.99	403	283	196	58.75	67.28		8	99.34	0.48	680	6	3	99.13	99.56
	10	62.72	0.99	403	283	196	58.75	67.28		10	99.93	0.48	686	0	1	100	99.85
	15	62.72	0.99	403	283	196	58.75	67.28		15	96.39	0.49	640	46	2	93.29	99.69
	20	62.72	0.99	403	283	196	58.75	67.28		20	88.11	1.68	578	108	48	84.26	92.33
30	62.72	0.99	403	283	196	58.75	67.28	30	87.88	1.45	562	124	31	81.92	94.77		
TS-CERUTTI	2	57.34	1.29	371	315	237	54.08	61.02	PCA	2	94.71	1.61	618	68	1	90.09	99.84
	4	57.34	1.29	371	315	237	54.08	61.02		4	95.51	0.70	648	38	23	94.46	96.57
	6	57.34	1.29	371	315	237	54.08	61.02		6	94.89	0.66	641	45	24	93.44	96.39
	8	63.20	1.10	407	279	195	59.33	67.61		8	97.65	0.64	664	22	10	96.79	98.52
	10	63.20	1.10	407	279	195	59.33	67.61		10	94.76	0.72	642	44	27	93.59	95.96
	15	63.20	1.10	407	279	195	59.33	67.61		15	94.11	0.88	615	71	6	89.65	99.03
	20	63.20	1.10	407	279	195	59.33	67.61		20	99.34	0.44	678	8	1	98.83	99.85
30	63.20	1.10	407	279	195	59.33	67.61	30	98.46	0.43	670	16	5	97.67	99.26		
TS-LP	2	52.52	1.44	333	353	249	48.54	57.22		2	52.52	1.44	333	353	249	48.54	57.22
	4	52.52	1.44	333	353	249	48.54	57.22		4	52.52	1.44	333	353	249	48.54	57.22
	6	52.52	1.44	333	353	249	48.54	57.22		6	52.52	1.44	333	353	249	48.54	57.22
	8	56.87	1.37	360	326	220	52.48	62.07		8	56.87	1.37	360	326	220	52.48	62.07
	10	56.87	1.37	360	326	220	52.48	62.07		10	56.87	1.37	360	326	220	52.48	62.07
	15	56.87	1.37	360	326	220	52.48	62.07		15	56.87	1.37	360	326	220	52.48	62.07
	20	56.87	1.37	360	326	220	52.48	62.07		20	56.87	1.37	360	326	220	52.48	62.07
30	58.97	1.37	378	308	218	55.10	63.42	30	58.97	1.37	378	308	218	55.10	63.42		

Table B.7: Extracted fECG raw results for the Case 1 (SNR 3 dB)

3db																	
	No. Leads	F ₁	MAE	TP	FN	FP	SE	PPV		No. Leads	F ₁	MAE	TP	FN	FP	SE	PPV
AF-LMS	2	99.56	0.47	681	4	2	99.42	99.71	TS-PCA	2	98.02	0.52	668	17	10	97.52	98.53
	4	99.56	0.47	681	4	2	99.42	99.71		4	98.02	0.52	668	17	10	97.52	98.53
	6	99.56	0.47	681	4	2	99.42	99.71		6	98.02	0.52	668	17	10	97.52	98.53
	8	99.56	0.47	681	4	2	99.42	99.71		8	98.02	0.52	668	17	10	97.52	98.53
	10	99.56	0.47	681	4	2	99.42	99.71		10	98.02	0.52	668	17	10	97.52	98.53
	15	99.56	0.47	681	4	2	99.42	99.71		15	98.02	0.52	668	17	10	97.52	98.53
	20	99.56	0.47	681	4	2	99.42	99.71		20	98.02	0.52	668	17	10	97.52	98.53
30	99.56	0.47	681	4	2	99.42	99.71	30	98.02	0.52	668	17	10	97.52	98.53		
AF-RLS	2	99.34	0.43	681	4	5	99.42	99.27	FASTICA-DEF	2	99.71	1.85	682	3	1	99.56	99.85
	4	99.34	0.43	681	4	5	99.42	99.27		4	94.77	2.19	643	42	29	93.87	95.69
	6	99.34	0.43	681	4	5	99.42	99.27		6	96.37	1.76	651	34	15	95.04	97.75
	8	99.34	0.43	681	4	5	99.42	99.27		8	97.69	1.08	654	31	0	95.47	100
	10	99.34	0.43	681	4	5	99.42	99.27		10	87.73	0.76	536	149	1	78.25	99.81
	15	99.34	0.43	681	4	5	99.42	99.27		15	95.18	1.44	622	63	0	90.80	100
	20	99.34	0.43	681	4	5	99.42	99.27		20	77.41	1.50	497	188	102	72.56	82.97
30	99.34	0.43	681	4	5	99.42	99.27	30	80.64	1.41	504	181	61	73.58	89.20		
AF-ESN	2	99.12	0.40	679	6	6	99.12	99.12	FASTICA-SYM	2	100	1.14	685	0	0	100	100
	4	98.47	0.40	674	11	10	98.39	98.54		4	91.55	1.59	607	78	34	88.61	94.70
	6	98.76	0.42	676	9	8	98.69	98.83		6	95.90	0.84	631	54	0	92.12	100
	8	99.05	0.49	678	7	6	98.98	99.12		8	97.46	0.63	651	34	0	95.04	100
	10	98.69	0.42	676	9	9	98.69	98.69		10	87.98	0.96	538	147	0	78.54	100
	15	98.98	0.38	678	7	7	98.98	98.98		15	92.30	0.76	587	98	0	85.69	100
	20	98.83	0.41	677	8	8	98.83	98.83		20	92.36	2.29	598	87	12	87.30	98.03
30	98.83	0.42	676	9	7	98.69	98.98	30	83.63	1.37	526	159	47	76.79	91.80		
TS	2	98.09	0.52	669	16	10	97.66	98.53	JADE	2	100	0.49	685	0	0	100	100
	4	98.09	0.52	669	16	10	97.66	98.53		4	100	0.45	685	0	0	100	100
	6	98.09	0.52	669	16	10	97.66	98.53		6	97.80	0.47	666	19	11	97.23	98.38
	8	98.09	0.52	669	16	10	97.66	98.53		8	97.15	0.80	648	37	1	94.599	99.85
	10	98.09	0.52	669	16	10	97.66	98.53		10	96.29	0.75	636	49	0	92.847	100
	15	98.09	0.52	669	16	10	97.66	98.53		15	94.62	0.78	615	70	0	89.781	100
	20	98.09	0.52	669	16	10	97.66	98.53		20	86.96	1.4383	527	158	0	76.934	100
30	98.09	0.52	669	16	10	97.66	98.53	30	86.04	1.4109	533	152	21	77.81	96.209		
TS-CERUTTI	2	98.32	0.53	671	14	9	97.96	98.68	PCA	2	100	0.49	685	0	0	100	100
	4	98.32	0.53	671	14	9	97.96	98.68		4	100	0.57	685	0	0	100	100
	6	98.32	0.53	671	14	9	97.96	98.68		6	99.49	0.58	681	4	3	99	99.56
	8	98.32	0.53	671	14	9	97.96	98.68		8	99.85	0.58	684	1	1	100	99.85
	10	98.32	0.53	671	14	9	97.96	98.68		10	99.71	0.32	682	3	1	100	100
	15	98.32	0.53	671	14	9	97.96	98.68		15	99.34	0.38	680	5	4	99	99.42
	20	98.32	0.53	671	14	9	97.96	98.68		20	99.71	0.43	682	3	1	100	99.85
30	98.32	0.53	671	14	9	97.96	98.68	30	99.34	0.41	679	6	3	99	99.56		
TS-LP	2	92.07	0.66	621	64	43	90.66	93.52		2	92.07	0.66	621	64	43	90.66	93.52
	4	92.07	0.66	621	64	43	90.66	93.52		4	92.07	0.66	621	64	43	90.66	93.52
	6	92.07	0.66	621	64	43	90.66	93.52		6	92.07	0.66	621	64	43	90.66	93.52
	8	92.07	0.66	621	64	43	90.66	93.52		8	92.07	0.66	621	64	43	90.66	93.52
	10	92.07	0.66	621	64	43	90.66	93.52		10	92.07	0.66	621	64	43	90.66	93.52
	15	92.07	0.66	621	64	43	90.66	93.52		15	92.07	0.66	621	64	43	90.66	93.52
	20	92.07	0.66	621	64	43	90.66	93.52		20	92.07	0.66	621	64	43	90.66	93.52
30	92.07	0.66	621	64	43	90.66	93.52	30	92.07	0.66	621	64	43	90.66	93.52		

Table B.14: Extracted fECG raw results for the Case 2 (SNR 9 dB)

9db																	
	No. Leads	F ₁	MAE	TP	FN	FP	SE	PPV		No. Leads	F ₁	MAE	TP	FN	FP	SE	PPV
AF-LMS	2	99.18	0.48	661	8	3	98.80	99.55	TS-PCA	2	99.18	0.49	662	7	4	98.95	99.40
	4	99.18	0.48	661	8	3	98.80	99.55		4	99.18	0.49	662	7	4	98.95	99.40
	6	99.18	0.48	661	8	3	98.80	99.55		6	99.18	0.49	662	7	4	98.95	99.40
	8	99.18	0.48	661	8	3	98.80	99.55		8	99.18	0.49	662	7	4	98.95	99.40
	10	99.18	0.48	661	8	3	98.80	99.55		10	99.18	0.49	662	7	4	98.95	99.40
	15	99.18	0.48	661	8	3	98.80	99.55		15	99.18	0.49	662	7	4	98.95	99.40
	20	99.33	0.56	664	5	4	99.25	99.40		20	99.18	0.49	662	7	4	98.95	99.40
30	99.85	0.51	667	2	0	99.70	100	30	99.48	0.53	666	3	4	99.55	99.40		
AF-RLS	2	99.85	0.50	668	1	1	99.85	99.85	FASTICA-DEF	2	64.27	2.86	411	258	199	61.44	67
	4	99.85	0.50	668	1	1	99.85	99.85		4	100	0.52	669	0	0	100	100
	6	99.85	0.50	668	1	1	99.85	99.85		6	100	1.23	668	1	0	100	100
	8	99.93	0.54	669	0	1	100	99.85		8	83.07	3.16	547	122	101	81.76	84.41
	10	99.93	0.54	669	0	1	100	99.85		10	100	1.48	668	1	0	100	100
	15	99.93	0.54	669	0	1	100	99.85		15	83.35	0.74	548	121	98	81.91	84.83
	20	99.93	0.54	669	0	1	100	99.85		20	100	1.19	669	0	0	100	100
30	99.93	0.54	669	0	1	100	99.85	30	100	2.10	666	3	2	100	100		
AF-ENS	2	99.78	0.47	667	2	1	99.70	99.85	FASTICA-SYM	2	93.35	1.23	611	58	29	91.33	95.47
	4	99.63	0.48	666	3	2	99.55	99.70		4	99.93	1.45	668	1	0	99.85	100
	6	99.78	0.47	667	2	1	99.70	99.85		6	83.24	0.98	539	130	87	80.57	86.10
	8	99.93	0.50	668	1	0	99.85	100		8	100	2.51	669	0	0	100	100
	10	99.93	0.50	668	1	0	99.85	100		10	84.03	0.87	542	127	79	81.02	87.28
	15	99.93	0.50	668	1	0	99.85	100		15	96.83	1.40	641	28	14	95.82	97.86
	20	99.93	0.54	668	1	0	99.85	100		20	100	1.75	668	1	0	100	100
30	99.93	0.52	668	1	0	99.85	100	30	100	2.37	669	0	0	100	100		
TS	2	99.63	0.49	667	2	3	99.70	99.55	JADE	2	100	0.52	669	0	0	100	100
	4	99.63	0.49	667	2	3	99.70	99.55		4	100	0.51	668	1	0	100	100
	6	99.63	0.49	667	2	3	99.70	99.55		6	99.93	0.50	668	1	0	99.85	100
	8	99.63	0.55	667	2	3	99.70	99.55		8	100	0.51	668	1	0	100	100
	10	99.63	0.64	667	2	3	99.70	99.55		10	100	0.51	668	1	0	100	100
	15	99.63	0.64	667	2	3	99.70	99.55		15	100	0.51	668	1	0	100	100
	20	99.63	0.59	667	2	3	99.70	99.55		20	100	0.52	668	1	0	100	100
30	99.78	0.53	668	1	2	99.85	99.70	30	100	0.52	668	1	0	100	100		
TS-CERUTTI	2	99.40	0.50	665	4	4	99.40	99.40	PCA	2	99.93	2.00	668	1	0	99.85	100
	4	99.40	0.50	665	4	4	99.40	99.40		4	100	0.56	669	0	1	100	100
	6	99.40	0.50	665	4	4	99.40	99.40		6	100	0.58	669	0	1	100	100
	8	99.40	0.50	665	4	4	99.40	99.40		8	100	0.58	669	0	1	100	100
	10	99.40	0.50	665	4	4	99.40	99.40		10	100	0.60	669	0	1	100	100
	15	99.40	0.50	665	4	4	99.40	99.40		15	100	0.61	669	0	2	100	100
	20	99.40	0.50	665	4	4	99.40	99.40		20	100	0.64	669	0	6	100	99.11
30	99.48	0.49	666	3	4	99.55	99.40	30	100	0.61	669	0	2	100	100		
TS-LP	2	95.31	0.49	630	39	23	94.17	96.48									
	4	95.31	0.49	630	39	23	94.17	96.48									
	6	95.31	0.49	630	39	23	94.17	96.48									
	8	95.31	0.49	630	39	23	94.17	96.48									
	10	95.31	0.49	630	39	23	94.17	96.48									
	15	95.31	0.49	630	39	23	94.17	96.48									
	20	95.31	0.49	630	39	23	94.17	96.48									
30	95.48	0.56	633	36	24	94.62	96.35										

B.4 Case 3 - Uterine Contraction + Noise

Table B.16: Extracted fECG raw results for the Case 3 (SNR 0 dB)

odb																	
	No. Leads	F ₁	MAE	TP	FN	FP	SE	PPV		No. Leads	F ₁	MAE	TP	FN	FP	SE	PPV
AF-LMS	2	76.12	0.91	526	191	139	73.36	79.10	TS-PCA	2	69.21	1.00	427	290	90	59.55	82.59
	4	76.12	0.91	526	191	139	73.36	79.10		4	69.21	1.00	427	290	90	59.55	82.59
	6	76.12	0.91	526	191	139	73.36	79.10		6	69.21	1.00	427	290	90	59.55	82.59
	8	76.12	0.91	526	191	139	73.36	79.10		8	69.21	1.00	427	290	90	59.55	82.59
	10	76.12	0.91	526	191	139	73.36	79.10		10	69.21	1.00	427	290	90	59.55	82.59
	15	76.12	0.91	526	191	139	73.36	79.10		15	69.21	1.00	427	290	90	59.55	82.59
	20	76.12	0.91	526	191	139	73.36	79.10		20	69.21	1.00	427	290	90	59.55	82.59
30	76.12	0.91	526	191	139	73.36	79.10	30	69.21	1.00	427	290	90	59.55	82.59		
AF-RLS	2	76.82	0.96	532	185	136	74.20	79.64	FASTICA-DEF	2	61.54	1.43	404	313	192	56.35	67.79
	4	76.82	0.96	532	185	136	74.20	79.64		4	64.25	1.28	416	301	162	58.02	71.97
	6	76.82	0.96	532	185	136	74.20	79.64		6	63.55	1.29	414	303	172	57.74	70.65
	8	76.82	0.96	532	185	136	74.20	79.64		8	64.14	1.22	415	302	162	57.88	71.92
	10	76.82	0.96	532	185	136	74.20	79.64		10	64.64	1.72	435	282	194	60.67	69.16
	15	76.82	0.96	532	185	136	74.20	79.64		15	65.18	1.44	423	294	158	59.00	72.81
	20	76.82	0.96	532	185	136	74.20	79.64		20	63.02	1.29	409	308	172	57.04	70.40
30	76.82	0.96	532	185	136	74.20	79.64	30	62.67	1.31	408	309	177	56.90	69.74		
AF-ENS	2	84.75	0.72	600	117	99	83.68	85.84	FASTICA-SYM	2	97.00	0.54	696	21	22	97.07	96.94
	4	84.11	0.74	593	124	100	82.71	85.57		4	95.03	2.23	679	38	33	94.70	95.37
	6	84.50	0.75	597	120	99	83.26	85.78		6	64.71	1.42	441	276	205	61.51	68.27
	8	84.60	0.77	596	121	96	83.12	86.13		8	64.38	1.57	440	277	210	61.37	67.69
	10	83.22	0.72	585	132	104	81.59	84.91		10	63.60	1.35	415	302	173	57.88	70.58
	15	83.88	0.71	593	124	104	82.71	85.08		15	99.65	1.24	715	2	3	99.72	99.58
	20	84.40	0.75	595	122	98	82.99	85.86		20	65.23	2.96	438	279	188	61.09	69.97
30	83.75	0.72	590	127	102	82.29	85.26	30	63.85	2.48	431	286	202	60.11	68.09		
TS	2	69.54	0.82	427	290	84	59.55	83.56	JADE	2	96.86	0.54	695	22	23	96.93	96.80
	4	69.54	0.82	427	290	84	59.55	83.56		4	99.37	0.52	713	4	5	99.44	99.30
	6	69.54	0.82	427	290	84	59.55	83.56		6	99.37	0.50	713	4	5	99.44	99.30
	8	69.54	0.82	427	290	84	59.55	83.56		8	99.30	0.51	713	4	6	99.44	99.17
	10	69.54	0.82	427	290	84	59.55	83.56		10	65.67	0.49	353	364	5	49.23	98.60
	15	69.54	0.82	427	290	84	59.55	83.56		15	65.92	0.49	354	363	3	49.37	99.16
	20	69.54	0.82	427	290	84	59.55	83.56		20	65.12	0.52	350	367	8	48.82	97.77
30	69.54	0.82	427	290	84	59.55	83.56	30	64.74	0.52	348	369	10	48.54	97.21		
TS-CERUTTI	2	69.16	0.90	425	292	87	59.28	83.01	PCA	2	97.63	0.54	701	16	18	97.77	97.50
	4	69.16	0.90	425	292	87	59.28	83.01		4	84.04	2.09	582	135	86	81.17	87.13
	6	69.16	0.90	425	292	87	59.28	83.01		6	93.35	0.54	667	50	45	93.03	93.68
	8	69.16	0.90	425	292	87	59.28	83.01		8	93.49	0.54	668	49	44	93.17	93.82
	10	69.16	0.90	425	292	87	59.28	83.01		10	94.82	0.53	677	40	34	94.42	95.22
	15	69.16	0.90	425	292	87	59.28	83.01		15	96.78	0.50	692	25	21	96.51	97.06
	20	69.16	0.90	425	292	87	59.28	83.01		20	98.33	0.51	705	12	12	98.33	98.33
30	69.16	0.90	425	292	87	59.28	83.01	30	96.77	0.54	690	27	19	96.23	97.32		
TS-LP	2	63.52	1.29	390	327	121	54.39	76.32		2	63.52	1.29	390	327	121	54.39	76.32
	4	63.52	1.29	390	327	121	54.39	76.32		4	63.52	1.29	390	327	121	54.39	76.32
	6	63.52	1.29	390	327	121	54.39	76.32		6	63.52	1.29	390	327	121	54.39	76.32
	8	63.52	1.29	390	327	121	54.39	76.32		8	63.52	1.29	390	327	121	54.39	76.32
	10	63.52	1.29	390	327	121	54.39	76.32		10	63.52	1.29	390	327	121	54.39	76.32
	15	63.52	1.29	390	327	121	54.39	76.32		15	63.52	1.29	390	327	121	54.39	76.32
	20	63.52	1.29	390	327	121	54.39	76.32		20	63.52	1.29	390	327	121	54.39	76.32
30	63.52	1.29	390	327	121	54.39	76.32	30	63.52	1.29	390	327	121	54.39	76.32		

Table B.17: Extracted fECG raw results for the Case 3 (SNR 3 dB)

3db																	
	No. Leads	F ₁	MAE	TP	FN	FP	SE	PPV		No. Leads	F ₁	MAE	TP	FN	FP	SE	PPV
AF-LMS	2	83.26	0.69	587	130	106	81.87	84.70	TS-PCA	2	82.48	0.72	539	178	51	75.17	91.36
	4	83.26	0.69	587	130	106	81.87	84.70		4	82.48	0.72	539	178	51	75.17	91.36
	6	83.26	0.69	587	130	106	81.87	84.70		6	82.48	0.72	539	178	51	75.17	91.36
	8	83.26	0.69	587	130	106	81.87	84.70		8	82.48	0.72	539	178	51	75.17	91.36
	10	83.26	0.69	587	130	106	81.87	84.70		10	82.48	0.72	539	178	51	75.17	91.36
	15	83.26	0.69	587	130	106	81.87	84.70		15	82.48	0.72	539	178	51	75.17	91.36
	20	83.26	0.69	587	130	106	81.87	84.70		20	82.48	0.72	539	178	51	75.17	91.36
30	83.26	0.69	587	130	106	81.87	84.70	30	82.48	0.72	539	178	51	75.17	91.36		
AF-RLS	2	84.03	0.72	592	125	100	82.57	85.55	FASTICA-DEF	2	63.47	1.52	430	287	208	59.97	67.40
	4	84.03	0.72	592	125	100	82.57	85.55		4	61.28	1.67	413	304	218	57.60	65.45
	6	84.03	0.72	592	125	100	82.57	85.55		6	98.82	0.52	709	8	9	98.88	98.75
	8	84.03	0.72	592	125	100	82.57	85.55		8	79.50	0.75	543	174	106	75.73	83.67
	10	84.03	0.72	592	125	100	82.57	85.55		10	96.77	1.70	690	27	19	96.23	97.32
	15	84.03	0.72	592	125	100	82.57	85.55		15	95.47	1.32	685	32	33	95.54	95.40
	20	84.03	0.72	592	125	100	82.57	85.55		20	99.23	0.50	712	5	6	99.30	99.16
30	84.03	0.72	592	125	100	82.57	85.55	30	96.16	1.06	688	29	26	95.96	96.36		
AF-ENS	2	88.81	0.72	627	90	68	87.45	90.22	FASTICA-SYM	2	96.80	0.52	695	22	24	96.93	96.66
	4	88.39	0.68	624	93	71	87.03	89.78		4	60.52	1.25	394	323	191	54.95	67.35
	6	89.77	0.67	636	81	64	88.70	90.86		6	78.30	2.55	534	183	113	74.48	82.54
	8	88.62	0.70	627	90	71	87.45	89.83		8	66.67	1.95	443	274	169	61.79	72.39
	10	89.85	0.70	637	80	64	88.84	90.87		10	88.57	1.25	616	101	58	85.91	91.40
	15	88.97	0.72	629	88	68	87.73	90.24		15	69.59	1.31	469	248	162	65.41	74.33
	20	88.02	0.68	621	96	73	86.61	89.48		20	99.23	1.44	712	5	6	99.30	99.16
30	88.91	0.68	629	88	69	87.73	90.12	30	90.83	1.09	644	73	57	89.82	91.87		
TS	2	85.02	0.67	556	161	35	77.55	94.08	JADE	2	96.59	0.52	693	24	25	96.65	96.52
	4	85.02	0.67	556	161	35	77.55	94.08		4	83.44	1.70	582	135	96	81.17	85.84
	6	85.02	0.67	556	161	35	77.55	94.08		6	98.68	0.52	708	9	10	98.75	98.61
	8	85.02	0.67	556	161	35	77.55	94.08		8	82.79	0.52	517	200	15	72.11	97.18
	10	85.02	0.67	556	161	35	77.55	94.08		10	98.54	0.50	707	10	11	98.61	98.47
	15	85.02	0.67	556	161	35	77.55	94.08		15	99.16	0.50	712	5	7	99.30	99.03
	20	85.02	0.67	556	161	35	77.55	94.08		20	80.87	1.69	556	161	102	77.55	84.50
30	85.02	0.67	556	161	35	77.55	94.08	30	98.75	0.51	709	8	10	98.88	98.61		
TS-CERUTTI	2	83.81	0.72	546	171	40	76.15	93.17	PCA	2	94.69	1.99	678	39	37	94.56	94.83
	4	83.81	0.72	546	171	40	76.15	93.17		4	88.73	0.64	630	87	73	87.87	89.62
	6	83.81	0.72	546	171	40	76.15	93.17		6	85.67	0.67	589	128	69	82.15	89.51
	8	83.81	0.72	546	171	40	76.15	93.17		8	85.76	0.67	602	115	85	83.96	87.63
	10	83.81	0.72	546	171	40	76.15	93.17		10	86.21	0.61	591	126	63	82.43	90.37
	15	83.81	0.72	546	171	40	76.15	93.17		15	86.74	0.60	595	122	60	82.99	90.84
	20	83.81	0.72	546	171	40	76.15	93.17		20	87.37	0.61	602	115	59	83.96	91.07
30	83.81	0.72	546	171	40	76.15	93.17	30	87.08	0.62	600	117	61	83.68	90.77		
TS-LP	2	77.77	0.90	516	201	94	71.97	84.59		2	77.77	0.90	516	201	94	71.97	84.59
	4	77.77	0.90	516	201	94	71.97	84.59		4	77.77	0.90	516	201	94	71.97	84.59
	6	77.77	0.90	516	201	94	71.97	84.59		6	77.77	0.90	516	201	94	71.97	84.59
	8	77.77	0.90	516	201	94	71.97	84.59		8	77.77	0.90	516	201	94	71.97	84.59
	10	77.77	0.90	516	201	94	71.97	84.59		10	77.77	0.90	516	201	94	71.97	84.59
	15	77.77	0.90	516	201	94	71.97	84.59		15	77.77	0.90	516	201	94	71.97	84.59
	20	77.77	0.90	516	201	94	71.97	84.59		20	77.77	0.90	516	201	94	71.97	84.59
30	77.77	0.90	516	201	94	71.97	84.59	30	77.77	0.90	516	201	94	71.97	84.59		

Table B.18: Extracted fECG raw results for the Case 3 (SNR 6 dB)

6db																	
	No. Leads	F ₁	MAE	TP	FN	FP	SE	PPV		No. Leads	F ₁	MAE	TP	FN	FP	SE	PPV
AF-LMS	2	69.48	1.21	469	249	163	65.32	74.21	TS-PCA	2	64.39	0.84	377	341	76	52.51	83.22
	4	69.48	1.21	469	249	163	65.32	74.21		4	64.39	0.84	377	341	76	52.51	83.22
	6	69.48	1.21	469	249	163	65.32	74.21		6	64.39	0.84	377	341	76	52.51	83.22
	8	69.48	1.21	469	249	163	65.32	74.21		8	64.39	0.84	377	341	76	52.51	83.22
	10	69.48	1.21	469	249	163	65.32	74.21		10	64.39	0.84	377	341	76	52.51	83.22
	15	69.48	1.21	469	249	163	65.32	74.21		15	64.39	0.84	377	341	76	52.51	83.22
	20	75.24	1.14	518	200	141	72.15	78.60		20	73.49	0.84	445	273	48	61.98	90.26
30	75.58	0.97	520	198	138	72.42	79.03	30	76.67	0.70	465	253	30	64.76	93.94		
AF-RLS	2	72.47	1.18	491	227	146	68.38	77.08	FASTICA-DEF	2	79.89	1.12	558	160	121	77.72	82.18
	4	72.47	1.18	491	227	146	68.38	77.08		4	73.14	1.34	505	213	158	70.33	76.17
	6	72.47	1.18	491	227	146	68.38	77.08		6	58.22	1.60	377	341	200	52.51	65.34
	8	72.47	1.18	491	227	146	68.38	77.08		8	52.52	2.17	339	379	234	47.21	59.16
	10	72.47	1.18	491	227	146	68.38	77.08		10	52.90	2.07	338	380	222	47.08	60.36
	15	72.47	1.18	491	227	146	68.38	77.08		15	64.37	1.06	421	297	169	58.64	71.36
	20	76.00	1.12	524	194	137	72.98	79.27		20	100	0.53	718	0	0	100	100
30	76.68	1.07	531	187	136	73.96	79.61	30	96.58	1.18	692	26	23	96.38	96.78		
AF-ENS	2	77.91	0.84	543	175	133	75.63	80.33	FASTICA-SYM	2	80.03	1.12	559	159	120	77.86	82.33
	4	77.73	0.80	541	177	133	75.35	80.27		4	57.67	1.78	376	342	210	52.37	64.16
	6	79.14	0.84	552	166	125	76.88	81.54		6	49.65	2.36	319	399	248	44.43	56.26
	8	78.57	0.83	548	170	129	76.32	80.95		8	63.96	1.48	426	292	188	59.33	69.38
	10	78.31	0.85	545	173	129	75.91	80.86		10	54.63	1.99	357	361	232	49.72	60.61
	15	78.17	0.85	546	172	133	76.05	80.41		15	89.94	0.79	639	79	64	89.00	90.90
	20	82.61	0.81	582	136	109	81.06	84.23		20	62.74	1.38	415	303	190	57.80	68.60
30	84.44	0.69	597	121	99	83.15	85.78	30	79.18	1.00	557	161	132	77.58	80.84		
TS	2	65.87	0.84	387	331	70	53.90	84.68	JADE	2	85.86	0.66	607	111	89	84.54	87.21
	4	65.87	0.84	387	331	70	53.90	84.68		4	62.60	2.46	421	297	206	58.64	67.15
	6	65.87	0.84	387	331	70	53.90	84.68		6	46.21	1.29	241	477	84	33.57	74.15
	8	65.87	0.84	387	331	70	53.90	84.68		8	63.88	1.52	420	298	177	58.50	70.35
	10	65.87	0.84	387	331	70	53.90	84.68		10	63.22	1.54	416	302	182	57.94	69.57
	15	65.87	0.84	387	331	70	53.90	84.68		15	64.04	1.50	422	296	178	58.77	70.33
	20	74.98	0.82	457	261	44	63.65	91.22		20	99.16	0.53	712	6	6	99.16	99.16
30	76.62	0.62	467	251	34	65.04	93.21	30	99.16	0.53	712	6	6	99.16	99.16		
TS-CERUTTI	2	64.85	0.82	381	337	76	53.06	83.37	PCA	2	80.43	1.12	565	153	122	78.69	82.24
	4	64.85	0.82	381	337	76	53.06	83.37		4	82.02	0.89	577	141	112	80.36	83.75
	6	64.85	0.82	381	337	76	53.06	83.37		6	77.28	1.12	529	189	122	73.68	81.26
	8	64.85	0.82	381	337	76	53.06	83.37		8	80.50	0.94	551	167	100	76.74	84.64
	10	64.85	0.82	381	337	76	53.06	83.37		10	81.12	1.01	567	151	113	78.97	83.38
	15	64.85	0.82	381	337	76	53.06	83.37		15	82.78	0.84	572	146	92	79.67	86.15
	20	75.16	0.80	457	261	41	63.65	91.77		20	95.19	0.56	682	36	33	94.99	95.39
30	75.66	0.73	460	258	38	64.07	92.37	30	91.90	0.57	647	71	43	90.11	93.77		
TS-LP	2	61.60	1.07	365	353	102	50.84	78.16		2	61.60	1.07	365	353	102	50.84	78.16
	4	61.60	1.07	365	353	102	50.84	78.16		4	61.60	1.07	365	353	102	50.84	78.16
	6	61.60	1.07	365	353	102	50.84	78.16		6	61.60	1.07	365	353	102	50.84	78.16
	8	61.60	1.07	365	353	102	50.84	78.16		8	61.60	1.07	365	353	102	50.84	78.16
	10	61.60	1.07	365	353	102	50.84	78.16		10	61.60	1.07	365	353	102	50.84	78.16
	15	61.60	1.07	365	353	102	50.84	78.16		15	61.60	1.07	365	353	102	50.84	78.16
	20	70.11	0.87	421	297	62	58.64	87.16		20	70.11	0.87	421	297	62	58.64	87.16
30	71.53	0.73	436	282	65	60.72	87.03	30	71.53	0.73	436	282	65	60.72	87.03		

Table B.19: Extracted fECG raw results for the Case 3 (SNR 9 dB)

9db																	
	No. Leads	F ₁	MAE	TP	FN	FP	SE	PPV		No. Leads	F ₁	MAE	TP	FN	FP	SE	PPV
AF-LMS	2	75.74	0.95	523	194	141	72.94	78.77	TS-PCA	2	76.82	0.63	459	258	19	64.02	96.03
	4	75.74	0.95	523	194	141	72.94	78.77		4	77.29	0.91	468	249	26	65.27	94.74
	6	75.74	0.95	523	194	141	72.94	78.77		6	77.29	0.91	468	249	26	65.27	94.74
	8	76.66	0.82	532	185	139	74.20	79.29		8	78.43	0.68	480	237	27	66.95	94.68
	10	77.84	0.91	541	176	132	75.45	80.39		10	79.84	0.69	491	226	22	68.48	95.71
	15	77.84	0.91	541	176	132	75.45	80.39		15	79.84	0.69	491	226	22	68.48	95.71
	20	80.03	0.81	559	158	121	77.96	82.21		20	81.84	0.66	516	201	28	71.97	94.85
30	80.03	0.81	559	158	121	77.96	82.21	30	81.84	0.66	516	201	28	71.97	94.85		
AF-RLS	2	75.06	0.92	516	201	142	71.97	78.42	FASTICA-DEF	2	70.49	1.19	455	262	119	63.46	79
	4	76.27	1.05	519	198	125	72.39	80.59		4	58.62	1.64	391	326	226	54.53	63.37
	6	76.27	1.05	519	198	125	72.39	80.59		6	82.03	1.89	573	144	107	79.92	84.27
	8	77.88	0.87	544	173	136	75.87	80.00		8	52.17	1.50	319	398	187	44.49	63.04
	10	78.19	0.86	545	172	132	76.01	80.50		10	56.30	1.67	362	355	207	50.49	63.62
	15	78.19	0.86	545	172	132	76.01	80.50		15	50.31	2.20	323	394	244	45.05	56.97
	20	80.37	0.86	565	152	124	78.80	82.00		20	61.94	1.19	406	311	188	56.63	68.35
30	80.37	0.86	565	152	124	78.80	82.00	30	51.88	1.44	317	400	188	44.21	62.77		
AF-ENS	2	77.27	0.85	537	180	136	74.90	79.79	FASTICA-SYM	2	73.45	1.37	484	233	117	67.50	80.53
	4	78.62	1.02	546	171	126	76.15	81.25		4	63.72	0.86	389	328	115	54.25	77.18
	6	79.71	1.08	554	163	119	77.27	82.32		6	68.61	1.20	436	281	118	60.81	78.70
	8	81.45	0.78	573	144	117	79.92	83.04		8	64.71	0.99	396	321	111	55.23	78.11
	10	82.48	0.84	579	138	108	80.75	84.28		10	51.74	1.85	335	382	243	46.72	57.96
	15	82.28	0.85	578	139	110	80.61	84.01		15	56.30	2.04	342	375	156	47.70	68.68
	20	83.84	0.70	589	128	99	82.15	85.61		20	78.41	1.15	534	183	111	74.48	82.79
30	84.68	0.77	597	120	96	83.26	86.15	30	78.93	2.48	532	185	99	74.20	84.31		
TS	2	77.19	0.61	462	255	18	64.44	96.25	JADE	2	80.75	0.83	562	155	113	78.38	83.26
	4	77.19	0.61	462	255	18	64.44	96.25		4	64.87	2.76	422	295	162	58.86	72.26
	6	77.19	0.61	462	255	18	64.44	96.25		6	79.13	0.94	544	173	114	75.87	82.68
	8	78.56	0.58	480	237	25	66.95	95.05		8	70.18	2.82	473	244	158	65.97	74.96
	10	79.25	0.63	489	228	28	68.20	94.58		10	63.83	2.78	413	304	164	57.60	71.58
	15	79.25	0.63	489	228	28	68.20	94.58		15	54.57	1.21	349	368	213	48.68	62.10
	20	80.89	0.61	510	207	34	71.13	93.75		20	76.24	1.75	515	202	119	71.83	81.23
30	80.89	0.61	510	207	34	71.13	93.75	30	78.29	1.73	530	187	107	73.92	83.20		
TS-CERUTTI	2	77.50	0.66	465	252	18	64.85	96.27	PCA	2	80.11	1.26	560	157	121	78.10	82.23
	4	77.50	0.66	465	252	18	64.85	96.27		4	54.30	1.95	341	376	198	47.56	63.27
	6	77.50	0.66	465	252	18	64.85	96.27		6	76.03	1.07	525	192	139	73.22	79.07
	8	79.67	0.62	486	231	17	67.78	96.62		8	76.20	0.81	522	195	131	72.80	79.94
	10	79.67	0.62	486	231	17	67.78	96.62		10	72.47	0.92	483	234	133	67.36	78.41
	15	79.67	0.62	486	231	17	67.78	96.62		15	78.41	0.68	543	174	125	75.73	81.29
	20	81.68	0.67	517	200	32	72.11	94.17		20	78.69	1.16	528	189	97	73.64	84.48
30	81.68	0.67	517	200	32	72.11	94.17	30	80.43	0.73	559	158	114	77.96	83.06		
TS-LP	2	71.72	0.77	421	296	36	58.72	92.12		2	71.72	0.77	421	296	36	58.72	92.12
	4	73.28	1.10	432	285	30	60.25	93.51		4	73.28	1.10	432	285	30	60.25	93.51
	6	73.28	1.10	432	285	30	60.25	93.51		6	73.28	1.10	432	285	30	60.25	93.51
	8	73.28	1.10	432	285	30	60.25	93.51		8	73.28	1.10	432	285	30	60.25	93.51
	10	73.56	0.81	441	276	41	61.51	91.49		10	73.56	0.81	441	276	41	61.51	91.49
	15	73.56	0.81	441	276	41	61.51	91.49		15	73.56	0.81	441	276	41	61.51	91.49
	20	75.69	0.77	464	253	45	64.71	91.16		20	75.69	0.77	464	253	45	64.71	91.16
30	75.69	0.77	464	253	45	64.71	91.16	30	75.69	0.77	464	253	45	64.71	91.16		

Table B.20: Extracted fECG raw results for the Case 3 (SNR 12 dB)

12db																	
	No. Leads	F ₁	MAE	TP	FN	FP	SE	PPV		No. Leads	F ₁	MAE	TP	FN	FP	SE	PPV
AF-LMS	2	81.03	0.93	566	151	114	78.94	83.24	TS-PCA	2	80.45	0.55	504	213	32	70.29	94.03
	4	81.03	0.93	566	151	114	78.94	83.24		4	80.45	0.55	504	213	32	70.29	94.03
	6	81.03	0.93	566	151	114	78.94	83.24		6	80.45	0.55	504	213	32	70.29	94.03
	8	81.03	0.93	566	151	114	78.94	83.24		8	80.54	0.73	509	208	38	70.99	93.05
	10	81.03	0.93	566	151	114	78.94	83.24		10	80.54	0.73	509	208	38	70.99	93.05
	15	81.03	0.93	566	151	114	78.94	83.24		15	80.54	0.73	509	208	38	70.99	93.05
	20	81.03	0.93	566	151	114	78.94	83.24		20	80.54	0.73	509	208	38	70.99	93.05
30	81.03	0.93	566	151	114	78.94	83.24	30	80.95	0.69	510	207	33	71.13	93.92		
AF-RLS	2	80.69	0.97	564	153	117	78.66	82.82	FASTICA-DEF	2	89.85	0.58	642	75	70	89.54	90.17
	4	80.69	0.97	564	153	117	78.66	82.82		4	63.52	1.32	417	300	179	58.16	69.97
	6	80.69	0.97	564	153	117	78.66	82.82		6	91.99	1.37	649	68	45	90.52	93.52
	8	80.69	0.97	564	153	117	78.66	82.82		8	66.61	2.51	420	297	124	58.58	77.21
	10	80.69	0.97	564	153	117	78.66	82.82		10	84.82	1.46	581	136	72	81.03	88.97
	15	80.69	0.97	564	153	117	78.66	82.82		15	64.71	2.91	429	288	180	59.83	70.44
	20	80.69	0.97	564	153	117	78.66	82.82		20	65.65	1.20	410	307	122	57.18	77.07
30	80.69	0.97	564	153	117	78.66	82.82	30	65.65	1.20	410	307	122	57.18	77.07		
AF-ENS	2	85.13	0.79	601	116	94	83.82	86.48	FASTICA-SYM	2	84.48	1.21	596	121	98	83.12	85.88
	4	84.58	0.78	595	122	95	82.99	86.23		4	67.76	1.50	454	263	169	63.32	72.87
	6	85.25	0.76	601	116	92	83.82	86.72		6	69.15	2.75	455	262	144	63.46	75.96
	8	85.37	0.77	601	116	90	83.82	86.98		8	68.57	1.43	456	261	157	63.60	74.39
	10	84.52	0.85	595	122	96	82.99	86.11		10	91.83	2.12	652	65	51	90.93	92.75
	15	85.17	0.81	600	117	92	83.68	86.71		15	92.34	2.06	657	60	49	91.63	93.06
	20	85.11	0.82	600	117	93	83.68	86.58		20	66.62	1.06	438	279	160	61.09	73.24
30	85.13	0.79	601	116	94	83.82	86.48	30	67.67	1.40	449	268	161	62.62	73.61		
TS	2	81.50	0.62	511	206	26	71.27	95.16	JADE	2	90.21	0.59	645	72	68	89.96	90.46
	4	81.50	0.62	511	206	26	71.27	95.16		4	94.63	0.51	678	39	38	94.56	94.69
	6	81.50	0.62	511	206	26	71.27	95.16		6	94.26	0.52	673	44	38	93.86	94.66
	8	81.50	0.62	511	206	26	71.27	95.16		8	95.62	0.52	687	30	33	95.82	95.42
	10	81.50	0.62	511	206	26	71.27	95.16		10	95.83	0.52	689	28	32	96.10	95.56
	15	81.50	0.62	511	206	26	71.27	95.16		15	96.10	0.51	690	27	29	96.23	95.97
	20	81.50	0.62	511	206	26	71.27	95.16		20	94.78	0.58	681	36	39	94.98	94.58
30	81.82	0.70	513	204	24	71.55	95.53	30	95.07	0.57	684	33	38	95.40	94.74		
TS-CERUTTI	2	81.30	0.66	513	204	32	71.55	94.13	PCA	2	90.20	0.50	640	77	62	89.26	91.17
	4	81.30	0.66	513	204	32	71.55	94.13		4	85.47	0.56	597	120	83	83.26	87.79
	6	81.30	0.66	513	204	32	71.55	94.13		6	73.05	0.60	473	244	105	65.97	81.83
	8	81.30	0.66	513	204	32	71.55	94.13		8	76.53	0.58	507	210	101	70.71	83.39
	10	81.30	0.66	513	204	32	71.55	94.13		10	78.96	0.62	531	186	97	74.06	84.55
	15	81.30	0.66	513	204	32	71.55	94.13		15	72.73	0.61	472	245	109	65.83	81.24
	20	81.30	0.66	513	204	32	71.55	94.13		20	71.87	0.63	465	252	112	64.85	80.59
30	81.65	0.72	514	203	28	71.69	94.83	30	73.32	1.90	496	221	140	69.18	77.99		
TS-LP	2	72.70	0.66	442	275	57	61.65	88.58		2	72.70	0.66	442	275	57	61.65	88.58
	4	72.70	0.66	442	275	57	61.65	88.58		4	72.70	0.66	442	275	57	61.65	88.58
	6	72.70	0.66	442	275	57	61.65	88.58		6	72.70	0.66	442	275	57	61.65	88.58
	8	72.70	0.66	442	275	57	61.65	88.58		8	72.70	0.66	442	275	57	61.65	88.58
	10	72.70	0.66	442	275	57	61.65	88.58		10	72.70	0.66	442	275	57	61.65	88.58
	15	72.70	0.66	442	275	57	61.65	88.58		15	72.70	0.66	442	275	57	61.65	88.58
	20	72.70	0.66	442	275	57	61.65	88.58		20	72.70	0.66	442	275	57	61.65	88.58
30	74.51	0.78	453	264	46	63.18	90.78	30	74.51	0.78	453	264	46	63.18	90.78		

B.5 Case 4 - Ectopic Beats + Noise

Table B.21: Extracted fECG raw results for the Case 4 (SNR 0 dB)

odb																	
	No. Leads	F ₁	MAE	TP	FN	FP	SE	PPV		No. Leads	F ₁	MAE	TP	FN	FP	SE	PPV
AF-LMS	2	83.80	0.66	551	134	79	80.44	87.46	TS-PCA	2	79.91	0.77	523	162	101	76.35	83.81
	4	83.80	0.66	551	134	79	80.44	87.46		4	79.91	0.77	523	162	101	76.35	83.81
	6	83.80	0.66	551	134	79	80.44	87.46		6	79.91	0.77	523	162	101	76.35	83.81
	8	83.80	0.66	551	134	79	80.44	87.46		8	79.91	0.77	523	162	101	76.35	83.81
	10	83.80	0.66	551	134	79	80.44	87.46		10	79.91	0.77	523	162	101	76.35	83.81
	15	83.80	0.66	551	134	79	80.44	87.46		15	79.91	0.77	523	162	101	76.35	83.81
	20	83.80	0.66	551	134	79	80.44	87.46		20	79.91	0.77	523	162	101	76.35	83.81
30	83.80	0.66	551	134	79	80.44	87.46	30	79.91	0.77	523	162	101	76.35	83.81		
AF-RLS	2	83.31	0.65	549	136	84	80.15	86.73	FASTICA-DEF	2	82.03	1.45	525	160	70	76.64	88.24
	4	83.31	0.65	549	136	84	80.15	86.73		4	83.69	1.54	531	154	53	77.52	90.93
	6	83.31	0.65	549	136	84	80.15	86.73		6	84.34	2.20	544	141	61	79.42	89.92
	8	83.36	0.82	546	139	79	79.71	87.36		8	84.53	0.52	522	163	28	76.20	94.91
	10	83.36	0.82	546	139	79	79.71	87.36		10	84.58	0.55	524	161	30	76.50	94.59
	15	83.36	0.82	546	139	79	79.71	87.36		15	84.67	0.52	519	166	22	75.77	95.93
	20	83.36	0.82	546	139	79	79.71	87.36		20	84.71	0.51	518	167	20	75.62	96.28
30	83.36	0.82	546	139	79	79.71	87.36	30	84.64	0.51	518	167	21	75.62	96.10		
AF-ENS	2	83.61	0.57	528	157	50	77.08	91.35	FASTICA-SYM	2	83.85	0.58	532	153	52	77.66	91.10
	4	84.49	0.60	531	154	41	77.52	92.83		4	56.09	1.28	364	321	249	53.14	59.38
	6	84.38	0.62	532	153	44	77.66	92.36		6	84.96	2.20	548	137	57	80.00	90.58
	8	84.15	0.58	531	154	46	77.52	92.03		8	84.40	0.52	522	163	30	76.20	94.57
	10	84.09	0.60	531	154	47	77.52	91.87		10	84.56	0.54	523	162	29	76.35	94.75
	15	84.39	0.70	535	150	48	78.10	91.77		15	85.51	1.51	534	151	30	77.96	94.68
	20	84.29	0.58	531	154	44	77.52	92.35		20	84.86	1.84	513	172	11	74.89	97.90
30	84.06	0.62	530	155	46	77.37	92.01	30	84.64	0.51	518	167	21	75.62	96.10		
TS	2	78.10	0.85	510	175	111	74.45	82.13	JADE	2	83.71	0.58	532	153	54	77.66	90.79
	4	78.10	0.85	510	175	111	74.45	82.13		4	84.30	0.52	521	164	30	76.06	94.56
	6	78.10	0.85	510	175	111	74.45	82.13		6	84.72	0.52	521	164	24	76.06	95.60
	8	78.10	0.85	510	175	111	74.45	82.13		8	84.67	0.52	522	163	26	76.20	95.26
	10	78.10	0.85	510	175	111	74.45	82.13		10	55.80	1.43	349	336	217	50.95	61.66
	15	78.10	0.85	510	175	111	74.45	82.13		15	85.03	0.51	517	168	14	75.47	97.36
	20	78.10	0.85	510	175	111	74.45	82.13		20	85.01	0.51	516	169	13	75.33	97.54
30	78.10	0.85	510	175	111	74.45	82.13	30	84.80	0.51	516	169	16	75.33	96.99		
TS-CERUTTI	2	79.79	0.76	521	164	100	76.06	83.90	PCA	2	84.36	1.42	523	162	32	76.35	94.23
	4	79.79	0.76	521	164	100	76.06	83.90		4	83.91	0.69	545	140	69	79.56	88.76
	6	79.79	0.76	521	164	100	76.06	83.90		6	85.87	0.55	571	114	74	83.36	88.53
	8	79.79	0.76	521	164	100	76.06	83.90		8	85.71	0.58	570	115	75	83.21	88.37
	10	79.79	0.76	521	164	100	76.06	83.90		10	85.54	0.60	571	114	79	83.36	87.85
	15	79.79	0.76	521	164	100	76.06	83.90		15	86.20	0.67	578	107	78	84.38	88.11
	20	79.79	0.76	521	164	100	76.06	83.90		20	85.00	0.69	558	127	70	81.46	88.85
30	79.79	0.76	521	164	100	76.06	83.90	30	84.53	0.66	560	125	80	81.75	87.50		
TS-LP	2	75.29	0.90	492	193	130	71.83	79.10		2	75.29	0.90	492	193	130	71.83	79.10
	4	75.29	0.90	492	193	130	71.83	79.10		4	75.29	0.90	492	193	130	71.83	79.10
	6	75.29	0.90	492	193	130	71.83	79.10		6	75.29	0.90	492	193	130	71.83	79.10
	8	75.29	0.90	492	193	130	71.83	79.10		8	75.29	0.90	492	193	130	71.83	79.10
	10	75.29	0.90	492	193	130	71.83	79.10		10	75.29	0.90	492	193	130	71.83	79.10
	15	75.29	0.90	492	193	130	71.83	79.10		15	75.29	0.90	492	193	130	71.83	79.10
	20	75.29	0.90	492	193	130	71.83	79.10		20	75.29	0.90	492	193	130	71.83	79.10
30	75.29	0.90	492	193	130	71.83	79.10	30	75.29	0.90	492	193	130	71.83	79.10		

Table B.23: Extracted fECG raw results for the Case 4 (SNR 6 dB)

6db																	
	No. Leads	F ₁	MAE	TP	FN	FP	SE	PPV		No. Leads	F ₁	MAE	TP	FN	FP	SE	PPV
AF-LMS	2	80.88	0.80	531	154	97	77.52	84.55	TS-PCA	2	81.77	0.83	536	149	90	78.25	85.62
	4	80.88	0.80	531	154	97	77.52	84.55		4	81.77	0.83	536	149	90	78.25	85.62
	6	80.88	0.80	531	154	97	77.52	84.55		6	81.77	0.83	536	149	90	78.25	85.62
	8	80.88	0.80	531	154	97	77.52	84.55		8	81.77	0.83	536	149	90	78.25	85.62
	10	80.88	0.80	531	154	97	77.52	84.55		10	81.77	0.83	536	149	90	78.25	85.62
	15	80.88	0.80	531	154	97	77.52	84.55		15	81.77	0.83	536	149	90	78.25	85.62
	20	81.25	0.88	533	152	94	77.81	85.01		20	82.13	0.88	540	145	90	78.83	85.71
30	82.03	0.84	541	144	93	78.98	85.33	30	83.25	0.71	549	136	85	80.15	86.59		
AF-RLS	2	82.66	0.80	541	144	83	78.98	86.70	FASTICA-DEF	2	80.16	1.39	507	178	73	74.02	87.41
	4	82.66	0.80	541	144	83	78.98	86.70		4	81.99	0.72	512	173	52	74.75	90.78
	6	82.66	0.80	541	144	83	78.98	86.70		6	66.67	1.78	409	276	133	59.71	75.46
	8	82.66	0.80	541	144	83	78.98	86.70		8	69.34	1.91	423	262	112	61.75	79.07
	10	82.66	0.80	541	144	83	78.98	86.70		10	78.54	2.23	538	147	147	78.54	78.54
	15	82.66	0.80	541	144	83	78.98	86.70		15	82.33	0.68	508	177	41	74.16	92.53
	20	82.66	0.80	541	144	83	78.98	86.70		20	82.13	1.49	508	177	44	74.16	92.03
30	82.66	0.80	541	144	83	78.98	86.70	30	81.95	1.90	497	188	31	72.56	94.13		
AF-ENS	2	80.31	0.69	524	161	96	76.50	84.52	FASTICA-SYM	2	82.64	2.04	514	171	45	75.04	91.95
	4	81.43	0.84	535	150	94	78.10	85.06		4	69.83	1.65	434	251	124	63.36	77.78
	6	80.97	0.75	532	153	97	77.66	84.58		6	80.82	2.10	493	192	42	71.97	92.15
	8	81.47	0.77	534	151	92	77.96	85.30		8	81.84	0.63	507	178	47	74.02	91.52
	10	81.50	0.78	533	152	90	77.81	85.55		10	77.40	2.37	524	161	145	76.50	78.33
	15	81.33	0.96	527	158	84	76.93	86.25		15	75.24	1.92	471	214	96	68.76	83.07
	20	82.20	0.83	515	170	53	75.18	90.67		20	81.66	2.12	512	173	57	74.75	89.98
30	82.08	0.83	513	172	52	74.89	90.80	30	78.63	1.53	493	192	76	71.97	86.64		
TS	2	67.80	1.14	439	246	171	64.09	71.97	JADE	2	82.82	0.79	523	162	55	76.35	90.48
	4	67.80	1.14	439	246	171	64.09	71.97		4	82.56	0.70	516	169	49	75.33	91.33
	6	67.80	1.14	439	246	171	64.09	71.97		6	81.22	0.62	506	179	55	73.87	90.20
	8	67.80	1.14	439	246	171	64.09	71.97		8	80.80	0.64	505	180	60	73.72	89.38
	10	67.80	1.14	439	246	171	64.09	71.97		10	78.34	2.05	537	148	149	78.39	78.28
	15	67.85	1.21	438	247	168	63.94	72.28		15	77.49	1.96	530	155	153	77.37	77.60
	20	70.93	1.24	460	225	152	67.15	75.16		20	78.90	3.39	516	169	107	75.33	82.83
30	73.91	1.07	483	202	139	70.51	77.65	30	76.90	3.68	506	179	125	73.87	80.19		
TS-CERUTTI	2	81.90	0.81	536	149	88	78.25	85.90	PCA	2	83.81	1.34	515	170	29	75.18	94.67
	4	81.90	0.81	536	149	88	78.25	85.90		4	81.17	0.96	528	157	88	77.08	85.71
	6	81.90	0.81	536	149	88	78.25	85.90		6	81.65	1.02	536	149	92	78.25	85.35
	8	81.90	0.81	536	149	88	78.25	85.90		8	83.02	1.07	545	140	83	79.56	86.78
	10	81.90	0.81	536	149	88	78.25	85.90		10	81.57	0.76	509	176	54	74.31	90.41
	15	81.90	0.81	536	149	88	78.25	85.90		15	81.47	0.59	532	153	89	77.66	85.67
	20	82.42	0.87	544	141	91	79.42	85.67		20	82.91	1.20	485	200	0	70.80	100
30	82.71	0.82	543	142	85	79.27	86.47	30	81.62	1.05	535	150	91	78.10	85.46		
TS-LP	2	76.66	0.84	496	189	113	72.41	81.45		2	76.66	0.84	496	189	113	72.41	81.45
	4	76.66	0.84	496	189	113	72.41	81.45		4	76.66	0.84	496	189	113	72.41	81.45
	6	76.66	0.84	496	189	113	72.41	81.45		6	76.66	0.84	496	189	113	72.41	81.45
	8	76.66	0.84	496	189	113	72.41	81.45		8	76.66	0.84	496	189	113	72.41	81.45
	10	76.66	0.84	496	189	113	72.41	81.45		10	76.66	0.84	496	189	113	72.41	81.45
	15	79.36	0.91	521	164	107	76.06	82.96		15	79.36	0.91	521	164	107	76.06	82.96
	20	80.70	0.88	531	154	100	77.52	84.15		20	80.70	0.88	531	154	100	77.52	84.15
30	80.70	0.88	531	154	100	77.52	84.15	30	80.70	0.88	531	154	100	77.52	84.15		

Table B.24: Extracted fECG raw results for the Case 4 (SNR 9 dB)

9db																	
	No. Leads	F ₁	MAE	TP	FN	FP	SE	PPV		No. Leads	F ₁	MAE	TP	FN	FP	SE	PPV
AF-LMS	2	83.04	0.55	514	172	38	74.93	93.12	TS-PCA	2	83.42	0.71	546	140	77	79.59	87.64
	4	83.04	0.55	514	172	38	74.93	93.12		4	83.42	0.71	546	140	77	79.59	87.64
	6	83.04	0.55	514	172	38	74.93	93.12		6	83.42	0.71	546	140	77	79.59	87.64
	8	83.42	0.54	513	173	31	74.78	94.30		8	84.39	0.82	554	132	73	80.76	88.36
	10	83.44	0.69	524	162	46	76.39	91.93		10	84.39	0.82	554	132	73	80.76	88.36
	15	83.55	0.61	518	168	36	75.51	93.50		15	84.63	0.79	559	127	76	81.49	88.03
	20	83.55	0.61	518	168	36	75.51	93.50		20	84.63	0.79	559	127	76	81.49	88.03
30	84.38	0.55	513	173	17	74.78	96.79	30	84.63	0.79	559	127	76	81.49	88.03		
AF-RLS	2	84.39	0.49	508	178	10	74.05	98.07	FASTICA-DEF	2	83.79	1.95	517	169	31	75.36	94.34
	4	84.39	0.49	508	178	10	74.05	98.07		4	83.95	0.50	510	176	19	74.34	96.41
	6	84.86	0.50	510	176	6	74.34	98.84		6	83.96	0.56	518	168	30	75.51	94.53
	8	85.07	0.50	510	176	3	74.34	99.42		8	83.71	1.29	514	172	28	74.93	94.83
	10	85.07	0.50	510	176	3	74.34	99.42		10	83.74	1.28	515	171	29	75.07	94.67
	15	85.07	0.50	510	176	3	74.34	99.42		15	83.10	1.84	531	155	61	77.41	89.70
	20	85.07	0.50	510	176	3	74.34	99.42		20	83.92	1.31	514	172	25	74.93	95.36
30	85.07	0.50	510	176	3	74.34	99.42	30	84.35	1.27	512	174	16	74.64	96.97		
AF-ENS	2	83.94	0.45	507	179	15	73.91	97.13	FASTICA-SYM	2	84.37	1.24	521	165	28	75.95	94.90
	4	84.25	0.46	508	178	12	74.05	97.69		4	84.32	1.11	511	175	15	74.49	97.15
	6	84.76	0.51	509	177	6	74.20	98.84		6	84.33	1.24	514	172	19	74.93	96.44
	8	84.62	0.51	509	177	8	74.20	98.45		8	84.01	0.54	515	171	25	75.07	95.37
	10	84.69	0.51	509	177	7	74.20	98.64		10	74.86	3.21	472	214	103	68.81	82.09
	15	84.69	0.51	509	177	7	74.20	98.64		15	70.94	2.58	454	232	140	66.18	76.43
	20	84.79	0.51	510	176	7	74.34	98.65		20	75.09	2.29	505	181	154	73.62	76.63
30	84.60	0.50	508	178	7	74.05	98.64	30	74.98	2.31	505	181	156	73.62	76.40		
TS	2	72.90	0.94	468	218	130	68.22	78.26	JADE	2	83.21	0.57	518	168	41	75.51	92.67
	4	72.90	0.94	468	218	130	68.22	78.26		4	83.88	0.49	510	176	20	74.34	96.23
	6	72.90	0.94	468	218	130	68.22	78.26		6	84.06	0.52	514	172	23	74.93	95.72
	8	72.90	0.94	468	218	130	68.22	78.26		8	62.92	1.74	414	272	216	60.35	65.71
	10	72.90	0.94	468	218	130	68.22	78.26		10	59.58	1.62	370	316	186	53.94	66.55
	15	72.90	0.94	468	218	130	68.22	78.26		15	70.94	1.02	443	243	120	64.58	78.69
	20	78.27	0.91	508	178	104	74.05	83.01		20	74.69	3.27	506	180	163	73.76	75.64
30	82.48	0.73	525	161	62	76.53	89.44	30	76.28	3.28	505	181	133	73.62	79.15		
TS-CERUTTI	2	83.44	0.73	544	142	74	79.30	88.03	PCA	2	84.99	1.35	521	165	19	75.95	96.48
	4	83.44	0.73	544	142	74	79.30	88.03		4	84.07	0.76	525	161	38	76.53	93.25
	6	83.44	0.73	544	142	74	79.30	88.03		6	84.41	0.79	528	158	37	76.97	93.45
	8	83.44	0.73	544	142	74	79.30	88.03		8	84.45	0.62	524	162	31	76.39	94.41
	10	83.44	0.73	544	142	74	79.30	88.03		10	84.20	0.81	525	161	36	76.53	93.58
	15	83.59	0.76	550	136	80	80.18	87.30		15	84.36	0.80	526	160	35	76.68	93.76
	20	83.59	0.76	550	136	80	80.18	87.30		20	84.12	0.80	527	159	40	76.82	92.95
30	83.59	0.76	550	136	80	80.18	87.30	30	84.35	0.72	520	166	27	75.80	95.06		
TS-LP	2	83.08	0.81	545	141	81	79.45	87.06		2	83.08	0.81	545	141	81	79.45	87.06
	4	83.08	0.81	545	141	81	79.45	87.06		4	83.08	0.81	545	141	81	79.45	87.06
	6	83.08	0.81	545	141	81	79.45	87.06		6	83.08	0.81	545	141	81	79.45	87.06
	8	83.08	0.81	545	141	81	79.45	87.06		8	83.08	0.81	545	141	81	79.45	87.06
	10	83.08	0.81	545	141	81	79.45	87.06		10	83.08	0.81	545	141	81	79.45	87.06
	15	83.30	0.85	551	135	86	80.32	86.50		15	83.30	0.85	551	135	86	80.32	86.50
	20	83.30	0.85	551	135	86	80.32	86.50		20	83.30	0.85	551	135	86	80.32	86.50
30	83.39	0.74	532	154	58	77.55	90.17	30	83.39	0.74	532	154	58	77.55	90.17		

Table B.25: Extracted fECG raw results for the Case 4 (SNR 12 dB)

12db																	
	No. Leads	F ₁	MAE	TP	FN	FP	SE	PPV		No. Leads	F ₁	MAE	TP	FN	FP	SE	PPV
AF-LMS	2	82.98	0.51	495	190	13	72.26	97.44	TS-PCA	2	83.09	0.57	501	184	20	73.14	96.16
	4	82.98	0.51	495	190	13	72.26	97.44		4	83.36	1.32	551	134	86	80.44	86.50
	6	82.98	0.51	495	190	13	72.26	97.44		6	83.43	0.67	511	174	29	74.60	94.63
	8	82.98	0.51	495	190	13	72.26	97.44		8	83.81	0.57	497	188	4	72.56	99.20
	10	82.98	0.51	495	190	13	72.26	97.44		10	83.81	0.57	497	188	4	72.56	99.20
	15	83.03	0.51	494	191	11	72.12	97.82		15	83.82	0.61	500	185	8	72.99	98.43
	20	83.03	0.51	494	191	11	72.12	97.82		20	83.82	0.61	500	185	8	72.99	98.43
30	83.10	0.51	494	191	10	72.12	98.02	30	83.82	0.61	500	185	8	72.99	98.43		
AF-RLS	2	83.56	0.52	493	192	2	71.97	99.60	FASTICA-DEF	2	79.19	1.48	487	198	58	71.10	89.36
	4	83.56	0.52	493	192	2	71.97	99.60		4	81.75	0.60	504	181	44	73.58	91.97
	6	83.56	0.52	493	192	2	71.97	99.60		6	83.40	0.55	495	190	7	72.26	98.61
	8	83.63	0.52	493	192	1	71.97	99.80		8	82.25	1.41	505	180	38	73.72	93.00
	10	83.63	0.52	493	192	1	71.97	99.80		10	82.27	0.80	501	184	32	73.14	94.00
	15	83.63	0.52	493	192	1	71.97	99.80		15	82.40	1.83	494	191	20	72.12	96.11
	20	83.63	0.52	493	192	1	71.97	99.80		20	82.44	1.89	493	192	18	71.97	96.48
30	83.63	0.52	493	192	1	71.97	99.80	30	82.49	1.28	497	188	23	72.56	95.58		
AF-ENS	2	83.11	0.49	492	193	7	71.83	98.60	FASTICA-SYM	2	74.96	2.34	461	224	84	67.30	84.59
	4	82.97	0.49	492	193	9	71.83	98.20		4	80.09	2.46	513	172	83	74.89	86.07
	6	82.87	0.49	491	194	9	71.68	98.20		6	81.77	1.42	498	187	35	72.70	93.43
	8	82.80	0.54	491	194	10	71.68	98.00		8	81.52	1.91	503	182	46	73.43	91.62
	10	83.08	0.51	491	194	6	71.68	98.79		10	80.29	0.51	501	184	62	73.14	88.99
	15	82.94	0.57	491	194	8	71.68	98.40		15	81.75	0.59	504	181	44	73.58	91.97
	20	83.01	0.52	491	194	7	71.68	98.59		20	76.15	1.51	487	198	107	71.10	81.99
30	83.32	0.76	552	133	88	80.58	86.25	30	78.92	1.46	498	187	79	72.70	86.31		
TS	2	82.88	0.66	501	184	23	73.14	95.61	JADE	2	81.75	0.60	504	181	44	73.58	91.97
	4	82.88	0.66	501	184	23	73.14	95.61		4	82.15	0.55	504	181	38	73.58	92.99
	6	82.88	0.66	501	184	23	73.14	95.61		6	81.82	0.58	504	181	43	73.58	92.14
	8	83.31	0.60	499	186	14	72.85	97.27		8	82.09	0.55	504	181	39	73.58	92.82
	10	83.31	0.60	499	186	14	72.85	97.27		10	82.15	0.53	504	181	38	73.58	92.99
	15	83.31	0.60	499	186	14	72.85	97.27		15	81.69	0.61	504	181	45	73.58	91.80
	20	83.31	0.60	499	186	14	72.85	97.27		20	81.75	0.61	504	181	44	73.58	91.97
30	83.31	0.60	499	186	14	72.85	97.27	30	73.87	3.42	492	193	155	71.83	76.04		
TS-CERUTTI	2	82.98	0.52	495	190	13	72.26	97.44	PCA	2	83.25	1.18	492	193	5	71.83	98.99
	4	82.98	0.52	495	190	13	72.26	97.44		4	81.95	0.58	504	181	41	73.58	92.48
	6	82.98	0.52	495	190	13	72.26	97.44		6	82.12	0.59	503	182	37	73.43	93.15
	8	83.56	0.51	493	192	2	71.97	99.60		8	83.60	1.36	502	183	14	73.29	97.29
	10	83.56	0.51	493	192	2	71.97	99.60		10	83.24	0.68	499	186	15	72.85	97.08
	15	83.56	0.51	493	192	2	71.97	99.60		15	83.28	1.24	493	192	6	71.97	98.80
	20	83.56	0.51	493	192	2	71.97	99.60		20	82.86	0.55	498	187	19	72.70	96.33
30	83.56	0.51	493	192	2	71.97	99.60	30	82.50	0.62	502	183	30	73.29	94.36		
TS-LP	2	83.20	0.68	500	185	17	72.99	96.71		2	83.20	0.68	500	185	17	72.99	96.71
	4	83.20	0.68	500	185	17	72.99	96.71		4	83.64	1.00	506	179	19	73.87	96.38
	6	83.64	1.00	506	179	19	73.87	96.38		6	83.64	1.00	506	179	19	73.87	96.38
	8	83.64	1.00	506	179	19	73.87	96.38		8	83.64	1.00	506	179	19	73.87	96.38
	10	83.64	1.00	506	179	19	73.87	96.38		10	84.47	1.22	525	160	33	76.64	94.09
	15	84.47	1.22	525	160	33	76.64	94.09		15	84.47	1.22	525	160	33	76.64	94.09
	20	84.47	1.22	525	160	33	76.64	94.09		20	84.47	1.22	525	160	33	76.64	94.09
30	84.47	1.22	525	160	33	76.64	94.09	30	84.47	1.22	525	160	33	76.64	94.09		

B.6 Case 5 - Twin Pregnancy + Noise

Table B.26: Extracted fECG raw results for the Case 5 (SNR 0 dB)

		0dB															
		Fetus 1								Fetus 2							
	No. Leads	F ₁	MAE	TP	FN	FP	SE	PPV	No. Leads	F ₁	MAE	TP	FN	FP	SE	PPV	
FASTICA-DEF	2	99.85	0.49	685	0	2	100	99.71	2	19.45	6.35	113	362	574	23.79	16.45	
	4	63.00	1.60	418	267	224	61.02	65.11	4	19.63	6.24	102	373	462	21.47	18.09	
	6	99.05	1.66	679	6	7	99.12	98.98	6	36.97	4.35	193	282	376	40.63	33.92	
	8	96.32	1.32	654	31	19	95.47	97.18	8	40.69	3.01	213	262	359	44.84	37.24	
	10	93.48	2.20	631	54	34	92.12	94.89	10	32.12	2.50	168	307	403	35.37	29.42	
	15	99.85	1.82	685	0	2	100	99.71	15	72.60	0.75	371	104	176	78.11	67.82	
	20	99.85	1.81	685	0	2	100	99.71	20	100	1.16	475	0	0	100	100	
	30	99.85	1.77	685	0	2	100	99.71	30	100	2.17	475	0	0	100	100	
FASTICA-SYM	2	97.14	1.23	662	23	16	96.64	97.64	2	22.03	6.06	127	348	551	26.74	18.73	
	4	65.70	1.77	429	256	192	62.63	69.08	4	20.84	6.45	114	361	505	24.00	18.42	
	6	99.85	0.48	685	0	2	100	99.71	6	54.65	1.04	285	190	283	60.00	50.18	
	8	99.85	0.49	685	0	2	100	99.71	8	53.32	1.00	277	198	287	58.32	49.11	
	10	99.42	1.08	682	3	5	99.56	99.27	10	37.61	4.56	198	277	380	41.68	34.26	
	15	99.85	1.22	685	0	2	100	99.71	15	92.76	1.35	461	14	58	97.05	88.83	
	20	96.76	0.93	656	29	15	95.77	97.77	20	76.77	0.69	385	90	143	81.05	72.92	
	30	99.85	1.21	685	0	2	100	99.71	30	99.58	1.72	475	0	4	100	99.17	
JADE	2	99.85	0.49	685	0	2	100	99.71	2	19.45	6.35	113	362	574	23.79	16.45	
	4	99.85	0.47	685	0	2	100	99.71	4	21.08	6.45	109	366	450	22.95	19.50	
	6	99.85	0.47	685	0	2	100	99.71	6	39.66	5.52	210	265	374	44.21	35.96	
	8	99.85	0.48	685	0	2	100	99.71	8	38.17	5.65	200	275	373	42.11	34.90	
	10	99.85	0.48	685	0	2	100	99.71	10	57.55	0.92	301	174	270	63.37	52.72	
	15	99.85	0.52	685	0	2	100	99.71	15	95.18	0.20	474	1	47	99.79	90.98	
	20	99.85	0.48	685	0	2	100	99.71	20	100	0.29	475	0	0	100	100	
	30	99.85	0.49	685	0	2	100	99.71	30	86.59	1.12	426	49	83	89.68	83.69	
PCA	2	99.85	0.48	685	0	2	100	99.71	2	19.45	6.42	113	362	574	23.79	16.45	
	4	98.61	0.54	674	11	8	98.39	98.83	4	20.40	5.89	118	357	564	24.84	17.30	
	6	95.36	0.48	648	37	26	94.60	96.14	6	31.01	5.34	160	315	397	33.68	28.73	
	8	96.85	0.49	661	24	19	96.50	97.21	8	40.55	2.84	205	270	331	43.16	38.25	
	10	99.05	0.45	677	8	5	98.83	99.27	10	34.44	3.08	186	289	419	39.16	30.74	
	15	99.42	0.42	681	4	4	99.42	99.42	15	61.92	0.89	326	149	252	68.63	56.40	
	20	99.85	0.47	685	0	2	100	99.71	20	66.67	0.80	349	126	223	73.47	61.01	
	30	87.59	0.80	582	103	62	84.96	90.37	30	71.95	2.10	368	107	180	77.47	67.15	

Table B.27: Extracted fECG raw results for the Case 5 (SNR 3 dB)

3dB																
		Fetus 1							Fetus 2							
	No. Leads	F ₁	MAE	TP	FN	FP	SE	PPV	No. Leads	F ₁	MAE	TP	FN	FP	SE	PPV
FASTICA-DEF	2	99.93	0.49	686	0	1	100	99.85	2	25.10	4.85	162	553	414	22.66	28.13
	4	99.93	0.48	686	0	1	100	99.85	4	74.76	1.58	514	201	146	71.89	77.88
	6	82.13	0.65	533	153	79	77.70	87.09	6	100	1.08	715	0	0	100	100
	8	99.42	2.11	682	4	4	99.42	99.42	8	100	1.76	715	0	0	100	100
	10	87.71	2.15	589	97	68	85.86	89.65	10	100	0.33	715	0	0	100	100
	15	99.93	2.23	686	0	1	100	99.85	15	100	1.80	715	0	0	100	100
	20	99.93	0.47	686	0	1	100	99.85	20	100	1.11	715	0	0	100	100
	30	99.93	0.45	686	0	1	100	99.85	30	100	1.11	715	0	0	100	100
FASTICA-SYM	2	72.03	1.93	488	198	181	71.14	72.95	2	51.01	4.27	353	362	316	49.37	52.77
	4	99.93	0.53	686	0	1	100	99.85	4	100	0.45	715	0	0	100	100
	6	76.70	1.51	492	194	105	71.72	82.41	6	81.24	1.70	578	137	130	80.84	81.64
	8	87.80	2.16	590	96	68	86.01	89.67	8	100	1.75	715	0	0	100	100
	10	99.93	1.22	686	0	1	100	99.85	10	100	1.04	715	0	0	100	100
	15	99.93	0.41	686	0	1	100	99.85	15	100	0.44	715	0	0	100	100
	20	99.93	0.45	686	0	1	100	99.85	20	100	0.08	715	0	0	100	100
	30	99.93	0.43	686	0	1	100	99.85	30	100	0.14	715	0	0	100	100
JADE	2	99.93	0.49	686	0	1	100	99.85	2	25.33	4.66	164	551	416	22.94	28.28
	4	99.93	0.51	686	0	1	100	99.85	4	100	0.47	715	0	0	100	100
	6	99.93	0.51	686	0	1	100	99.85	6	100	0.43	715	0	0	100	100
	8	99.93	0.48	686	0	1	100	99.85	8	100	0.38	715	0	0	100	100
	10	99.93	0.48	686	0	1	100	99.85	10	100	0.38	715	0	0	100	100
	15	90.22	0.93	609	77	55	88.78	91.72	15	100	0.47	715	0	0	100	100
	20	99.93	0.47	686	0	1	100	99.85	20	100	0.49	715	0	0	100	100
	30	99.93	0.45	686	0	1	100	99.85	30	100	0.49	715	0	0	100	100
PCA	2	91.74	1.10	622	64	48	90.67	92.84	2	30.76	5.03	213	502	457	29.79	31.79
	4	99.93	0.53	686	0	1	100	99.85	4	99.23	0.56	708	7	4	99.02	99.44
	6	99.20	0.53	679	7	4	98.98	99.41	6	95.47	0.45	674	41	23	94.27	96.70
	8	98.76	0.55	676	10	7	98.54	98.98	8	100	0.49	715	0	0	100	100
	10	98.24	0.64	670	16	8	97.67	98.82	10	98.60	1.00	702	13	7	98.18	99.01
	15	99.93	0.42	686	0	1	100	99.85	15	100	0.36	715	0	0	100	100
	20	99.93	0.48	686	0	1	100	99.85	20	99.86	1.05	713	2	0	99.72	100
	30	99.93	0.51	685	1	0	99.85	100	30	100	1.91	715	0	0	100	100

Table B.28: Extracted fECG raw results for the Case 5 (SNR 6 dB)

6dB																		
Fetus 1									Fetus 2									
	No.	Leads	F ₁	MAE	TP	FN	FP	SE	PPV	No.	Leads	F ₁	MAE	TP	FN	FP	SE	PPV
FASTICA-DEF	2		83.65	1.19	560	125	94	81.75	85.63	2		28.69	5.03	180	421	474	29.95	27.52
	4		84.97	1.10	568	117	84	82.92	87.12	4		36.19	2.22	213	388	363	35.44	36.98
	6		100	0.52	685	0	0	100	100	6		100	0.52	601	0	0	100	100
	8		99.71	1.51	682	3	1	99.56	99.85	8		100	0.51	601	0	0	100	100
	10		99.85	2.14	685	0	2	100	99.71	10		100	1.37	601	0	0	100	100
	15		99.85	1.35	685	0	2	100	99.71	15		93.31	1.28	558	43	37	92.85	93.78
	20		99.85	0.48	685	0	2	100	99.71	20		89.80	2.34	537	64	58	89.35	90.25
	30		64.70	2.63	395	290	141	57.66	73.69	30		61.31	1.10	336	265	159	55.91	67.88
FASTICA-SYM	2		90.96	1.27	614	71	51	89.64	92.33	2		27.17	4.89	172	429	493	28.62	25.87
	4		93.94	1.25	636	49	33	92.85	95.07	4		34.04	3.15	202	399	384	33.61	34.47
	6		100	0.51	685	0	0	100	100	6		62.39	1.77	374	227	224	62.23	62.54
	8		100	1.99	685	0	0	100	100	8		84.40	2.27	503	98	88	83.69	85.11
	10		99.85	2.08	685	0	2	100	99.71	10		91.47	0.99	547	54	48	91.02	91.93
	15		99.85	2.36	685	0	2	100	99.71	15		100	2.26	601	0	0	100	100
	20		99.85	1.39	685	0	2	100	99.71	20		89.68	1.81	539	62	62	89.68	89.68
	30		89.65	1.34	602	83	56	87.88	91.49	30		100	2.31	601	0	0	100	100
JADE	2		95.00	0.56	646	39	29	94.31	95.70	2		26.02	5.08	166	435	509	27.62	24.59
	4		96.69	0.52	658	27	18	96.06	97.34	4		45.92	1.60	270	331	305	44.93	46.96
	6		100	0.51	685	0	0	100	100	6		100	0.52	601	0	0	100	100
	8		100	0.51	685	0	0	100	100	8		100	0.51	601	0	0	100	100
	10		99.85	0.50	685	0	2	100	99.71	10		86.51	1.32	516	85	76	85.86	87.16
	15		99.85	0.50	685	0	2	100	99.71	15		100	0.51	601	0	0	100	100
	20		99.85	0.48	685	0	2	100	99.71	20		100	0.51	601	0	0	100	100
	30		87.43	3.81	581	104	63	84.82	90.22	30		90.04	2.34	538	63	56	89.52	90.57
PCA	2		95.74	1.28	652	33	25	95.18	96.31	2		25.51	5.55	163	438	514	27.12	24.08
	4		91.94	0.80	622	63	46	90.80	93.11	4		28.68	4.19	182	419	486	30.28	27.25
	6		93.21	0.44	631	54	38	92.12	94.32	6		99.83	0.69	600	1	1	99.83	99.83
	8		88.53	0.47	594	91	63	86.72	90.41	8		100	0.53	601	0	0	100	100
	10		84.07	0.76	562	123	90	82.04	86.20	10		100	0.51	601	0	0	100	100
	15		97.22	0.39	664	21	17	96.93	97.50	15		100	0.56	601	0	0	100	100
	20		95.36	0.50	648	37	26	94.60	96.14	20		99.92	0.50	600	1	0	99.83	100
	30		97.80	0.40	668	17	13	97.52	98.09	30		84.24	1.24	513	88	104	85.36	83.14

Table B.29: Extracted fECG raw results for the Case 5 (SNR 9 dB)

9dB																		
Fetus 1									Fetus 2									
	No.	Leads	F ₁	MAE	TP	FN	FP	SE	PPV	No.	Leads	F ₁	MAE	TP	FN	FP	SE	PPV
FASTICA-DEF	2		30.22	4.45	218	468	539	31.78	28.80	2		92.33	0.82	728	92	29	88.78	96.17
	4		38.81	3.51	267	419	423	38.92	38.70	4		88.06	1.88	682	138	47	83.17	93.55
	6		59.21	2.86	397	289	258	57.87	60.61	6		100	0.77	820	0	0	100	100
	8		89.68	0.81	595	91	46	86.74	92.82	8		100	0.50	820	0	0	100	100
	10		98.01	0.54	666	20	7	97.09	98.96	10		100	0.50	820	0	0	100	100
	15		97.13	0.61	660	26	13	96.21	98.07	15		100	1.15	820	0	0	100	100
	20		96.99	0.64	660	26	15	96.21	97.78	20		100	0.76	820	0	0	100	100
	30		98.17	0.59	670	16	9	97.67	98.68	30		100	0.75	820	0	0	100	100
FASTICA-SYM	2		31.93	3.91	227	459	509	33.09	30.84	2		89.85	0.94	699	121	37	85.24	94.97
	4		38.50	3.67	261	425	409	38.05	38.96	4		90.41	1.26	712	108	43	86.83	94.31
	6		60.94	2.68	408	278	245	59.48	62.48	6		86.74	1.09	687	133	77	83.78	89.92
	8		93.00	1.51	624	62	32	90.96	95.12	8		100	0.73	820	0	0	100	100
	10		99.42	1.74	681	5	3	99.27	99.56	10		100	1.11	820	0	0	100	100
	15		94.64	1.93	644	42	31	93.88	95.41	15		100	1.16	820	0	0	100	100
	20		68.68	1.92	454	232	182	66.18	71.38	20		100	0.77	820	0	0	100	100
	30		97.88	1.32	669	17	12	97.52	98.24	30		100	0.75	820	0	0	100	100
JADE	2		31.48	4.00	224	462	513	32.65	30.39	2		90.30	0.92	703	117	34	85.73	95.39
	4		45.53	2.97	308	378	359	44.90	46.18	4		98.02	1.47	792	28	4	96.59	99.50
	6		59.78	1.96	399	287	250	58.16	61.48	6		100	0.52	820	0	0	100	100
	8		95.47	0.70	643	43	18	93.73	97.28	8		100	0.50	820	0	0	100	100
	10		99.41	0.53	679	7	1	98.98	99.85	10		100	0.41	820	0	0	100	100
	15		98.76	0.56	675	11	6	98.40	99.12	15		100	0.31	820	0	0	100	100
	20		67.02	1.88	441	245	189	64.29	70.00	20		100	0.35	820	0	0	100	100
	30		78.85	1.43	522	164	116	76.09	81.82	30		100	0.45	820	0	0	100	100
PCA	2		30.54	4.35	219	467	529	31.92	29.28	2		91.71	0.85	719	101	29	87.68	96.12
	4		37.85	3.67	264	422	445	38.48	37.24	4		86.12	0.79	661	159	54	80.61	92.45
	6		71.17	1.38	464	222	154	67.64	75.08	6		99.94	0.34	819	1	0	99.88	100
	8		97.65	0.55	665	21	11	96.94	98.37	8		99.94	0.72	819	1	0	99.88	100
	10		99.27	0.45	680	6	4	99.13	99.42	10		99.69	0.71	815	5	0	99.39	100
	15		79.07	0.87	529	157	123	77.11	81.14	15		99.94	0.26	819	1	0	99.88	100
	20		96.19	1.02	656	30	22	95.63	96.76	20		99.94	0.26	819	1	0	99.88	100
	30		92.33	1.50	626	60	44	91.25	93.43	30		99.88	0.27	818	2	0	99.76	100

Table B.30: Extracted fECG raw results for the Case 5 (SNR 12 dB)

12dB																		
Fetus 1									Fetus 2									
	No.	Leads	F ₁	MAE	TP	FN	FP	SE	PPV	No.	Leads	F ₁	MAE	TP	FN	FP	SE	PPV
FASTICA-DEF	2		94.61	1.35	641	45	28	93.44	95.82	2		21.74	6.12	130	397	539	24.67	19.43
	4		98.54	1.35	674	12	8	98.25	98.83	4		41.82	4.03	225	302	324	42.69	40.98
	6		81.79	1.48	530	156	80	77.26	86.89	6		99.91	2.04	527	0	1	100	99.81
	8		99.93	1.25	686	0	1	100	99.85	8		99.91	2.02	527	0	1	100	99.81
	10		99.93	1.28	686	0	1	100	99.85	10		99.91	2.05	527	0	1	100	99.81
	15		99.93	1.85	686	0	1	100	99.85	15		99.91	2.20	527	0	1	100	99.81
	20		99.93	0.83	686	0	1	100	99.85	20		80.86	2.46	412	115	80	78.18	83.74
	30		99.93	2.83	686	0	1	100	99.85	30		99.91	2.19	527	0	1	100	99.81
FASTICA-SYM	2		91.09	1.24	613	73	47	89.36	92.88	2		21.74	6.11	129	398	531	24.48	19.55
	4		98.17	1.39	671	15	10	97.81	98.53	4		41.33	3.92	224	303	333	42.51	40.22
	6		65.14	2.45	426	260	196	62.10	68.49	6		100	2.17	527	0	0	100	100
	8		99.93	0.57	686	0	1	100	99.85	8		100	2.00	527	0	0	100	100
	10		81.69	1.46	542	144	99	79.01	84.56	10		77.44	1.79	424	103	144	80.46	74.65
	15		99.93	1.36	686	0	1	100	99.85	15		100	0.76	527	0	0	100	100
	20		90.07	0.62	608	78	56	88.63	91.57	20		79.43	2.27	421	106	112	79.89	78.99
	30		99.93	3.25	686	0	1	100	99.85	30		100	2.41	527	0	0	100	100
JADE	2		99.56	0.49	682	4	2	99.42	99.71	2		19.82	6.25	120	407	564	22.77	17.54
	4		99.85	0.46	685	1	1	99.85	99.85	4		36.21	4.57	197	330	364	37.38	35.12
	6		99.85	0.42	685	1	1	99.85	99.85	6		99.91	2.09	527	0	1	100	99.81
	8		99.93	0.49	686	0	1	100	99.85	8		99.91	2.00	527	0	1	100	99.81
	10		99.93	0.49	686	0	1	100	99.85	10		100	2.01	527	0	0	100	100
	15		99.93	0.49	686	0	1	100	99.85	15		100	2.03	527	0	0	100	100
	20		99.93	0.48	686	0	1	100	99.85	20		99.81	2.02	527	0	2	100	99.62
	30		99.93	0.49	686	0	1	100	99.85	30		99.81	2.00	527	0	2	100	99.62
PCA	2		99.93	0.48	686	0	1	100	99.85	2		91.71	0.85	719	101	29	87.68	96.12
	4		99.56	0.50	682	4	2	99.42	99.71	4		86.12	0.79	661	159	54	80.61	92.45
	6		99.85	0.49	685	1	1	99.85	99.85	6		99.94	0.34	819	1	0	99.88	100
	8		99.93	0.50	686	0	1	100	99.85	8		99.94	0.72	819	1	0	99.88	100
	10		99.85	0.51	685	1	1	99.85	99.85	10		99.69	0.71	815	5	0	99.39	100
	15		99.93	0.50	686	0	1	100	99.85	15		99.94	0.26	819	1	0	99.88	100
	20		99.93	0.51	686	0	1	100	99.85	20		99.94	0.26	819	1	0	99.88	100
	30		99.93	0.51	686	0	1	100	99.85	30		99.88	0.27	818	2	0	99.76	100